

ADDIS ABABA UNIVERSITY
School of Graduate Studies
Faculty of Science

**LANDSLIDE HAZARD ZONATION MAPPING
ALONG RIGHT BANK OF GIBE RIVER**

A Thesis
submitted to
The School of Graduate Studies of Addis Ababa University
in Partial Fulfillment of the requirements for the Degree of Masters in
Engineering Geology

By
ENGDAWORK MULATU

June 2005



**ADDIS ABABA UNIVERSITY
DEPARTMENT OF EARTH
SCIENCES
SCHOOL OF GRADUATE STUDIES**

**LANDSLIDE HAZARD ZONATION MAPPING
ALONG RIGHT BANK OF GIBERIVER**

By

ENGDAWORK MULATU

JUNE 2005

ACKNOWLEDGEMENT

I would like to express my sincere appreciation to my advisors Dr. Tarun K. Raguhuvanshi who generously shared his knowledge, guided me during my fieldwork, supplied his personal resource, and sacrificed holidays in reading and correcting the thesis. I am also very grateful to my co-adviser Dr. Bekele Abebe for his continuous supervision, guidance and valuable comments.

I would like to express my heart felt and warmest gratitude to my friend, Sirak Bogale, for his financial support and valuable encouragement. I have exceptional affection to him, because without his financial support, I wouldn't have accomplished this work. I am also greatly indebted to my friend, Nehemia Solomon, for his unreserved encouragement and supports from the very beginning of my education up to now.

I would like to thank Ethiopian Electric Power Corporation (EEPCO), particularly Gilgel Gibe II Hydroelectric Power Project society, for providing me the necessary data of the study area and corporation provided during the field work. My special thanks go to Ato Sisay Woldatensae, Ato Smegnew Bekele and Ato Samson Cheneke for their kind assistance and approach through out my project work. The professional and moral assistance of GilgelGibe Geologists, Ato Belachew Kasa, Ato Yared Demle, and Ato Tegenachew Desse, is highly appreciable.

I also extends my sincere thank to Dr. Derje Ayalew, head of Department of Earth science of Addis Ababa University, for his persistent help in administrative and academic issues.

I am thankful to all staff members of Earth science department and my friends who support me directly or indirectly during my stay in the university.

I would like to acknowledge all my family, who contributed more for the success of this work in one or other ways.

More thanks and praise shall be for my heavenly GOD who always assists me in every dimension of my life

TABLE OF CONTENTS

Acknowledgement	I
List of Figures	V
List of Plates	VI
List of Tables	VII
Abstract	VIII
 CHAPTER- 1 Introduction	
1.1 Preamble	1
1.2 Location and Accessibility	2
1.3 Importance of the Study	2
1.4 Climate of the Area	4
1.5 Physiography	5
1.6 Earthquake Activity (Sismicity of the area)	7
1.7 Previous Works	8
1.8 Objectives	9
1.8.1 <i>General Objectives</i>	9
1.8.2 <i>Specific Objectives</i>	10
1.9 Approach and Methodology	10
1.10 Limitations of the Study	11
1.11 Proposed Outcome of the Study	11
 CHAPTER- 2 Landslide Hazard Evaluations	
2.1 General	12
2.2 Literature Review	12
2.3 Methodology for LHEF Rating Scheme	14

CHAPTER- 3 Geological Setup of the Area

3.1	Regional Geological Setting -----	16
3.1.1	<i>Pre- rift Succession</i> -----	17
3.1.1.1	Basal Red Sandstone -----	17
3.1.1.2	Early Flood Basalts -----	19
3.1.1.3	Salic, Basaltic, and Intermediate Flows and Pyroclastic Rocks -----	19
3.1.1.4	Trachyte, Rhyolite, Tuff, Breccia, Ignimbrite and Intercalated Basalt -----	19
3.1.1.5	Mekonnen Basalt -----	21
3.1.2	The post- Rift Succession -----	21
3.1.2.1	<i>Nazreth Group, Rhyolitic, Trachytic Flows. and Ignimbrites</i> -----	21
3.1.2.2	<i>Omo Group</i> -----	22
3.1.2.3	<i>Basalt Flows, Trachyte, Ash & Tuff</i> -----	23
3.1.2.4	<i>Holocene Sediment Deposits</i> -----	24
3.2	Geology of the Area -----	24
3.2.1	<i>Rhyolitic Tuff</i> -----	25
3.2.2	<i>Basalt</i> -----	25
3.2.3	<i>Dolerite</i> -----	25
3.3	Regional Structural Setup -----	27
3.3.1	<i>Pre- rift Structures</i> -----	27
3.3.2	<i>Rift Structure</i> -----	28

CHAPTER- 4 Landslide Hazard Evaluation and Zonation of the study area

4.1	Preamble -----	29
4.2	Landslide Hazard Evaluation Factor (LHEF) Rating Scheme -----	30
4.3	Geology -----	30
4.4	Lithology -----	31
4.5	Structure -----	31
4.6	Slope Morphometry -----	32
4.7	Relative Relief -----	32
4.8	Landuse and Land cover -----	34
4.9	Ground Water Condition -----	34

4.10	Landslide Hazard Evaluation in the Study Area	37
4.11	Landslide Hazard Zonation Mapping of the Study Area	38
4.11.1	<i>Low Hazard Area</i>	38
4.11.2	<i>Moderately Hazard Area</i>	38
4.11.3	<i>High Hazard Area</i>	38

CHAPTER- 5 Detail Slope Stability Studies

5.1	Preamble	43
5.2	Identification of Potential Unstable Slopes	43
5.3	Engineering Property of Rocks and Soils	44
5.3.1	<i>Rock mass classification</i>	44
5.3.2	<i>Soil classification</i>	48
5.4	Discontinuity Analysis	49
5.5	Geometry and Geology of the Critical Slope Sections	50
5.6	Kinematic Check	55
5.7	Limit Equilibrium Analysis for Critical Slope Sections	55
5.7.1	<i>Factor of Safety Analysis</i>	58
5.7.1.1	Plane Mode of Failure Analysis	59
5.7.1.2	Wedge Mode of Failure Analysis	63
5.7.1.3	Circular Mode of Failure Analysis	67

CHAPTER- 6 Slope Design and Remedial Measures

6.1	Overall Stability Condition	72
6.2	Remedial Measures for Slope Sections Having Plane Mode of Failure	74
6.2.1	<i>Slope Design</i>	74
6.2.2	<i>Rock Bolting</i>	74
6.3	Remedial Measures for Slope Sections Having Wedge Mode of Failure	80
6.4	Remedial Measures for Slope Sections Having Rotational Mode of Failure	81

CHAPTER- 7 Conclusion

References	85
Annexures	89

List of Figures		Page
Figure 1.1	Location Map of The Study area	3
Figure 1.2	Minimum and Maximum Temperature and Average Monthly Rainfall as observed at Sekoru Meteorological station (1989 -2004)	5
Figure 1.3	Topography of the study area	6
Figure 1.4	Seismic risk map of Ethiopia 100 years return period, 0.99 probability	8
Figure 3.1	Regional Geological Map of Omo- Gibe sub-basin	18
Figure 3.2	Geological map of the study area	26
Figure 4.1	Slope Morphometry of the study area	33
Figure 4.2	Relative Relief Map of the study area	35
Figure 4.3	Landuse and Landcover map of the study area	36
Figure 4.4	Landslide Hazard Zonation Map of the study area	39
Figure 5.1	RMR data locations and Critical slopes	47
Figure 5.2	The preferred orientations on various critical rock slope sections in the study area	51
Figure 5.3	Geological cross sections have been prepared along all the critical slope sections	52
Figure 5.4	Possible Mode of Failure in Critical Rock slope Sections	56
Figure 5.5	Geometry of the slope for modified technique	60
Figure 5.6	Stability condition of critical slopes having plane mode of failure for existing and anticipated worst conditions	64
Figure 5.7	Critical Slope section for Rotational Mode of Failure	68
Figure 6.1	Overall Stability of critical slopes under existing and possible	

	worst conditions	73
Figure 6.2	Shows the design for SL 1, SL2, SL3,SL4,SL5 and SL7 slope sections	74
Figure 6.3	Different Type of Rock Bolts	78
Figure 6.4	Rock bolt plan for Slope Section SL6 Designed for Anticipated Adverse Condition	80
Plate 5.1	Possible plane mode of failure in rock mass	58
Plate 5.2	Wedge Mode of Failures along the road cut	65
Plate 5.3	Critical soil slope section SL 10, having possible circular mode of failure	69

List of Tables		Page
Table 3.1	Geological Succession of Omo-Gibe sub-basin	20
Table 4.1:	Proposed maximum LHEF rating for different contributory factors for macro-zonation	30
Table 4.2	TEHD ratings, facet wise, for the study area	40
Table 5.1	RMR data collected from various locations at critical slope sections	46
Table 5.2	Shear strength Parameters and Modulus of Deformation 'Ed' as determined from RMR	48
Table 5.3	Index Properties, as determined from the soil samples collected from critical slope sections	49
Table 5.4	Shear strength properties and Unit weight of soil at critical slope sections	49
Table 5.5	Preferred orientations, as observed on various critical rock slope sections in the study area	50
Table 5.6	The Geometry of Critical Slope Sections	54
Table 5.7	Possible mode of failures of critical slope sections in the study area	57
Table 5.8	Input Parameters for the determination of Factor of Safety for Plane failure analysis of Critical Slope Sections	63
Table 5.9	Stability Condition of Critical Slopes having Plane Mode of Failure	64
Table 5.10	Input Data Sheet for Wedge failure Analysis for SL 8 Slope Section	66
Table 5.11	Stability Condition of Critical Slopes having Wedge Mode of Failure	67
Table 5.12	Input data sheet for possible circular mode of failure	70
Table 5.13	Stability Condition of Slope having possible wedge mode of failure	71
Table 6.1	Safe slope Design angles for different height	78
Table 6.2	Recommended bolt number and separation of bolts for SL 6 slope section	79

Abstract

The hillside and road cuttings of most parts of the north, south and western regions of the Ethiopian Plateau have a record of instability in both the superficial materials and the bedrock. Landslide-generated problems claimed many lives and property damages in the country.

Landslide hazard zonation is a rapid technique of hazard assessment of the land surface. It is used to classify the land surface into zones of varying degree of hazard based on the estimated significance of causative factors which influence the stability of the land. Since the study area is extremely rugged and the variation in elevation is very large additionally landslide problems are common in the area. Hence the study of landslide and susceptibility zonation using LHEF is crucial. The geology of the area is dominated by sheared and discontinuous rhyolite, rhyolitic tuff, and doleritic intrusions which are liable to failure.

The "Landslide Hazard Evaluation Factor" (LHEF) rating scheme, is a numerical system which is based on major inherent causative factors of slope instability such as geology, slope morphometry, relative relief; land use and land cover and groundwater conditions. In the present study on the basis of Total Estimated Hazard (TEHD) of LHEF, three categories of landslide hazard zones have been identified. These are low hazard which occupies 12% of the total study area, moderate hazard (34%), and high hazard (54%).

Further, potentially unstable critical slopes have been identified from the High Hazard and Moderately Hazard zones. Later, detailed stability analyses have been carried out for potential unstable slopes using 'limit equilibrium method'. The stability analysis of critical slope sections has been carried out for static and dynamic conditions under varied water saturation situations. For the stability studies data pertaining to structural discontinuities, Geomechanics (RMR) rock mass classification system and the slope geometry were collected from the field. Later these data were used for the computation of Factor of safety. In addition soil samples were collected and analyzed for the index properties. From the study, it is found that some slope sections are unstable for anticipated worst conditions. Therefore, safe slope design has been worked out and remedial measures have also been suggested for these slope sections.

1.1 Problem Definition

The term landslide includes all varieties of mass movement from a hill slope and can be defined as the downward and outward movement of slope forming materials composed of rocks, soils, artificial fills or a combination of these. Although, landslides are primarily associated with mountainous terrains, they can also occur in areas of low relief especially, in surface excavations or highways, buildings and open pit mines (Legget, 1962). All type of landslides are associated with a movement of material constituting part of the earth's crust, movement caused fundamentally by gravity and taking place because of some inherent instability in the arrangement of the materials concerned.

Most of the landslides occur naturally; these may develop during the course of civil engineering work. Generally, landslides contribute to the erosion of parts of the earth's crust in which work is being carried out. In all cases, although the exact cause of the slide may be difficult to determine, they will be due to either one or a combination of several factors (Legget, 1962).

All types of landslides are dependent completely on the nature of the materials involved and on their relative arrangement. The major engineering aspects of landslides are related to geological phenomena. Therefore, a study of local geology is a satisfactory way of starting an investigation for landslides, either actual or incipient. In other word, on the local geology at the site of the slide. Therefore, it should be possible to anticipate many landslide if the necessary preliminary investigations are made, that to say, if the local geology is studied with unusual care. The fact that all too often such investigations are made after a landslide has occurred is probably the reason why the value of preliminary studies is not better appreciated. Natural landslides may affect the work of civil engineering in many ways.

In Ethiopia, the hillside and road cuttings of most parts of the north, south and western regions of the Ethiopian Plateau have records of instability in both the superficial materials and the bedrock (Ayalew, 1999).

In the past, landslides or landslide-generated problems have claimed about 300 lives, damaged over 100 km of asphalt road, demolished more than 200 dwelling houses and

devastated in excess of 500 ha of land in Ethiopia within seven years from 1992 to 1998. Almost 60% of the total population in Ethiopia lives in the highlands with an altitude of more than 1750 m. The mean annual rainfall in these regions exceeds 1200 mm and accounts for some 70% of the total precipitation the country receives each year (Ayalew, 1999).

1.2 Location and Accessibility

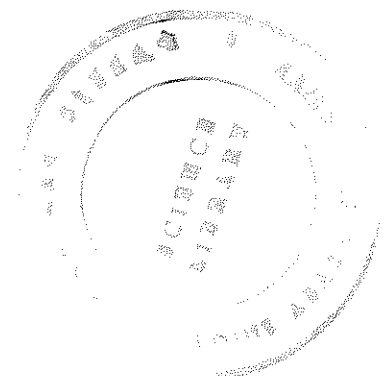
The project area lies in the Southern Nations, Nationalities and Peoples (SNNP) regional state in the central western margin of Main Ethiopian Rift. The area is about 280 km from Addis Ababa along Jimma road. It is by Oromia Administrative Region and by Gibe River in the western and eastern side respectively.

Geographically, the area is bounded by latitude of 7°45' and 7°52'N and longitude of 37°30' and 37°35' E. The study area falls in the Survey of Ethiopia Topographical sheet No. 0737 B1. The study area has a total surface area of 108 km² and project area falls within the Omo - Gibe River Basin (Fig. 1.1).

The project area can be accessed from Addis Ababa by road to Fofa town and the new road from Fofa to Gilgel-Gibe II Hydroelectric Power House. Access to many localities in the project area is difficult because of the undulating topographic relief. Most of the existing foot trails, as marked on the topographical sheet, are buried due to the construction of new road and road cut disposals.

1.3 Importance of the study

A landslide hazard zonation (LHZ) map is an important tool for designers, field engineers, and geologists. It is used to classify the land surface into zones of varying degree of hazard, based on the estimated significance of causative factors which influence the stability (Anbalagan, 1992). The LHZ map is a rapid technique of hazard assessment of the land surface. It is useful for the following purposes:



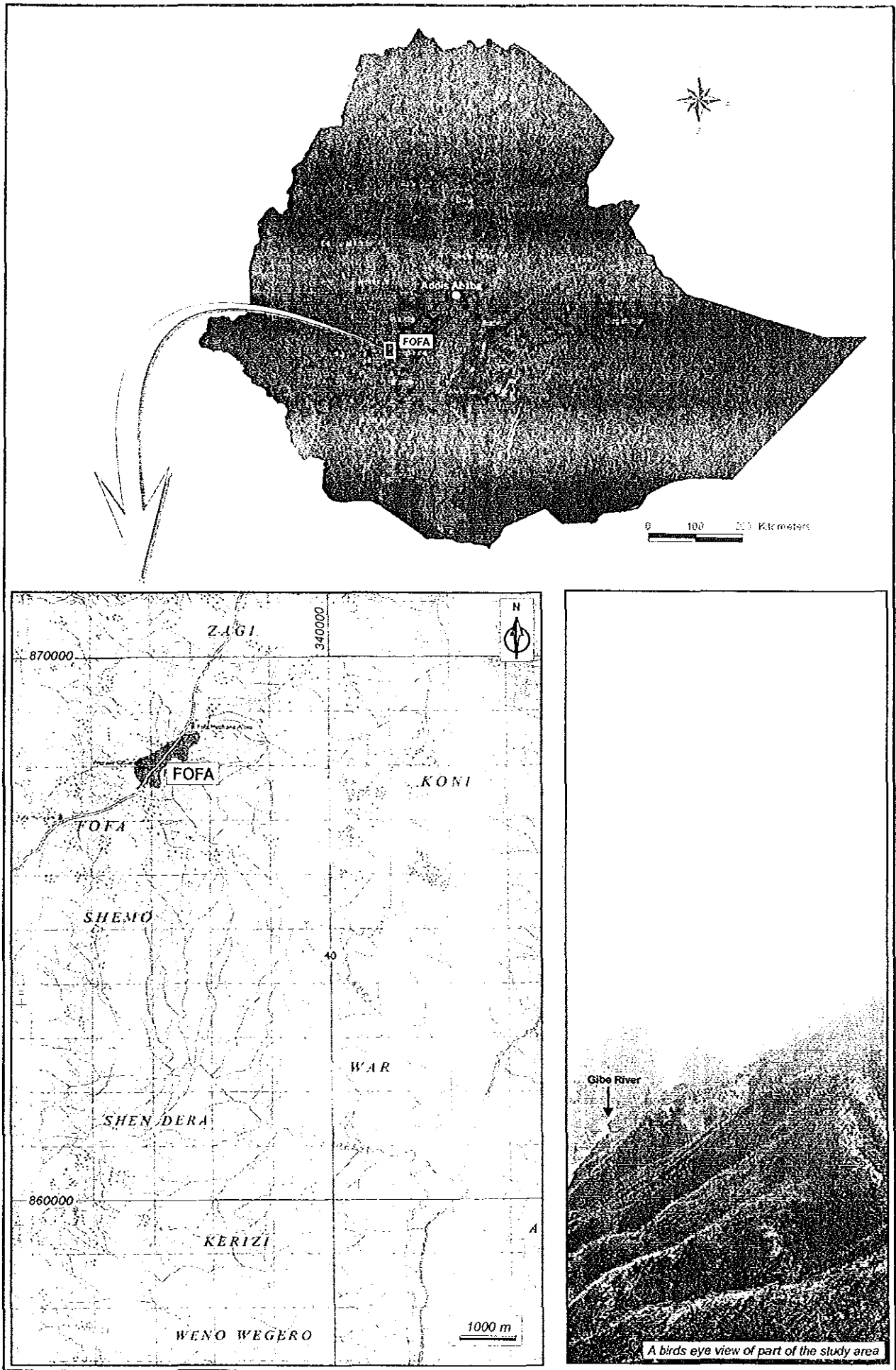


FIG. 1.1 Location map of the study area

- i) The LHZ map help the planners and field engineers to identify the hazard prone areas and therefore enable one to choose favorable locations for site development schemes. In case the site cannot be changed and it is hazardous, the zonation before construction helps to adopt proper precautionary measures to tackle the hazard problems.
- ii) These maps identify and delineate the hazardous area of instability for adopting proper remedial measure to tackle hazard problems.
- iii) Geotechnical monitoring of structures on the hill should be done specially in the hazardous area by preparing a contour map of displacement rates. Landslide control measures and construction control may be identified accordingly for the safety of building on the hilly areas.

Since, the project area is extremely rugged and the new road cut has higher economical importance therefore, this new road is the only access for the newly constructing hydropower project and for the future extension of the road to the nearest towns and villages. For this reason, the safe functioning of this road becomes more important for the safe and proper execution of the hydropower project and safe access to the nearby towns and villages. Keeping the above facts in mind the present study is planned to provide information on the landslide hazardous zones and proper remedial measures to prevent any serious damage to this new road.

1.4 Climate of the Area

The climate of the area is semiarid with temperature that may exceed 30°C. To workout the climatic conditions in the study area, data from Sekoru metrological station, which is about 25 km away from the study area, have been utilized. The precipitation and temperature data for the period 1989-2004, for Sekoru station has been collected from National Meteorological Service Agency. The analysis of this data reveals that the daily average temperature varies between 12°C to 28°C. However, the average annual temperature ranges between 13° to 6°C, with a maximum daily temperature variation recorded during the low rainy seasons, i.e. February to March and November to December.

The data indicates that the area has 1320 mm annual average precipitation. The highest monthly average precipitation recorded was 314 mm in July 1996. The precipitation graph (Fig. 1.2) shows that, there is only one distinct rainy season from June to August. The minimum monthly rainfall of 15.7mm was recorded in the month of December for all 25 years.

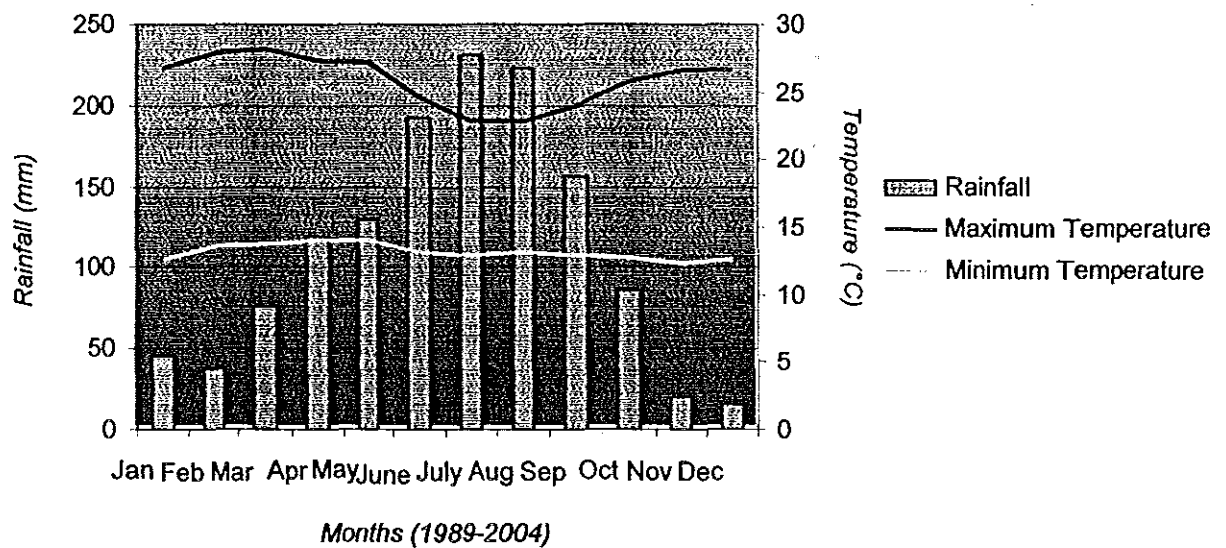


Fig. 1.2 Minimum and Maximum Temperature and Average Monthly Rainfall as observed at Sekoru Meteorological station (1989 -2004)

1.5 Physiography

The study area falls in the Yen Zone, which is found partly in the western margin of main Ethiopian rift, which is bordered by Gibe River in the eastern side. The area is extremely rugged and the variation in the elevation is very large. The maximum elevation in the project area is about 2640 meter near Fofa and the minimum elevation (920m) is found at the bed of Gibe River. Most of the streams flow along escarpments (Plate 6a). The study area is bounded in the eastern side by major escarpment along Gibe River which has similar orientation with main Ethiopian rift system in the eastern side of the river. Most of the escarpments are aligned parallel with two major tributary rivers, Derbu and Kora, for Gibe River. At the higher elevation area relative relief is moderate which lies between 101m to 300m. In these areas population density is high. Out of the total study area, around 75% of the area falls in high relative relief which is more than 300 m, which means the local relief of

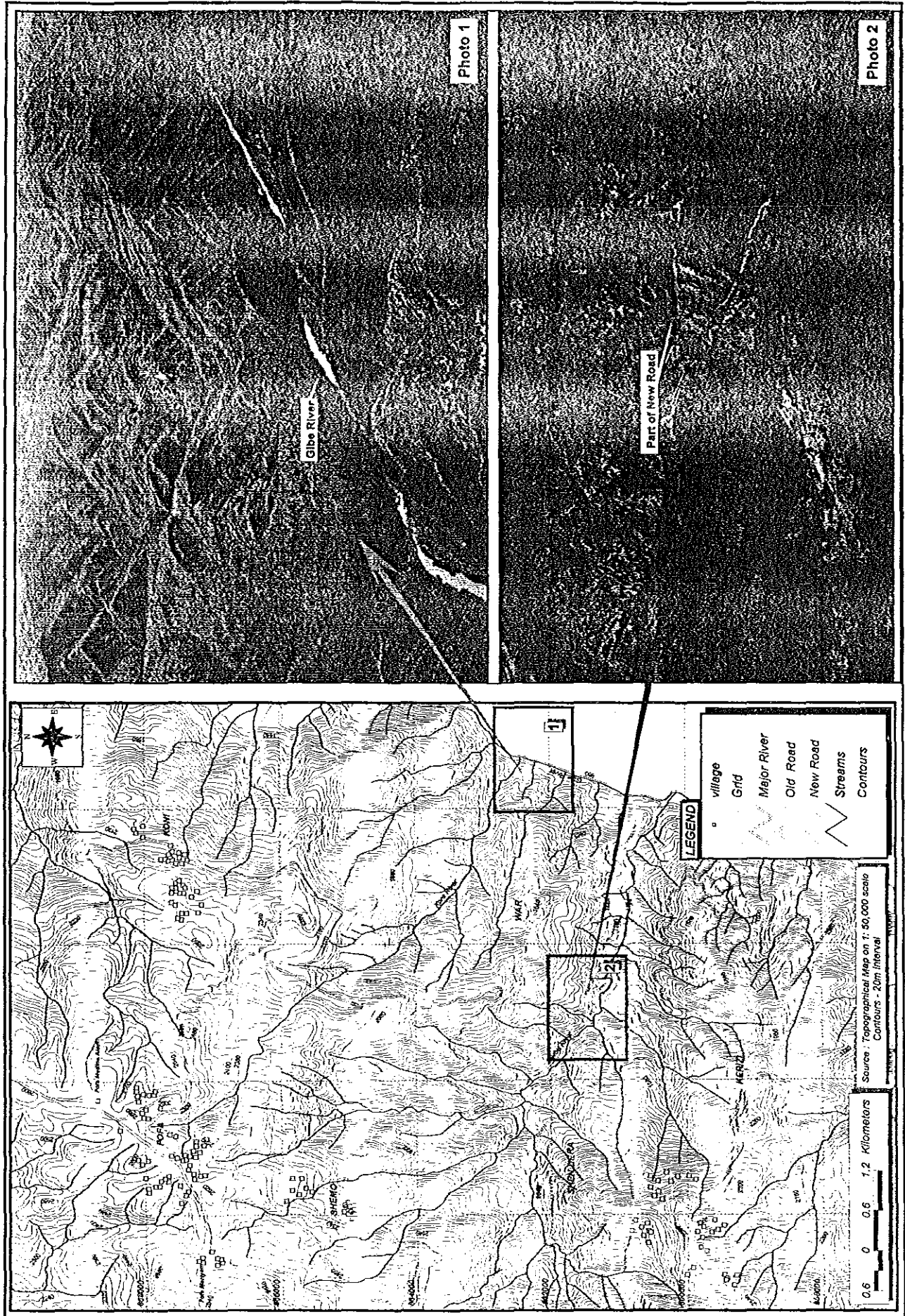


Fig. 1.3 General Topography of the project Area

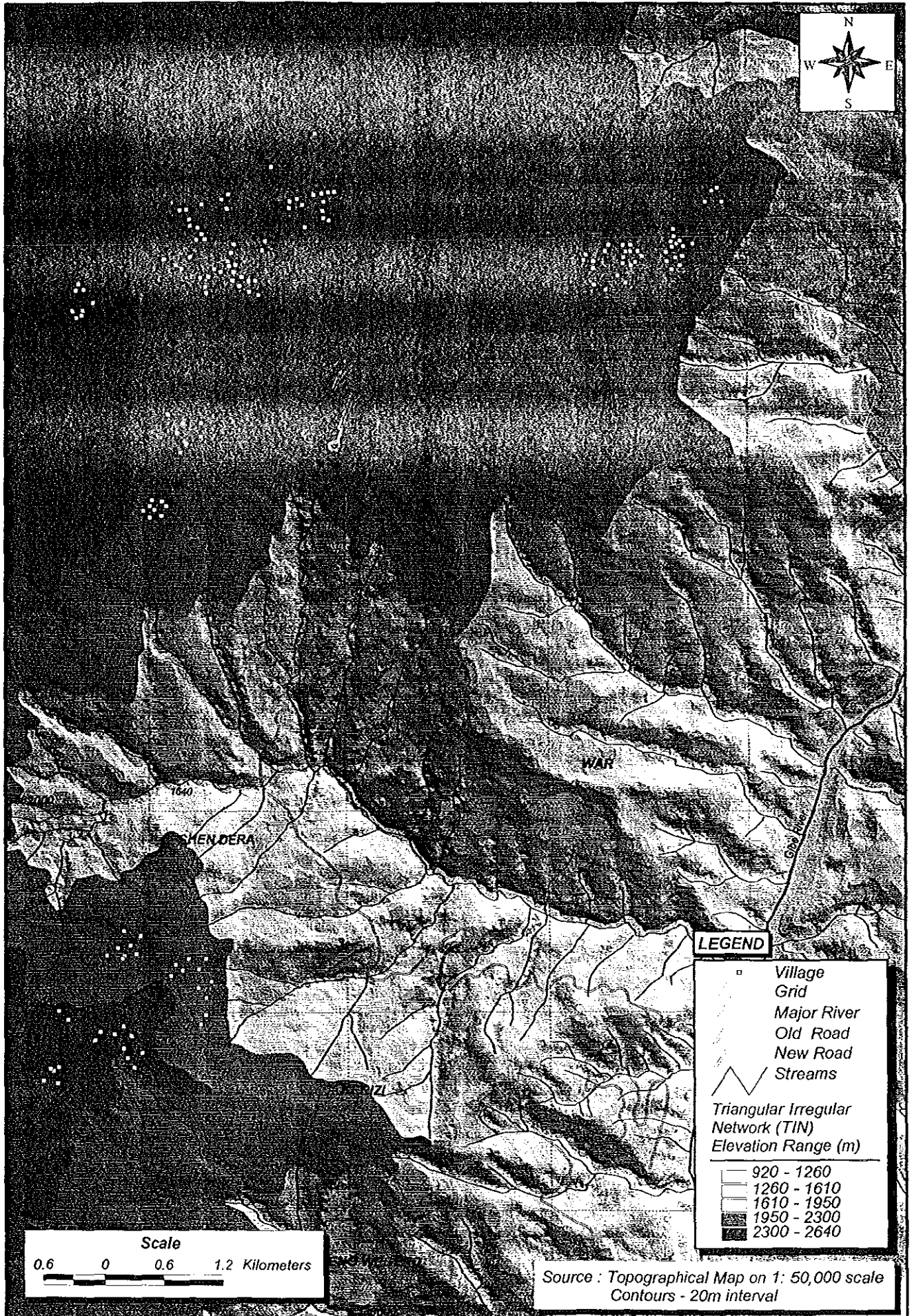


Fig. 1.3a Triangular Irregular Network (TIN) Model of the Area

maximum height between the ridge top and the valley floor within an individual facet is more than 300 meter (Fig.1.3 & fig.1.3a).

The drainage pattern of the project area is dendritic type and most of the tributary streams flows following structural weaknesses like fault and joints. The major tributaries of Gibe River are Derbu and Kora streams, which are dry in dry period but these are big rivers during rainy season.

1.6 Earthquake Activity (Siesmicity of the area)

The Omo River basin is bordered on the northeast by the Main Ethiopian Rift, on the southeast by the Chew Bahir rift systems and on the south by the Lake Turkana rift which extends northwards from Kenya into Ethiopia. These rift systems and adjacent escarpment bounded regions, are earthquake prone zones. Several earthquakes of magnitude greater than 4 have been documented within the project area during the period 1900-1993 (Gouin, 1979; Asfaw, 1990, 1992. AAU, Geophysical Observatory, 1995). List of earthquake events recorded between 1900-1993 for the region between latitudes 40 N and 100 N, and longitudes 350 E and 400 E is presented at Annexure I. Most of these earthquakes are associated with the Lake Turkana, Chew Bahir and Main Ethiopian rift systems. Figure 1.4 shows seismic risk map of Ethiopia.

Six earthquakes of magnitude greater than 4.5 have been recorded in the Omo-Gibe River basin, three of them being within the Turkana rift and three of them centered in the highland Quaternary volcanics. Outside the Project area, three have been recorded in northern Kenya, just south of the basin within the southern extension of the Lake Turkana and Chew Bahir rift systems, and several more have been registered in nearby regions southeast and northeast of the Project area associated with the chew Bahir and Main Ethiopian Rift systems. Main centers of seismic activity related to these earthquake events plot mainly along the eastern margin of the Tukana rift and the western margin of the Chew Bahir rift. No earthquake activity has been recorded in the basin area west and northwest of the Omo River.

The earthquakes in the region are exclusively related to the major rift structures. The earthquake data available suggests that the Main Ethiopian and Chew Bahir rift systems are probably more seismically active than the Turkana rift system. However, the Turkana rift itself is seismically active, and this is confirmed by recent earthquake events recorded (Gouin,

1979). This indicates the necessity of conducting a closer study of seismic risks to large scale construction projects that may be contemplated on being executed in the region (dam construction sites, large bridges, etc.)

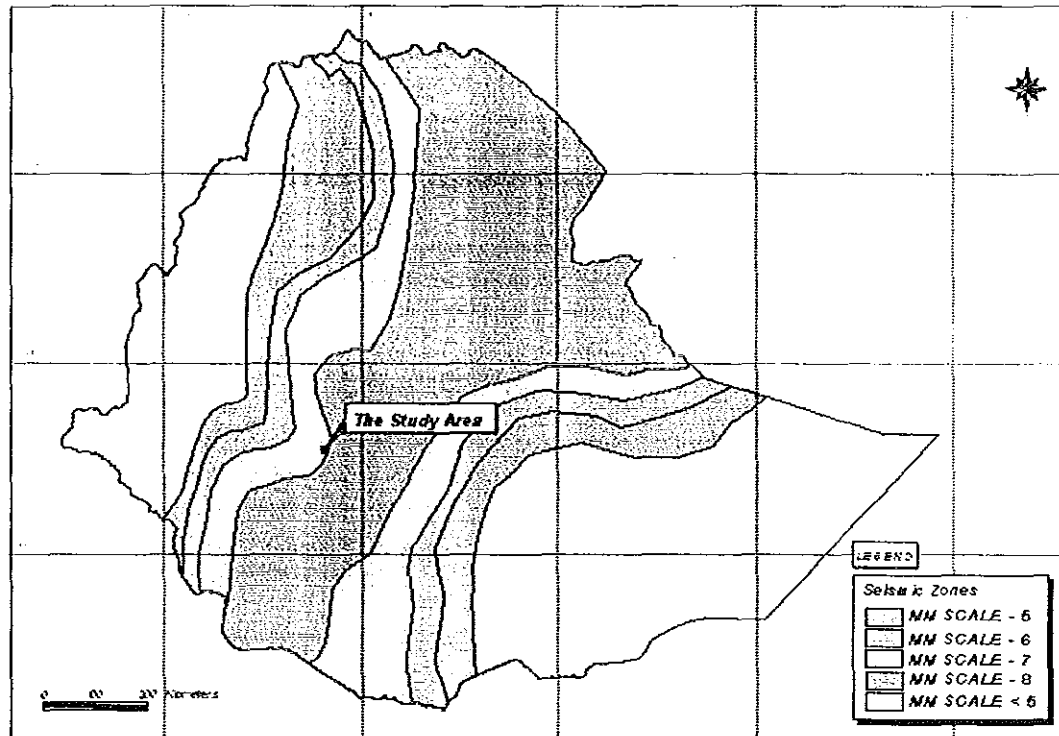


Fig 1.4 Seismic risk map of Ethiopia 100 years return period, 0.99 probability.

(After LaikeMariam Asfaw, 1986)

1.7 Previous works

A systematic regional geological mapping and mineral exploration programme was undertaken in South-Western Ethiopia between 1972 and 1974 under an Ethiopian - Canadian co-operation agreement (the Omo River Project, Davidson et al., 1973, 1976, 1983) by Ethio-Canadian teams. Prior to this period, very little was known about the geology of the region. Kazmin (1971, 1972, 1975a, 1975b 1978, 1979) proposed the first stratigraphic subdivision and tectonic synthesis of the Precambrian rocks of Ethiopia, and interpreted the geology of Western and South-Western Ethiopia in light of plate tectonic considerations.

Giday et al. (1992) describe the geology and the major structural settings of central sector of main Ethiopian rift and adjacent areas in his paper of rift basin development along main Ethiopian Rift. Giday et al. describes Guraghe section, which is the North East margin of the

present study area, in terms of geology, major structures, volcanic flow history and stratigraphic sequence. Stratigraphic successions of various sections along the rift margin and the adjacent rift shoulders, cross rift structural relationships and age of rifting are also described.

Lulseged A. (2001) studied the weathered rock mass characterization of Gilgel-Gibe area based on engineering geological parameters. He also describes geology and the effect of weathering on reduction of strength in rockmass. In his engineering geological study he describes the source of uncertainty in design and construction of engineering structures using statistical approach to handle geological parameters. This study was done in the west margin of this study area.

The recent study conducted by the Ethiopian Electric power corporation (EEPCO) near Gibe River area is the geological study for the purpose of tunnel excavation for Gilgel-Gibe II hydroelectric power project. The geology, geotechnical and petrographic characteristics of different rocks in the area along the tunnel alignment have been studied in details. The relevant data generated through this study has been utilized for the present study (EEPCO, 2004).

1.8 Objective

1.8.1 General objective

This present research work, in general, is aimed to achieve the following objectives:

- i) To prepare landslide hazard zonation map using LHEF technique based on different causative factors.
- ii) To workout the slope stability conditions for existing and possible worst conditions along the road cut from Fofa to Gilgelgibe II power house.
- iii) To find out suitable remedial measures for the stabilization of unstable slopes sections along the road cut.

1.8.2 Specific objective

- i) To prepare maps for different landslide causative factors including facet map, slope map, relief map, lithological map, structural map, landuse and land cover map of the study area.
- ii) Based on LHZ mapping identification of critical slope sections within Very high hazard and high hazard zones.
- iii) To prepare the geological cross sections along potentially unstable slope sections.
- iv) To determine the shear strength properties of the rock mass.
- v) To identify the possible kinematic mode of failure.
- vi) To determine the stability condition based on limit equilibrium method for static and dynamic ground conditions under varying water saturation Conditions, representing existing and possible worst conditions.
- vii) Based on the results of factor of safety to work out possible remedial measures for the slope stabilization.

1.9 Approach and Methodology

The following systematic methodology have been employed to achieve the objectives for the present study:

- i) Literature review on geology, structure, geomorphology, hydrology, and engineering geology of the Yem Zone from both published and unpublished reports, maps and journals.
- ii) Preparation of different types of base maps like facet map, topographic map, geological map of the study area and structures available from previous work and to refine the maps by undertaking fieldwork.
- iii) To acquire good understanding of the hydrological and climatical conditions of the area, hydro-meteorological data of the area has been collected and compiled.
- iv) After evaluating the compiled data, additional actual data has been collected from the field to fill the gap between the available and the required data. The field investigations have been concentrated on geological, structural, and geotechnical mapping, sampling and insitu measurements.

- v) To determine the geotechnical properties of the rocks in the study area, laboratory analysis has been conducted on samples.
- vi) After compilation of the actual field observations and the analyzed results, the data has been systematically grouped and analyzed using available techniques and computer programmes.
- vii) Interpretation of the results has been made in-view of the objective of the research and a draft of the thesis has been prepared.
- viii) Based on the result, conclusion and recommendations have been drawn.

1.10 Limitations of the study

The present study has been conducted with all positive efforts and sufficient technical inputs in the form of actual field data collection, analysis and technical interpretation. However, this study has certain limitations which are highlighted below;

1. The physiography of the area is highly rugged and the access to various locations is difficult. Most of the existing foot trails, as marked on the topographical sheet are buried due to the new road construction and road cut disposals.
2. Lack of sufficient existing data related to the present study.
3. Limitation of time and financial constraint to workout the present study.
4. The absence of related references for the present study.

1.11 Proposed outcome of the study

In general, this work may contribute to the understanding of the slope stability conditions of the area. The LHZ map prepared for the present study area will help planners and field engineers to identify hazard prone areas thus, enable them to identify potentially unstable zones along the existing new road. This will help planners in adopting proper remedial measure to tackle hazard problems along critical sections. Moreover, the present study will also provide recommendations on proper remedial measures in the form of safe slope design, rock slope support and retaining structures for the probable critical sections along the existing new road.

2.1 General

When planning a new development there can be several objectives. For example, promotion of accessibility to homes and other urban facilities, efficient use of resources, zoning of activities into those with compatible landuse and ensuring that the development is pleasant (Keeble, 1964)

It is difficult to achieve these objectives without considering the factor of the physical condition of ground or in other words, geological and geotechnical factors. To fulfill these objectives, attempts have been made towards classification of terrain systems and preparation of engineering geology and hazard maps on the basis of a combination of geological, geomorphological parameters with landslide and using them in the rating system.

The landslide hazard evaluation factor (LHEF) rating scheme is based on an empirical approach which combines past experience gained from the study of causative factors and their impact on landslides with conditions anticipated in the area of study.

The LHEF rating scheme is a numerical system which is based on major inherent causative factors of slope instability such as geology, slope morphometry, relative relief, landuse and land cover and ground water conditions. Factors like rainfall and seismicity are not included for the purpose of landslide hazard zonation mapping.

2.2 Literature review

For landslide hazard zonation mapping, different researchers apply different schemes based on different causative factors. Specially, in the case of slope cut and underground mining activities, the hazard or failure zones identification schemes have been developing for over 100 years since Ritter (1879) attempted to formalize an empirical approach to tunnel design, particularly for determination of support requirements. While the classification schemes are appropriate for their original application especially, if used within the bounds of the case histories from which they were developed, considerable caution must be exercised in applying rock mass classifications to other rock engineering problems. Different classification systems place different emphases on the various Parameters. Most of the multi- parameters

classification schemes were developed from civil engineering case histories in which all of the components of the engineering geological character of rock mass were included.

Terzaghi (1946) classify rock mass, based on those characteristics that dominate rock mass behavior, particularly in situations where gravity constitutes the dominant driving force. He gave clear and concise definitions for the terms like, intact rock, stratified rock, moderately jointed, blocky and seamy, crushed rock, squeezing and swelling rock.

Wickham et al., (1972) described a quantitative method for describing the quality of a rock mass and for selecting appropriate support on the basis of their Rock Structure Rating (*RSR*) classification. The significance of the *RSR* system is that it introduced the concept of rating on each of the three components, Geology, Geometry and effect of groundwater inflow on joint condition.

• Bieniawski (1976) introduced a rock mass classification system called the Geomechanics Classification or the Rock Mass Rating (*RMR*) system. In applying this classification system, the rock mass is divided into number of structural regions and each region is classified, separately. The *RMR* system requires, assigning rating for each of the six parameters like: Uniaxial compressive strength of rock material (*UCS*), Rock Quality Designation (*RQD*), Spacing of discontinuities, Condition of discontinuities, Groundwater conditions and Orientation of discontinuities. Sum of these ratings gives *RMR*, based on which the quality of rock mass can be defined. Further, *RMR* may also be utilized to determine the shear strength parameters of the rock mass and the deformability character of the rock mass.

Barton et al., (1974) of the Norwegian Geotechnical Institute proposed a Tunneling Quality Index (*Q*) for the determination of rock mass characteristics and tunnel support requirements on the basis of an evaluation of a large number of case histories of underground excavations. Barton uses six parameters and gave rating for each parameter, these parameters are the rock quality designation, joint set number, joint roughness number, joint alteration number, joint water reduction factor and stress reduction factor.

Romana (1985) introduced slope Mass Rating (*SMR*) as an application of Rock mass Rating (*RMR*) of Beniawski (1979). It takes into consideration the parameters such as attitudes of discontinuities, disposition of slope failure modes as well as slope excavation methods. This approach only accounts for plane and toppling mode of failures. For wedge failure it is

suggested that the different planes, forming the wedge should be analyzed, separately. However, Anbalagan et al., (1992) has modified the approach of Romana (1985) and generalized it to incorporate wedge mode of failure. In the modified SMR approach the line of intersection of two wedge forming planes is considered and accordingly new ratings were assigned.

In recent years, a vast change has taken place in the use of computer software to handle geographic data (Tomlinson, 1976). Geographical information system (GIS) have been defined as a powerful set of tools for collecting, storing, retrieving, transferring and displaying spatial data from the real world for a particular set of purpose. GIS based landslide hazard zonation mapping is the easy way of handling different causative factors for landslide (Gupta et al, 2000).

RMR and Q-systems are originally designed for tunnel excavation geotechnical studies and support requirements. Both methods are applied for specific zone of excavation or they may need more time and money to apply for large area coverage studies like landslide hazard zonation mapping.

Considering the above limitations for stability studies, LHEF scheme is selected for this study because of its advantage to handle different causative factors for evaluation of landslide hazard, easily and quickly, without any computer knowledge. LHEF scheme can cover large area of study by considering the most important geological factors and rating them based on their influence on landslide.

2.3 Methodology for LHEF rating scheme

The landslide hazard zonation (LHZ) mapping is a macro zonation approach showing the probability of landslide hazards. The LHZ maps are generally prepared on 1:25000 to 1:50000 scales. The LHZ mapping comprises mainly two components; desk study and field investigation. The desk study consists of preparation of prefield maps showing the status of causative factors in the study area with the help of aerial photographs, satellite imageries topographic maps and geological maps. The prefield maps, lithological map, structural map, slope morphometry map, relative relief map, rock outcrop and soil cover map, and land use land cover map, are prepared. The information collected from the desk study helps to plan and execute the field investigation, systematically. During the field study, more detailed

lithological and structural maps can be prepared .Further; the desk study can be verified in the field and modified wherever necessary.

The field study is carried out to collect the required data, *facet- wise*, for estimating the total hazards of the facets. A facet is a part of hill slope which has more or less similar characteristics of slope showing consistent slope direction and inclination. The facet boundaries are ridges, spurs, streams, and rivers. The facet map is the base map for the LHEF scheme. Thus, for the present study the facet map was prepared and according to the LHEF rating scheme various other thematic maps were prepared utilizing the facet map as base map.

3.1 Regional Geological Setting

The study area is found in Omo-Gibe river basin which is one of the largest basins in south west Ethiopia. The geology of the Omo-Gibe river basin comprises of Precambrian crystalline basement, Eocene to Miocene volcanic rocks and Quaternary lacustrine and alluvial sediments and volcanic flows (Davidson, 1983).

The crystalline basement comprised of high grade metamorphic rocks consisting of upper amphibolite facies, ortho and para- gneisses, migmatites and granulites. These include a complex of northwest trending, strongly deformed, recrystallized and migmatized gneisses, such as hornblende, biotite- hornblende, biotite, quartzo-feldspatic, garnet-augite, hypertine, garnet-sillimenite and calcsilicate gneisses and marble.

The main marine incursion into the Ethiopian region from the east and northeast that resulted in the formation of Mesozoic sediments, in much of the eastern and central Ethiopia, between Triassic and Jurassic times does not extend into the Project area. This is evident, from the absence of Mesozoic marine sediments in past and present geological mapping programmes conducted in the region. Hence, in the Project area, Tertiary volcanic rocks rest directly on the Precambrian crystalline basement.

The crystalline basement rocks mainly outcrop in the southern half of the Omo-Gibe River basin.

In the Omo river canyon more than 1.2 Km of thick volcanic rocks and sedimentary strata are exposed along two fault scarps. The volcanic rocks along the eastern canyon wall are dominated by mid -Miocene rhyolite, trachyte, basalt, and Pliocene vitric tuff in ascending order (Woldegebriel and Aronson, 1987). The chemistry of the vitric tuff in the Motti tuff at east Turkana , Kenya (Cerling and Brown,1985) , with an age of $4.10 \pm 0.07\text{My}$ (Mcdougall,1985). Preceding both south-southwest, and north of the Omo canyon, Eocene to Oligocene ages have been previously reported on flood basalts and rhyolite flow (Davidson and Rex, 1980).

The lack of exposure of these widespread paliogine flood basalt at Omo canyon despite an elevation lower than the floor of the MER is likely due to burial and is consistent with a

hypothesis that Omo canyon is an ancestral, now failed rift valley (Giday and Aronson, 1987). For convenience of description of the Cenozoic geology of the Omo-Gibe River basin in southwestern Ethiopia, Davidson (1983) has sub-divided it into two major groups of rocks as;

1. The "pre-rift succession", Eocene to mid Miocene in age, and
2. The "post-rift succession", late Miocene to Holocene in age.

Volcanism in southwest Ethiopia commenced as early as the Eocene. The hypabyssal phonolites and related intrusions and flows, emplaced before the formation of major rift topography, are middle Miocene in age (Davidson and Rex, 1980). This succession is referred to as the "pre-rift succession". The location of volcanic and sedimentary rocks deposited after this time is controlled by the topography that was formed as a result of major rifting and its accompanying erosion, and the rocks formed during this period are referred to as the "post-rift succession".

The age of the pre-rift succession in the present Project area ranges from late Eocene to middle Miocene in age and underlies approximately 70% of the area. The post-rift succession covers approximately 20% of the Project area and underlies mainly the Lake Turkana rift floor in the southern part of the area and the edge of the western escarpment of the main Ethiopian Rift Valley.

The Regional Geological Map of the area is shown as Fig. 3.1. and the geological succession is presented as table 3.1.

3.1.1 *Pre-rift Succession*

The major rock units consisting the pre-rift succession are described separately in the following section :

3.1.1.1 Basal Red Sandstone

In the south-western and north-eastern parts of the Omo-Gibe basin, the Precambrian crystalline basement is separated from the overlying Tertiary volcanic succession by a 6 to 8m thick unit comprised of red sandstone and conglomerate (Davidson, et al., 1973, 1976, 1983). The unit is devoid of any fossils and sedimentary structures and is poorly sorted and moderately to poorly

cemented. These features suggest that the unit is non-marine in origin, and in all likelihood represents slightly re-worked laterized basement gneiss material deposited on peneplained

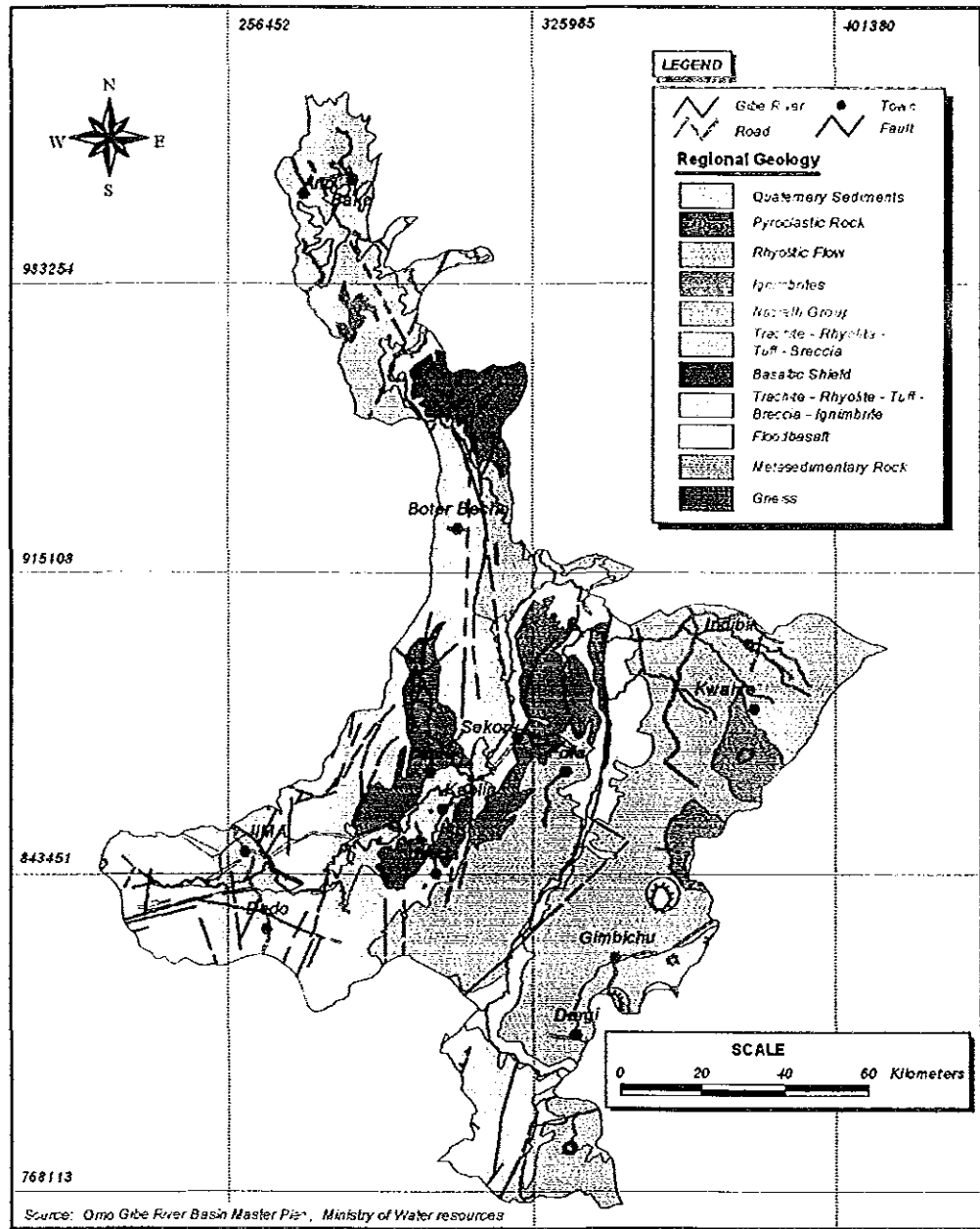


Fig. 3.1 Regional Geological Map of Omo- Gibe sub-basin

crystalline basement surface with little transport from source. Its absolute age has not been determined.

3.1.1.2 Early Flood Basalts

Basalts represent the thickest and most widespread rock type of the Tertiary volcanic sequence in the Omo-Gibe river basin. The early flood basalts are products of fissure eruptions, and are characterized by thin, extensive flows, locally columnar and with jointing parallel to flow layering. The basalts overlie the red basal sandstone already described above, and where the sandstone is missing, directly rest on the Precambrian basement. The main occurrences of this unit is in three separate areas in the basin, namely in the south-western, south-eastern and along the north-eastern parts of the Omo River valley.

The flood basalts are mostly soft weathering, consequently giving rise to a subdued topography in their areas of occurrence. They are either aphyric or porphyritic, containing olivine or plagioclase phenocrysts or both. Pyroxene-phyric basalts are less common. Amygdales containing zeolites, calcite and chalcedony are present in places.

3.1.1.3 Salic, Basaltic, and Intermediate Flows and Pyroclastic Rocks

In the south-western segment of Omo-gibe basin, a map unit containing intercalated basaltic, intermediate, and salic volcanic rocks has been mapped (Davidson et al., 1976). In this area, the early flood basalts are separated from the overlying thick salic lavas and pyroclastic rocks with minor intercalated basalt flows of the Tertiary volcanic sequence by a zone of mixed rocks containing intercalated resistant salic rocks and less resistant basaltic and intermediate flows. The intermediate rocks in this unit are massive, medium grey and plagioclase-phyric, with a notably lower groundmass color index than basalt, and are probably andesitic in composition.

3.1.1.4 Trachyte, Rhyolite, Tuff, Breccia, Ignimbrite and Intercalated Basalt

Salic volcanic rocks occupy a dominant portion of the Tertiary volcanic succession within the Project area. A thick succession of salic volcanic flows, pyroclastic rocks and subordinate intercalated basalt flows dominate the upper portion of the pre-rift volcanic succession. A significant part of the Omo-Gibe basin stretching from far north to the south is occupied by trachyte and rhyolite flows and pyroclastic rocks such as tuff, ignimbrite, and breccia with subordinate basalt flows, forming north and north-east trending zones. Basalt flows are present in parts of these predominantly salic sequences, just as salic flows occur within the flood basalts.

Table 3.1 Geological Succession of Omo-Gibe sub-basin

Period	Epoch	Rock type	Approximate age in Millions of years Before present
Quaternary- Tertiary	Holocene	-Fluviatile sand, silt -Lacustrine silt, clay -Alluvium	0.01
	Pleistocene-Holocene	- Trachyte, ash, & tuff - Basalt Flows - Undivided alluvial - fluviatile sediments - Fluviatile sand, silt - Lacustrine silt, clay - Alluvium	1.6
	Pliocene-Pleistocene	- Undivided - Sediments -Lacustrine sediments - Rhyolitic & trachytic lava flows - Ignimbrites	5.3
	Miocene	Nazareth Group : (Trachyte, rhyolite, ignimbrite, tuff & basalt flows) - Plugs & dykes of felsite phonolite, trachyte & granite -Trachyte, ignimbrite & phonolite - Surma basalt	23.7
	Oligocene-Miocene	- Makonnen Basalt - Trachyte, rhyolite, tuff, breccia ignimbrite & intercalated basalt - Salic, intermediate & basaltic flows & pyroclastic rocks	36.6
	Eocene-Oligocene	- Early flood basalt with minor intercalated trachyte, rhyolite ignimbrite & tuff	57.8
Archean Proterozoic	Precambrian Basement Rock	- Late tectonic granite -Syntectonic granite, granodiorite gabbroic gneiss	2500
		- Strongly lineated granitoid - orthogneiss - Cataclastic gneiss, - metasedimentary gneiss, amphibolite - muscovite-biotite granitoid gneiss & migmatite - biotite-quartz-feldspar gneiss	--

The salic flows (trachyte and rhyolite) in most parts are highly weathered to white, buff-brown or pink-brown colored rocks. They are well layered on millimeter scale in many places and massive in others, with layering inclined up to 30°NE or SW.

Rhyolite with both quartz and alkali feldspar phenocrysts is common. The basalts are commonly fresh and are either aphyric or porphyritic containing olivine or plagioclase phenocrysts or both.

Because the salic rocks and pyroclastic rocks are intensively weathered, the basalts are commonly quarried for building purposes. The salic and pyroclastic rocks are commonly used as road aggregates. Tuffs, ignimbrites, breccias, and volcanic agglomerates made up of mainly salic fragments are inter-layered with salic flows.

3.1.1.5 Mekonnen Basalt

This unit comprises up to 800m thick sub-horizontal flood basalts forming the high plateau of the Baro-Akobo River Basin (Davidson, 1983). The map unit mostly lies on the Precambrian crystalline basement rocks in the type area. K-Ar age dating has yielded an age range of 38.8-23.1 My, i.e. late Oligocene to early Miocene (Davidson and Rex, 1979; Davidson, 1983). The unit extends into the western part of the surveyed area, although it is difficult to mark its most western limit because of dense forest cover. The rocks are usually columnarly jointed, aphyric or porphyritic with plagioclase and olivine phenocrysts.

The extreme northern part of the Project area between Bako and Gedo towns is underlain by intercalated porphyritic basalt with phenocrysts of olivine and pyroxene, aphyritic-aphyric basalt and minor white weathering porphyritic trachyte. The basalts are locally amygdaloidal with fillings of chalcedony and chlorite.

3.1.2 The Post-Rift Succession

The major map units in the post- and syn-rift succession in the Project area include:

3.1.2.1 Nazreth Group, Rhyolitic, Trachytic Flows, and Ignimbrites

The name Nazreth Group is assigned to a thick succession of fiamme ignimbrite, pumice, trachyte, ash and rhyolitic flows and domes with minor intercalations of basalt flows which occur in the Main Ethiopian Rift floor, escarpments and adjacent plateau margins (Kazmin, 1979, Kazmin et al., 1978, 1981). The Nazreth Group rocks underlie the north-eastern border of the surveyed area. An age of 10-3 My has been assigned to these rocks (Kazmin and Seife M., 1978).

The rocks are interlayered on meter scale and show the feature of stratification of sedimentary rocks on aerial photographs. They lie unconformably on the early flood basalts with basalts

forming basal unit. The dominant rock type of the unit is trachyte containing feldspar phenocrysts (sanidine). Color generally ranges from light-pink to violet-grey. Porphyritic texture is common exhibiting flow alignment, and the ground mass is finely crystalline. Rhyolite intercalations with both quartz and alkali feldspar phenocrysts are common. The basalts are usually fresh. They are either aphyric or porphyritic with olivine, pyroxene and plagioclase phenocrysts. Ignimbrites and tuffs made up of mainly felsic fragments, and feldspar crystals are intercalated with the salic flows. The thickness of the unit reaches up to 200m and increases as the salic extrusive centers are approached.

Accumulation of the Nazareth Group rocks was accompanied by the formation of shield volcanoes on the western and eastern rift shoulders (Kazmin and Seife M, 1978; Kazmin et al., 1980). These are complex shield volcanoes of Pliocene age which developed on both sides of the rift shoulders and margins of the Main Ethiopian Rift. The clusters of central volcanic complexes show distinct NNE alignment. Some of these centers such as Teza, Ambricho, Wagebessa and Tembero mountains more or less lie on a line possibly indicating formations along a major fault trend. These centers straddle the boundary between the Omo-Gibe and the Rift Valley drainage systems, and are comprised of interlayered per-alkaline ignimbrites and trachytes showing flow structures. The dominant rock type is a highly porphyritic, dark grey trachyte with sanidine phenocrysts. The age of most of these volcanoes range from 3-4.5 My (Kazmin, Seife M. and Walsh, 1980).

3.1.2.2 Omo Group

The "Omo Beds" (Shungura Formation) are particularly famous among anthropological circles for the discoveries made within them of some of the world's oldest hominid fossil remains.

The Omo Group has been sub-divided into four formations (Davidson, 1983). These are; i) the Mursi Formation, ii) the Nkalabong Formation, iii) the Usno Formation and iv) the Shungura Formation.

The Mursi Formation is comprised of a lower sedimentary unit (NPom1) and an upper flood basalt. The lower sedimentary unit is exposed on the west side of the southern part of the Nkalabong range. It lies unconformably on the pre-rift succession, and is composed of

approximately 150 m of clays, silts and sands with minor tuff and pebble beds. The sediments are conformably overlain by flood basalt which is about 100 m thick and have been dated at 4.2 My (Fitch & Miller, 1976; Brown and Nash, 1976). The Mursi basalt is comprised of a few, thin, columnar flows of dark grey basalt, which is locally porphyritic with scattered phenocrysts of plagioclase and amygdales of chlorite.

The Nkalabong Formation occurs in its type area at the south-western end of the Nkalabong range and it is about 90 m thick. It is composed of grey to brown fluvial clastic sediments overlain by eolian sands, waterlain tuffs and tuffaceous sediments. It lies on weathered and faulted Mursi basalt. An age of 3.95 My has been obtained from the top part of the Formations (Fitch and Miller, 1969).

The Usno Formation is comprised of a minimum of 200 m of intercalating fluvial and lacustrine sediments with thin tuff horizons. An absolute age of 2.97 My is the most reliable age determined for the Usno Formation (Brown and Nash, 1976).

The Shungura Formation occurs along the west side of the Omo River comprises of a minimum of 760 m of clays, silts, sands, gravels, tuffs, marls and limestone. These sediments are inclined gently to the west and are overlain with shallow unconformity, by the Kibish formation. An age range of about 3-1.3 My has been reported for this unit (Brown and Nash, 1976).

3.1.2.3 Basalt Flows, Trachyte, Ash & Tuff

In the Baro-Akobo River basin a large tract of territory covered by shield basalt flows named as the Tepi basalt (Davidson et al., 1976, 1983) lying across the eroded unconformity between the Precambrian crystalline basement and the pre-rift volcanic succession. This unit extends from the west in the Baro-Akobo basin into the currently surveyed area. Basaltic lavas have flowed down pre-existing low topographies, and streams occupy new courses along the edges of these lava flows. The basalt of this unit forms columnar flows and is dark grey and vesicular. It is commonly porphyritic containing phenocrysts of olivine, augite and plagioclase.

In the northern part of the Project area, northwest of and around Weliso town, another large area made up of basaltic shield showing recent topographic features occurs. The area is composed of mainly basalt flows that have spread outwards from central volcanic complexes. This is usually

porphyritic with large phenocrysts of pyroxene, olivine and plagioclase, locally columnar and vesicular filled with zeolite and chalcedony. It lies on Nazreth Group rocks.

3.1.2.4 Holocene Sediment Deposits

An extensive area of Quaternary sedimentation occurs at the northwestern end of the Project area along the upper reaches of the Gibe River. Some relatively narrow grabens in the western part of the surveyed area are blanketed by recent unconsolidated alluvial sediments. The extensive area between Jimma and Sokoru is also covered by both recent alluvial sediments on which reddish brown soil, up to 10 m thick, has developed on the bed rock on both sides of the sediment deposits. The alluvial deposits occur along the Gilgel-Gibe River course and are mainly represented by sand, silt and clay. The soils are mainly reddish-brown and rarely are they black cotton soils. Figure 3.1 shows regional geology around the study area.

3.2 Geology of the area

The local geology is dominantly composed of Nazreth group rocks. A large tract of land stretching from south of Weliso to Welkite-Hosaina-Sodo and SelamBer and the adjacent plateau margin west of Omo River is underlain by a sequence of stratoid salic rocks, trachyte, rhyolite, ignimbrite and tuff with minor intercalated basalt flows characteristically containing lacustrine sediment deposits. An age of 9 to 3 Ma has been given to the Nazreth series on the basis of its relation to the Omo Mio-Pliocene lacustrine sediment of the Chorora Formation and some absolute K/Ar age determinations (Tierrcelin et al; 1980; Kazmin and Berhe, 1978). The Ignimbrite Unit is found just out of the project area boundary in the western side. The Basaltic rock Unit outcrops at the bed of Gibe river but its age is uncertain may be it has similar age with fault of Omo Formation or Welega Formation (EEPCO, 2004). The Jimma Volcanics which are considered analogous with the main volcanic sequence of Davidson (1983) form a thick succession of basalts and felsic rocks with basalt dominating the lower part of most sections. Davidson (1983) has reported K/Ar age of 42.7 to 30.5 Ma for Jimma volcanics.

Two units (Jimma Basalt and Jimma Rhyolites) which show a conformable relationship were identified. The Jimma Rhyolites being the younger of the two units in south western Ethiopia are equivalent to Maqdala Group of Kazmin (1972). The Jimma Volcanics almost always rest on the Precambrian Basement, the unconformity being marked by Basal residual Sandstone.

The Jimma Rhyolite in the study area is excessively intruded with dykes and sills which makes the geology extremely complex. The rhyolite has variable color including pink, white and yellow rhyolite. Figure 3.2 shows the Geological map of the study area.

The major dominating intercalated rock type in rhyolite is trachyte, and this unit is found in the rhyolite unit, just below rhyolitic tuff layer. The trachytic bed is not mappable.

3.2.1 Rhyolitic Tuff

The rhyolitic tuff unit is found in the upper reaches of the study area, this unit is the youngest formation of the study area. This is not well welded and is very weak, almost like loose soil mass. It is easily scratched with the thumb. This unit comprises of two types of tuff based on their color, one white tuff and other is red colored tuff. The red tuff is the parent material for the red clay soil and is well exposed near Fofa town.

From thin section analysis this rock shows a vitrophyric texture with vitreous fragments arranged as stripes weakly flattened, and not welded together. It is easy to find very small anhedral quartz crystals. In some cases it is possible to distinguish a vitreous matrix on the basis of textural and microscopic feature; this rock can be named as non welded vitreous rhyolitic tuff.

3.2.2 Basalt

The basaltic rock is outcropped near the bank of Gibe River which is the eastern margin of the project area; it may be Omo basalt or Welega basalt. From laboratory test result this rock shows a fluidal pilotassic oriented texture with vitreous matrix. The mineralogical assemblage is made by plagioclase, pyroxene, olivine, and accessory minerals. Plagioclase is euhedral with albite twinning. Crystal size dimensions are not bigger than millimeter. The extinction angle in symmetric zone is 20 to 24° (labradorite). Rare small phenocrysts with ophytic interstitial texture also occur. Pyroxene is colorless and ranges from subhedral to anhedral. Olivine is in micrometric crystals with high relief and high birefringence. Accessory minerals are magnetite. The basalt unit may not be visible in the geology map of the area, it is found as thin layer along Gibe river.

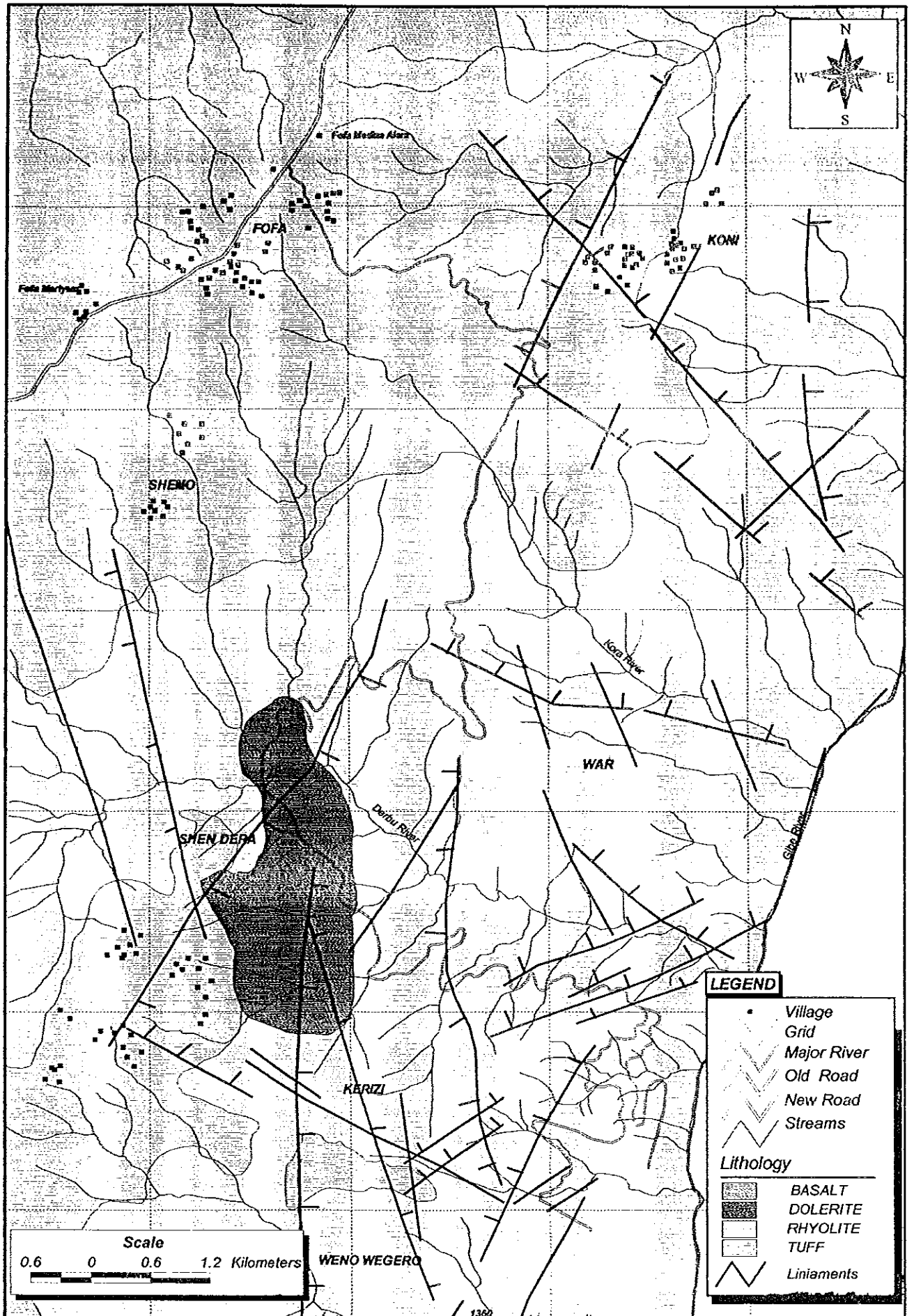


Fig. 3.2 Geological Map of the Study Area

3.2.3 Dolerite

This unit is found in the project area mostly as intrusive rocks. Most of Dykes and Sills in the rhyolitic bed are of doleritic rocks. However, there are Synite intrusions which are acidic rocks. The doleritic rocks are of different types. Which varies from course grained dark gray type to fine grained greenish type dolerite. Normally, this unit is very hard with UCS value greater than 200 Mpa (EEPCO, 2004). In the Gilgel Gibe-II hydroelectric power project area this rock has been used as an aggregate for the construction works. The fracture spacing in most doleritic rocks in the study area ranges from 10 cm to 50 cm, as indicated from the bore hole logging (EEPCO, 2004). Thin irregular calcite stringers along planes of weaknesses are also found. The thickness for most dykes of dolerite ranges from few centimeters to as thick as 50 m. The approximate age of this unit is late Miocene (EEPCO, 2004).

3.3 Regional Structural setup

In the south western part of the country there are two phases of deformations which are pre-rift and rift structures (Davidson, 1983).

3.3.1 Pre-rift Structures

Volcanism in south-western Ethiopia commenced in late Eocene time with the extrusion of flood basalts on the Precambrian crystalline basement peneplain. This was followed mainly by salic volcanism with intermittent outpouring of basalt lava through the Oligocene and Miocene. According Davidson (1983) uplift in south-western Ethiopia began immediately after the inception of volcanism of the main volcanic succession in the region. The process continued throughout the Oligocene and early Miocene concomitant with volcanism. The uplift produced an elevated land mass concave to the north-east with greater accumulation of volcanic products being in the central and eastern parts of the region. The rift valleys developed along this trend. The unconformity between the Precambrian crystalline basement and the pre-rift volcanic succession and the layering in the flows which were once more or less horizontal have now been tilted due to differential uplift and rift faulting. In pre rift units of rhyolite, trachyte, tuff and breccia ignimbrite in the Omo-Gibe river basin 5° to 40° westerly dips in the flows are common throughout the unit.

3.3.2 Rift Structure

According to Davidson (1983) the main development of rift began before 13 Million years. The orientation of the rift faults is controlled by the pre-existing structures of the Precambrian crystalline basement.

The most southern part of the Omo-Gibe river basin is occupied by the Lake Turkana rift system, a continuation into southern Ethiopia from northern Kenya. The Turkana rift branches into three in its northern part: the Kibish, the Omo and the Usno branches.

The Omo rift branch, oriented northerly, terminates in the high region. The Omo and Shoruni Rivers occupy the northern part of the Lake Turkana rift, where the rift is not well expressed. North of the Mwi River, this rift is bounded on its west side by a high escarpment that is the focus of a series of north to northeast trending faults with down-throw to the east and fault blocks tilted to the west. Down throw is probably more than 1km in the upper reaches of Mwi River valley. South of the Mwi River, the western edge of the Omo rift is sharply bounded by the Ilibai range, but the east side of the range does not show a clear fault scarp.

The Sawla rift valley, oriented north-easterly, is controlled by a major fault along its northwestern side. The block exposes crystalline rocks on its south-east facing escarpment, and has a northwest sloping surface capped by Tertiary volcanic flows. The rift appears to be part of the Lake Chew Bahr rift system. The fault along the middle Gibe River course that exposes Precambrian crystalline basement at its southeastern foot is probably related with the formation of the Lake Chew Bahr rift system.

The most north-eastern part of the Project area flanks the main Ethiopian rift valley and represents part of its western rift shoulder. The central part of Omo- Gibe basin is cut by a series of east-west trending, 2.5 km to 12 km wide and 20 to 30 km long shallow grabens. Four such grabens are traced from the aerial photographs. These basins are occupied by recent alluvial deposits. The upper reach of Gojeb River follows one of these structures. A similar graben occurs in the lower reaches of Gojeb River, just in the southern part of the project area.

The area is also cut by northeast-southwest trending major lineaments with subordinate north-west oriented ones identified on air photographs (Fig. 3.2).

4.1 Introduction

Every year a large number of landslides are reported all over the country during rainy season causing devastating damage to life, land and property. Most of such landslides are unnoticed, a very few of them get attention because of the damage caused by them such as; major casualties and large damage to infrastructure, mostly to roads and bridges. The damage due to possible landslides may be reduced considerably if such landslide prone areas are identified well in advance and accordingly necessary preventive measures are initiated prior to the slope failures. Thus, there is a need to execute a methodology which helps in preparing multipurpose terrain evaluation maps based on the geo-environment of mountainous terrain and using them as the basis for planning future development schemes.

Three types of mapping techniques are in practice based on various themes, such as danger, hazard, and risk maps (Anbalagan et al, 1996). Several types of maps can be produced based on the mapping techniques using the above themes.

Danger - Danger refers to an existing natural landslide phenomenon such as creep or rock fall or debris slide. The danger can exist, such as creep or a potential, as rock fall. The characterization does not include any forecasting of the events (Anbalagan et al, 1996). The danger map only shows the location of slide and the other characters such as type, size, nature of activity and failure probability. However, extents of damage are not shown on such maps.

Risk - Risk refers to the nature of damage likely to be caused in case of a failure. The damages may be in the form of loss of life and injures and/or loss of land and property. The extent of damage is dependent on the existing landuse pattern of the area, likely to be affected and the population, e.g. a major landslide in a remote area may cause lesser damage as compared to a smaller landslide in a densely populated area. Hence, risk is a function of hazard probability and the damage potential (Anbalagan et al., 1996). Risk assessment may be undertaken after evaluating the nature of hazard of a slope and its damage potential. The landslide risk is shown as very low risk, very high to very low damage potential.

Hazard - Hazard refers to a probability of occurrence of a landslide danger. The landslide hazard is shown as very high hazard, high hazard, moderate hazard, low hazard, and very low hazard to indicate very high to very low probability of occurrence of landslide. The period of time may be indicated in relative terms for different types of hazards. For example, in predicted high hazard slope, the landslide may occur early as compared to a moderate hazard slope, the landslide may occur easily as compared to moderate hazard or low hazard slope potential (Anbalagan et al., 1996).

4.2 Landslide Hazard Evaluation Factor (LHEF) Rating Scheme

The “Landslide Hazard Evaluation Factor Rating Scheme” (LHEF), developed by Anbalagan (1992), is a numerical rating system which is based on major inherent causative factors of slope instability such as geology, slope morphometry, relative relief, land use and land cover and groundwater conditions.

The field studies are carried out to collect the required data, Facet wise, for estimating the total hazards of the facet. A facet is a part of hill slope which has more or less similar characteristics of slope showing consistent slope direction and inclination, fig.4.1a. The maximum LHEF ratings for different categories are determined on the basis of their estimated significance in causing instability. Table 4.1 shows the proposed maximum LHEF rating for different contributory factors for macro-zonation (Anbalagan, 1992).

Table 4.1: Proposed maximum LHEF rating for different contributory factors for macro-zonation (after Anbalagan, 1992)

Contributory Factor	Maximum LHEF Rating
Lithology	2.0
Relationship of structural discontinuity with slope	2.0
Slope morphometry	2.0
Relative relief	1.0
Land use and land cover	2.0
Ground water condition	1.0
Total	10.0

The details of rating values for different factors is give in annex II

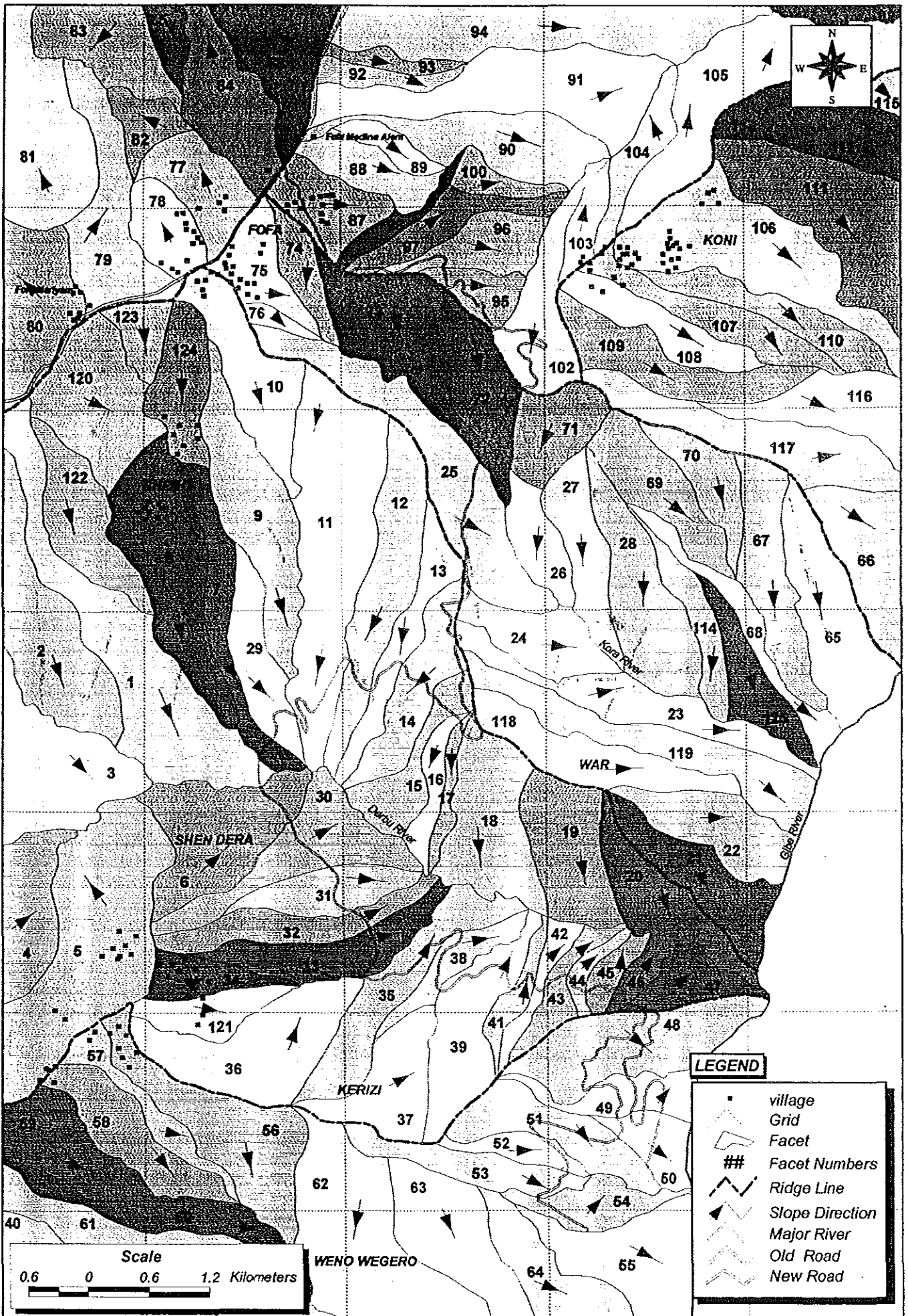


Fig. 4.1a Facet Map of the study area
30a

4.3 Geology

The Geological map provides information on the lithological and structural setting of the area. The lithological and structural maps may also be prepared separately for better representation. For the present study these two maps were prepared separately and are shown in Figures 3.2 (Chapter - 3).

4.4 Lithology

The erodeability or the response of rocks to the processes of weathering and erosion has been the main criteria in awarding the ratings for subcategories of lithology. Different rocks have different rate of weathering, therefore the lithology of individual facet should be properly identified, for example; rocks like quartzite, limestone and igneous rocks are generally hard, massive and resistant to erosion, forming steep slopes. In comparison, terrigenous sedimentary rocks are vulnerable to erosion and easily contribute to landslides. Phyllites and schists are characterized by flaky minerals which are more prone to weathering and thus, promote instability. A correction factor concerning the status of weathering of rocks has also been incorporated (Annexure -II).

In the case of soil, genesis and age, are the main considerations in awarding the ratings. Older alluvium is generally well compacted and has a high shearing resistance. Recent materials such as slide debris are loose and have low shearing resistance (Anbalagan, 1992).

In the project area three dominant lithological units are found, these are rhyolite, tuff and dolerite (Fig. 3.2). Rating for the rhyolite and dolerite unit is considered as 0.3, tuff unit is considered as soil because it is highly weathered and poorly compacted accordingly, a rating of 1.0 is assigned.

4.5 Structure

Structure includes primary and secondary discontinuities in the rocks such as bedding, joints, foliations and faults. The disposition of structural discontinuities in relation to slope inclination and direction has a great influence on the stability of slopes. In this context, the following three types of relations are considered important:

- (i) The extent of parallelism between the directions of the discontinuities, or the line of intersection of two discontinuities and the slope.

- (ii) The steepness of the dip of the discontinuity, or the plunge of the line of intersection of two discontinuities.
- (iii) The difference in the dip of the discontinuity, or the plunge of the line of intersection of the two discontinuities to the inclination of the slope.

The more the discontinuity or the line of intersection of two discontinuities tends to be parallel to the slope, the greater the risk of failure. When the dip of the discontinuity or plunge of the line of intersection of two discontinuities increases, the probability of failure also increases. This may lead to the satisfying a kinematic condition. Moreover, until the dip of the discontinuity plane or the plunge of the line of intersection of the two discontinuities does not exceed the inclination of the slope, the failure potential remains high. Accordingly, the LHEF ratings have been assigned for various stability conditions, broadly on the basis of the approach indicated by Romana (1985). In the case of soil, the inferred depth of the soil cover has been used for awarding the ratings.

In the project area the structures used for landslide hazard zonation mapping are joints and discontinuities. The collected structural data have been plotted on a stereonet for individual facet to get the preferred orientation of structures in relation with slope faces of each facet, later respective ratings have been awarded.

4.6 Slope Morphometry

Slope morphometry maps define slope categories on the basis of the frequency of occurrence of particular angles of slope. The distribution of the categories is dependent on the geomorphological history of the area; the angle of slope of each unit is a reflection of a series of localized processes and controls, which has been imposed on the facet. The slope morphometry map has been prepared by dividing the larger topographical map into smaller units. The contour lines have the same standard spacing, i.e., the same number of contour lines per km of horizontal distance. The chosen categories are six in number, representing the slopes of escarpment/cliff ($>40^\circ$), steep slope ($35^\circ-40^\circ$), moderately steep slope ($25^\circ-35^\circ$), gentle slope ($15^\circ-25^\circ$) and very gentle slope ($< 15^\circ$) (Annexure – II). In the study area most of the escarpments are concentrated along Derbu River. However, moderately steep slopes are extensively found in the central part, whereas the land near Fofa is classified as gentle slope ($< 15^\circ$). Figure 4.1 shows the Slope Morphometry Map of the study area.

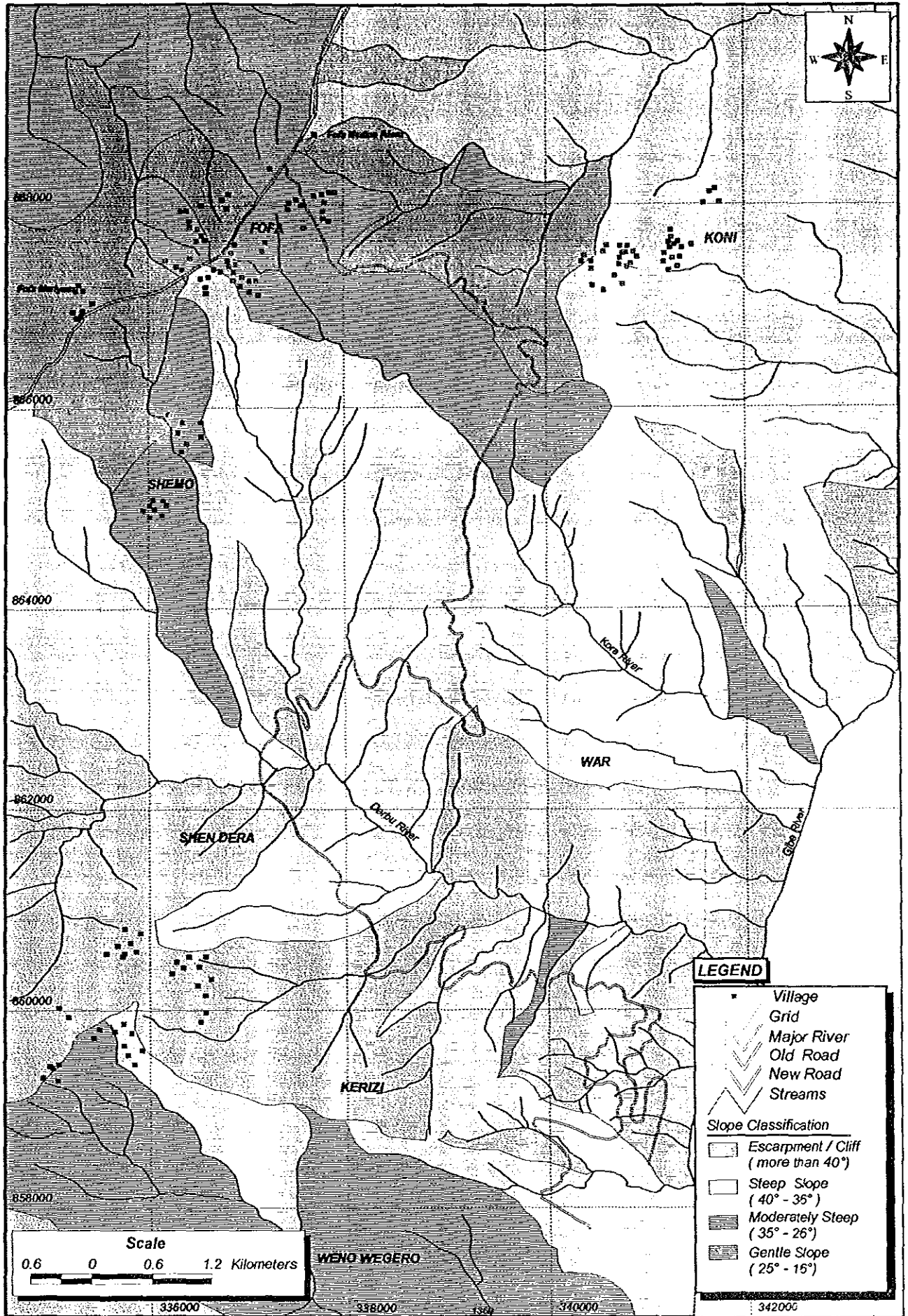


Fig. 4.1 Slope Morphometry Map of the Study Area

4.7 Relative relief

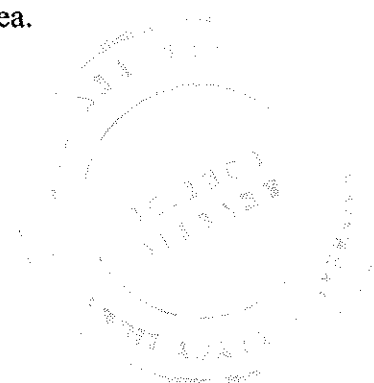
The relative relief map represents the local relief of maximum height between the ridge top and the valley floor within an individual facet. This shows the major breaks in the slopes of the study area. Three categories of slopes of relative relief have been chosen for hazard evaluation purposes, namely low (< 100 m), medium (101-300 m) and high (> 300 m).

According to Pachauri et al, (1991) incidence of landslide is greatest in the areas of high relief. Gravity sliding and debris flow has been more commonly noted in areas of higher relief. In the present study area more than 85% of the project area has high relative relief (>300m), therefore, the chances of slope instability is quite high in the study area. Figure 4.2 shows the Relative Relief map of the study area.

4.8 Land use and land cover

Land cover is an indirect indication of the stability of hill slopes. Barren and sparsely vegetated areas show faster erosion and greater instability as compared to reserve or protected forests, which are thickly vegetated and generally less prone to mass wasting processes. Forest cover, in general, reduces the action of climatic agents on the slopes and protects them from the effects of weathering and erosion. A well-spread root system increases the shearing resistance of slope material (Anbalagan, 1992). Agriculture, in general, is practiced on gentle to very gentle slopes, though moderately steep slopes are not spared at places for agricultural practices. However, the agricultural lands represent areas of repeated water charging for cultivation purposes and as such may be considered stable (Anbalagan, 1992). In the present study, based on the criteria of intensity of vegetation cover, the ratings have been awarded.

The present study area is highly rugged and most of the land is classified as steep slope. None of the area falls in the flat agricultural land. However, few isolated pockets of flat land are present near Fofa town which is being utilized for house construction. Most of the agricultural lands in the area are on the moderately steep lands and rarely in the highly steep lands. There are few isolated clusters of highly dense forest covers in the project area. The vegetation cover along the river banks is comparatively good with desert shrubs and bushes. Figure 4.3 shows the Landuse and Landcover map of the study area.



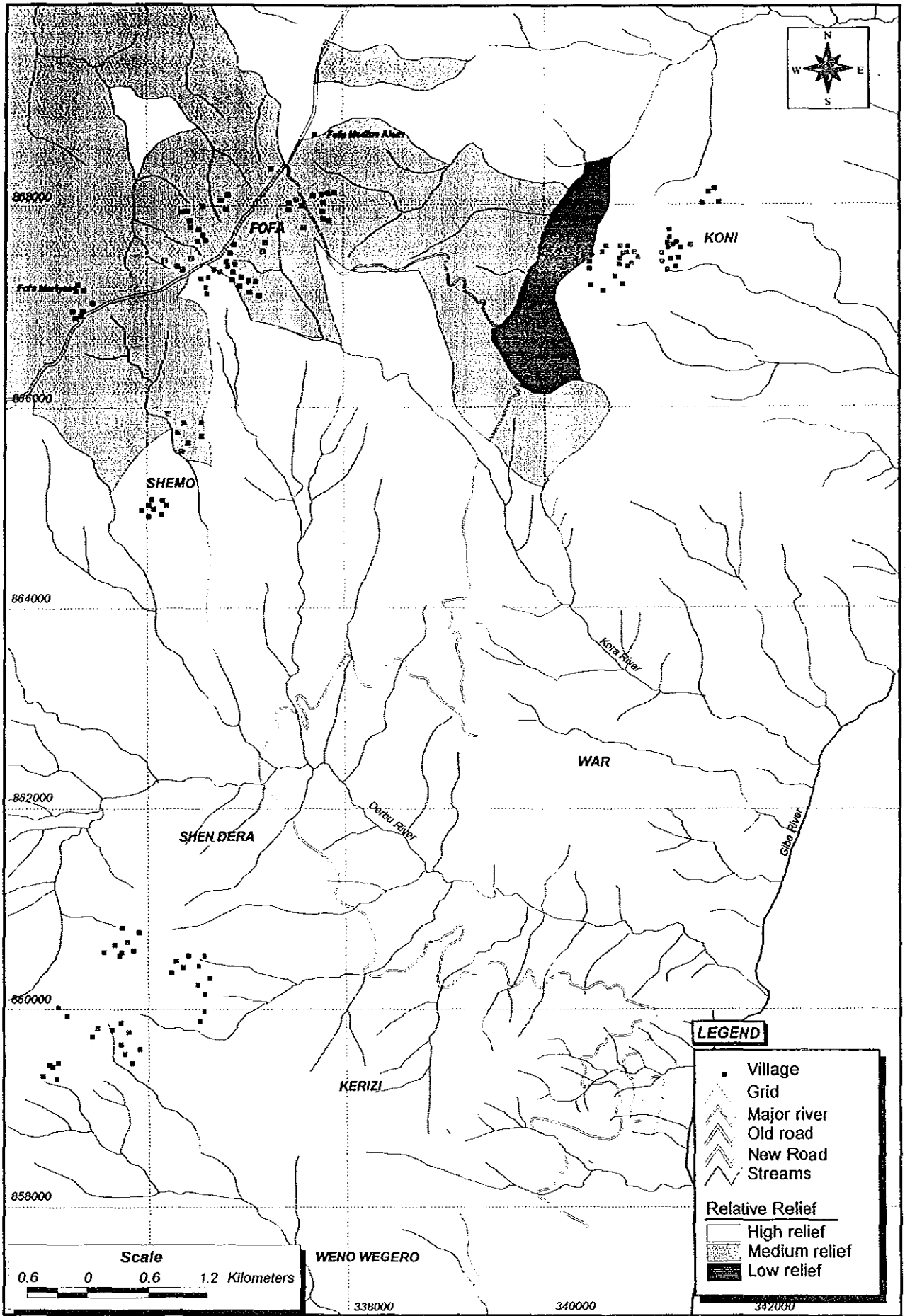


Fig. 4.2 Relative Relief Map of The Study Area

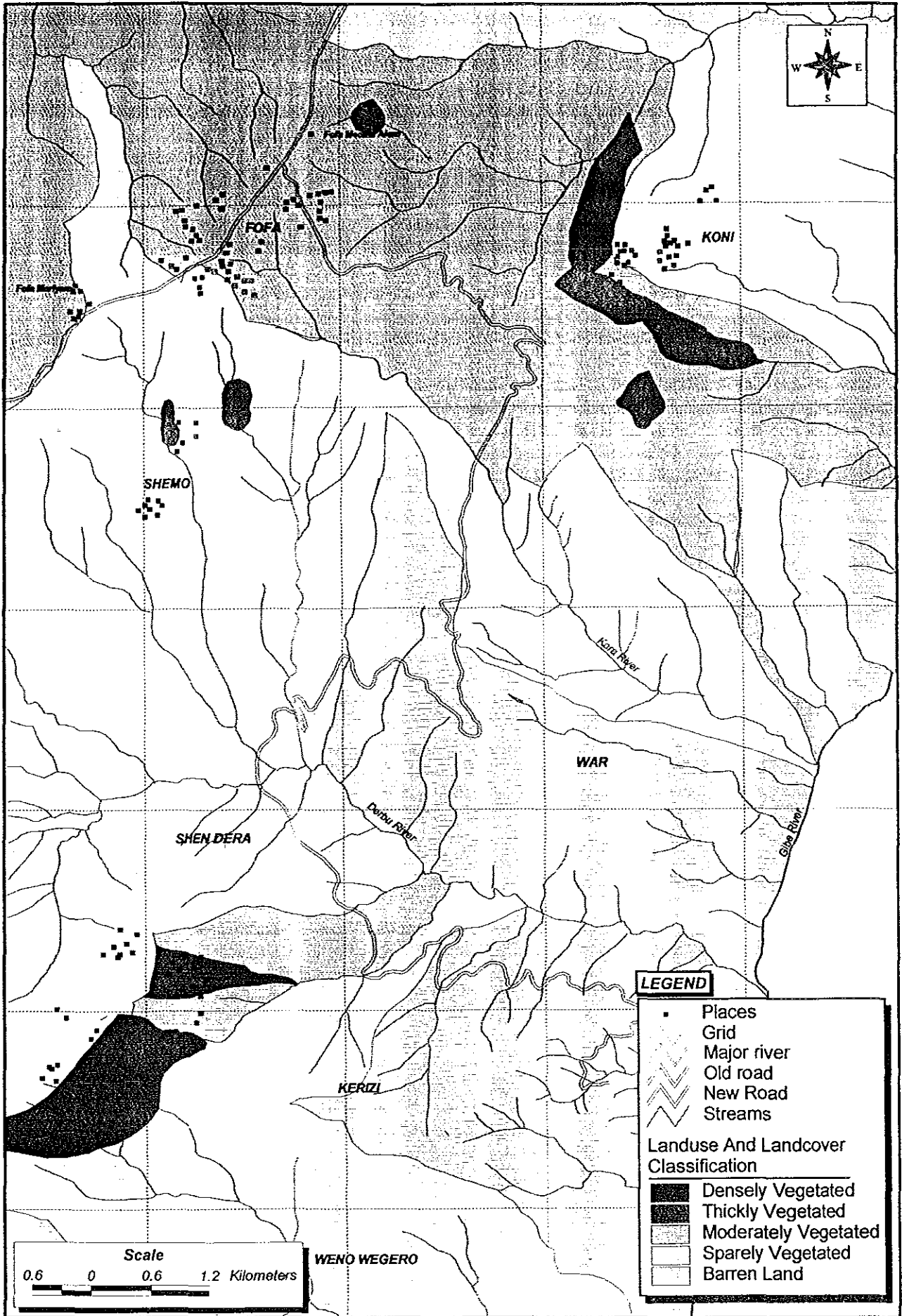


Fig. 4.3 Landue and Land cover Map of the Study Area

4.9 Ground water condition

In general, groundwater in hilly terrain is channeled along structural discontinuities of rocks and it does not have a uniform pattern. The evaluation of observations of the behavior of groundwater on hill slopes is not possible over large areas. Therefore, in order to make a quick appraisal, the nature of surface indications of the behavior of groundwater will provide valuable information on the stability of hill slopes for hazard mapping purposes (Anbalagan, 1992). Surface indications of water such as damp, wet, dripping, and flowing are used for rating purposes. The observations taken after the rainy season provide probably the possible worst groundwater conditions.

The present field work was carried out during the dry season and the surface water condition was almost dry through out the project area, except at very few places like those major rivers and near Fofa town where surface water was observed. However, for the present study the detailed stability analysis has been carried out for the possible worst conditions which are represented by moderately saturated slopes, as practically the entire slope cannot be fully saturated.

4.10 Landslide Hazard Evaluation in the study area

There are several Classification systems based on ranking for Landslide Hazard Evaluation (Howard and Ramson, 1978; Stevenson, 1977). In order to prepare a landslide hazard map on the basis of different causative factors, as described in previous section of this chapter, it is necessary to quantify the land using a weighting and rating system. All qualitative classes require a ranking method by which each class can be quantified and weighting given each factor to create a land hazard rank (Hensen, 1984; Varnes, 1984). The logical assumption is that the risk of occurrence of a damaging event or landslide is a direct consequence of these parameters. Therefore, these parameters can be given due weighting resulting in weighted landslide hazard values for each subclass. Each parameter is given a weighting depending on its degree of affiliation to the landslide hazard. The process and exact mechanisms involved in landslides is difficult to assess. This makes prediction quite difficult. Therefore, there is a substantial degree of uncertainty involved in any hazard evaluation process (Gupta et al., 2001).

The total estimated hazard (TEHD) indicates the net probability of instability and is calculated facet-wise, because adjoining facets may have entirely different stability conditions

(Anbalagan, 1995). The TEHD of an individual facet is obtained by adding the ratings of the individual causative factors obtained from the LHEF rating scheme (Annexure -2)

$$\text{Total estimated hazard (TEHD)} = \sum \text{Ratings of causative factors} \quad \dots\dots\dots 4.1$$

Or

$$\text{TEHD} = \text{Ratings of (lithology + structure + slope morphometry + relative relief + land use and land cover + groundwater conditions)}$$

On the basis of TEHD, there may be five categories of landslide hazard zones (Annexure - 2), namely, very low hazard (VLH), low hazard (LH), moderate hazard (MH), high hazard (HH) and very high hazard (VHH). In the present study, after evaluating TEHD it is found that there are only three classes, low hazard, moderate hazard and high hazard, the two opposite extremes namely; very low hazard and very high hazard are not present in the study area. Table 4.2 presents the TEHD ratings, facet wise, for the study area.

4.11 Landslide Hazard Zonation Mapping of the study area

Landslide Hazard Zonation Map is used to classify the land surface into zones of varying degree of hazard based on the estimated significance of causative factors which influence the stability of the area (Anbalagan, 1992). The LHZ map is a rapid assessment technique for hazard evaluation of the land surface.

4.11.1 Low Hazard

According to Anbalagan, (1992) low hazard zone has a TEHD value between 3.5 and 5.0. Out of total 125 facets in the study area 18 facets falls within low hazard zone. These areas are relatively flat land or low relief areas located in the northern part of the project area around Fofa. In terms of Percent this zone covers 12 % of the total area. This zone comprises mainly very weak rhyolitic tuff deposits (Fig.4.4).

4.12.2 Moderately Hazard

Moderately hazard zone has a TEHD value falling between 5.1 and 6.0 (Anbalagan, 1992). This zone covers most of the areas in the North- Eastern part and some areas around South-Western region of the study area. In total, 38 facets fall within moderately hazard zone. This hazard zone covers around 34 % of the total study area (Fig.4.4).



Fig. 4.4 Landslide Hazard Map of the

Table 4.2 TEHD ratings, facet wise, for the study area.

Face No	Structure	G-water condition	Geology	Relative relief	Land use	Slope Morphometry	Summation	TEHD
1	1.6	0	1	1	1.5	1.7	6.8	HH
2	1.6	0	1	1	1.5	1.7	6.8	HH
3	1.6	0	1	1	1.5	2	7.1	HH
4	1.6	0	1	1	1.5	2	7.1	HH
5	1.6	0	1	1	1.5	2	7.1	HH
6	1.6	0	0.9	1	1.7	2	7.2	HH
7	1.5	0	0.9	1	1.5	1.7	6.6	HH
8	1.6	0	0.9	1	1.5	1.2	6.2	HH
9	1.5	0	0.9	1	1.5	1.7	6.6	HH
10	1.5	0	0.9	1	1.5	1.7	6.6	HH
11	1.5	0	0.9	1	1.5	1.7	6.6	HH
12	1.5	0	0.9	1	2	1.7	7.1	HH
13	1.5	0	0.9	1	2	1.7	7.1	HH
14	1.2	0	0.9	1	2	1.7	6.8	HH
15	1.2	0	0.9	1	2	1.7	6.8	HH
16	1.2	0.2	0.9	1	2	1.7	7	HH
17	1.2	0.2	0.9	1	2	2	7.3	HH
18	1	0	0.9	1	2	2	6.9	HH
19	1	0	0.9	1	2	2	6.9	HH
20	1	0	0.9	1	2	2	6.9	HH
21	1	0	0.9	1	2	2	6.9	HH
22	1	0	0.9	1	2	2	6.9	HH
23	1	0	0.9	1	1.5	1.7	6.1	HH
24	1.1	0	0.9	1	1.5	1.7	6.2	HH
25	0.7	0.2	0.9	1	1.5	1.7	6	MH
26	1	0	0.9	1	1.5	1.7	6.1	HH
27	1	0.2	0.9	1	1.5	1.7	6.3	HH
28	1	0.2	0.9	1	1.5	1.7	6.3	HH
29	1.5	0	0.9	1	1.5	2	6.9	HH
30	1	0	0.9	1	1.5	1.7	6.1	HH
31	1.05	0	0.9	1	1.5	1.7	6.15	HH
32	1.05	0	0.9	1	1.1	1.7	5.75	MH
33	1.3	0	0.9	1	1.1	2	6.3	HH
34	1	0	0.9	1	0.8	2	5.7	MH
35	1	0	0.9	1	1.5	2	6.4	HH
36	1.2	0	0.9	1	1.5	2	6.6	HH
37	0.95	0	0.9	1	2	2	6.85	HH
38	1	0	0.9	1	2	1.7	6.6	HH
39	0.7	0	0.9	1	2	1.7	6.3	HH
40	1	0	0.9	1	2	2	6.9	HH
41	0.7	0	0.9	1	2	1.7	6.3	HH
42	1	0	0.9	1	2	1.2	6.1	HH
43	0.95	0	0.9	1	2	2	6.85	HH
44	1.2	0	0.9	1	2	1.7	6.8	HH
45	0.7	0	0.9	1	2	2	6.6	HH
46	1.3	0	0.9	1	2	2	7.2	HH

HH – High Hazard Zone, MH – Moderate High Hazard Zone, LH – Low Hazard Zone

Cont.....

Table 4.2 *Cont....*

Face t No	Structure	G-water condition	Geology	Relative relief	Land use	Slope Morphometry	Summation	TEHD
50	1.2	0	0.9	1	2	2	7.1	HH
51	1.3	0	0.9	1	2	1.7	6.9	HH
52	1.3	0	0.9	1	2	2	7.2	HH
53	1.3	0	0.9	1	2	1.7	6.9	HH
54	1.1	0	0.9	1	2	1.7	6.7	HH
55	0.8	0	0.9	1	2	1.7	6.4	HH
56	0.7	0	0.9	1	1.5	1.7	5.8	MH
57	0.7	0	0.9	1	1.5	1.2	5.3	MH
58	0.7	0	0.9	1	1.5	1.2	5.3	MH
59	0.7	0	0.9	1	1.5	1.2	5.3	MH
60	0.7	0	0.9	1	1.5	1.2	5.3	MH
61	0.7	0	0.9	1	1.5	1.2	5.3	MH
62	0.7	0	0.9	1	1.5	1.2	5.3	MH
63	0.7	0	0.9	1	1.5	1.2	5.3	MH
64	0.7	0	0.9	1	1.5	1.2	5.3	MH
65	1.3	0	0.9	1	2	1.7	6.9	HH
66	1.3	0	0.9	1	2	2	7.2	HH
67	1.3	0	0.9	1	1.5	1.7	6.4	HH
68	1.3	0	0.9	1	1.3	1.7	6.2	HH
69	1.3	0	0.9	1	1.3	1.7	6.2	HH
70	1.3	0	0.9	1	1	2	6.2	HH
71	1	0	0.9	0.6	1.2	1.2	4.9	LH
72	0.7	0	0.9	0.6	1.2	1.2	4.6	LH
73	0.7	0	0.9	1	1.2	1.2	5	LH
74	0.85	0	1	0.6	1.2	1.2	4.85	LH
75	0.85	0	1	0.6	1.2	1.2	4.85	LH
77	0.85	0.8	1	0.6	1.2	0.8	5.25	MH
78	0.85	0	1	0.6	1.2	1.2	4.85	LH
79	0.85	0	1	0.6	1.5	0.8	4.75	LH
80	0.85	0	1	0.6	1.2	0.8	4.45	LH
81	0.85	0.5	1	0.6	1.2	1.2	5.35	MH
82	0.85	0.5	1	1	1.2	1.2	5.75	MH
83	0.85	0.5	1	0.6	1.2	1.2	5.35	MH
84	0.85	0.5	1	0.6	1.2	1.2	5.35	MH
86	0.85	0.5	1	1	1.2	1.2	5.75	MH
85	0.85	0.5	1	1	1.2	1.2	5.75	MH
87	0.85	0	1	0.6	1.2	1.2	4.85	LH
88	0.85	0	1	0.6	1.2	2	5.65	MH
89	0.85	0	1	0.6	1.2	2	5.65	MH
90	0.85	0	1	1	1.2	1.7	5.75	MH
91	0.85	0	1	1	1.3	1.7	5.85	MH
92	0.85	0	1	0.6	1.2	2	5.65	MH
93	0.85	0	1	0.6	1.2	2	5.65	MH

HH – High Hazard Zone, MH – Moderate High Hazard Zone, LH – Low Hazard Zone

Cont.....

Table 4.2 *Cont...*

Face no	structure	G-water condition	Geology	Relative relief	Land use	Slope morphometry	summation	TEHD
94	0.85	0	1	1	1.5	1.7	6.05	MH
95	0.85	0	1	0.6	1.2	0.8	4.45	LH
96	0.85	0	1	0.6	1.2	0.8	4.45	LH
97	0.85	0	1	0.6	1.2	0.8	4.45	LH
98	0.85	0	1	0.6	1.2	0.8	4.45	LH
99	0.85	0	1	0.6	1.2	0.8	4.45	LH
100	0.85	0	1	0.6	1.2	1.2	4.85	LH
101	0.85	0	1	0.6	1.5	0.8	4.75	LH
101	0.85	0	1	0.6	1.2	1.2	4.85	LH
102	0.85	0	1	0.3	1.2	0.8	4.15	LH
103	0.85	0	1	0.3	1.2	0.8	4.15	LH
104	0.85	0	1	1	1.3	1.7	5.85	MH
105	0.85	0	1	1	1.5	1.7	6.05	MH
106	1.05	0	0.9	1	1.5	1.7	6.15	HH
107	1.05	0	0.9	1	1.2	1.7	5.85	MH
108	1.05	0	0.9	1	0.8	1.7	5.45	MH
109	0.9	0	0.9	1	1.3	1.7	5.8	MH
110	1.05	0	0.9	1	1.5	1.7	6.15	HH
111	1.05	0	0.9	1	1.5	1.7	6.15	HH
112	1.05	0	0.9	1	1.5	1.7	6.15	HH
113	1.05	0	0.9	1	1.5	1.7	6.15	HH
114	1.05	0	0.9	1	1.5	1.7	6.15	HH
115	1.05	0	0.9	1	1.5	1.7	6.15	HH
116	0.9	0	0.9	1	1.3	1.7	5.8	MH
117	0.9	0	0.9	1	1.3	1.7	5.8	MH
118	1	0	0.9	1	2	1.7	6.6	HH
119	1	0	0.9	1	2	1.7	6.6	HH
120	1	0	0.9	1	2	1.7	6.6	HH
121	1	0	0.9	1	1.1	2	6	MH
122	1	0	0.9	1	0.8	2	5.7	MH
123	1.6	0	0.9	1	1.5	1.7	6.7	HH
124	0.85	0	1	0.6	1.5	1.2	5.15	MH
125	0.85	0	1	1	1.5	1.2	5.55	MH

HH – High Hazard Zone, MH – Moderate High Hazard Zone, LH – Low Hazard Zone

4.12.3 High Hazard

In High Hazard zone TEHD value falls between 6.1 and 7.5 (Anbalagan, 1992). As a result of the geomorphological setting of the study area, most of the facets are in this group. Out of total 125 facets, 69 facets falls with in high hazard zone, which comprises 54 % of the total study area. A major part of the new road (Fofa to Powerhouse) is constructed in this zone (Fig.4.4).

Based on the TEHD values, 54% of the slopes in the study area falls in High Hazard, 34% in the Moderately Hazard and only 12% of the area falls in Low Hazard. These figures clearly indicates that most of the area in the study area falls into High Hazard or Moderately Hazard. Which implies that chances of slope failures is high in the study area.

However, a slope may only fail when the driving forces exceeds the resisting forces and the orientation of discontinuities is such that they favors sliding, either on single discontinuity or on a wedge formed by two intersecting discontinuities. Moreover, even if slope is potentially unstable, it does not mean that slope is actually going to fail, until or unless there is some driving force which triggers the sliding, such as heavy water saturation or earthquake loading.

5.1 Preamble

The Total estimated hazard (TEHD) values for the present study area indicates that 54% of the slopes in the study area falls in High Hazard, 34% in the Moderately Hazard and only 12% of the area falls in Low Hazard. From these results it can easily be concluded that the study area, in general, is prone to landslide activity. However, a slope may only fail when the driving forces exceeds the resisting forces and the orientation of discontinuities is such that they favor sliding, either on single discontinuity or on a wedge formed by two intersecting discontinuities. Slopes may also fail when the slope material is homogeneous like soils or slope material comprises of highly weathered and fractured rock mass. Moreover, even if a slope is potentially unstable, it does not mean that it is actually going to fail, until or unless there is some driving force which triggers sliding, such as heavy water saturation or earthquake loading. This is the reason why we have maximum landslides during rainy season. Thus, an attempt has been made to identify such potential unstable slopes in High Hazard and Moderately Hazard zones. Further, a detailed stability analysis has been carried out for potential unstable slopes in the study area.

5.2 Identification of Potential Unstable Slope

A thorough reconnaissance survey was carried out, particularly in the High Hazard and Moderately Hazard zones in the study area, to identify the potential unstable slopes, based on their field manifestations of instability, such as;

- i) Presence of scarp faces on steep slopes
- ii) Removal of toe support for road construction
- iii) Presence of evidences of slope distress, such as, development of tension cracks, bulging of slope face and other such features.
- iv) Orientation of discontinuities, such that they favor sliding, either on single discontinuity or on a wedge formed by two intersecting discontinuities.

Thus, based on the above mentioned field manifestations of instabilities total 10 No. of potential unstable slopes were identified in the study area. The detailed stability studies of these critical sections are discussed later in this chapter.

5.3 Engineering property of rocks and soils

The rock in its most general form is an anisotropic, discontinuous mass containing cracks, joints, and faults and bedding planes with varying degree of cohesion along these discontinuities. In practical design work any acceptable solution must take into account not only the isotropy of the rock mass but also the discontinuities which play a far more important role in the stability of a rock structure.

For most of the rock engineering problem, the engineering properties of a rock mass depends far more on the system of geological separations within the rock mass than on the strength of a rock mass, is in fact its residual strength which, together with its anisotropy, is governed by the interlocking bonds of the unit elements forming the rock mass (Lama et al, 1978).

Because of a vast range in properties of rocks due to different structures, fabrics and materials, it is difficult to determine the properties and to describe rocks quantitatively. Certain properties that are relatively easy to measure are used to classify the rock, these rock properties are unit weight, permeability, porosity, point load index and slaking and durability.

The term 'soil' in soil engineering is defined as an unconsolidated material, composed of solid particles, produced by the disintegration of rocks. Soils are formed by weathering of rocks due to mechanical disintegration or chemical decomposition (Arora, 1997). Most of the soil covers in the project area are residual soils which are developed from the parent rhyolitic tuff rock. Most of the sloppy terrains are covered with thin layers of colluvial soil having variety of grain sizes.

5.3.1 Rock mass classification

Rock Mass Classification, based on simple rating scheme, is an rapid and very effective method to determine the overall quality of the rock mass. Rock Mass rating Systems are also useful in assessing the shear strength and deformability of the rock mass. Though, there are several rating schemes available to classify the rock mass, however for the present study the Geomechanics Classification or the Rock Mass Rating System proposed by Bieniawski, 1989 has been utilized to workout the rock mass quality.

In order to workout the RMR, 6 basic parameters are used, these are;

- i) Uniaxial compressive strength of rock (UCS)

- ii) Rock Quality Designation (RQD)
- iii) Spacing of discontinuities
- iv) Condition of discontinuities
- v) Ground water condition
- vi) Orientation of discontinuities

The data pertaining to RMR has been collected from all 8 critical slope sections at several locations and based on the conditions the ratings for each of the 6 parameters were assigned from the standard RMR table and are added to get the RMR value.

For the present study, the uniaxial compressive strength of the rock has been determined by Schmidt hammer, using the empirical relation given by Barton and Choubey, 1977

$$\log_{10}(\sigma_c) = 0.00088\gamma R + 1.01 \quad \dots\dots\dots 5.1$$

Where;

σ_c = uniaxial compressive strength in MPa

γ = dry rock density in KN/m³

R = rebound number of Schmidt hammer

The Rock Quality Designation (RQD) has been determined by Palmstrom's Volumetric Count method (Palmstrom, 1982), according to which,

$$RQD = 115 - 3.3 J_v \quad \dots\dots\dots 5.2$$

Where;

RQD = Rock Quality Designation (%)

J_v = Total Number of discontinuities, greater than 10cm in length, in 1m cube of Rock mass.

For other parameters, like; Spacing, Condition of discontinuities, Ground water condition, and Orientation of discontinuities visual observations and measurements has been made and accordingly, the ratings were assigned from the standard RMR table. Figure 5.1 presents the RMR data collection locations at various critical slope sections. The RMR data collected from various locations is summarized in Table 5.1.

Table 5.1 RMR data collected from various locations at critical slope sections

RMR Data points	Parameters Ratings										RMR	Rock Mass Class
	UCS			RQD			Sp.	Con	GWC	Ori		
	SHV	UCS	Ra	Jv	RQD	Ra						
SL1	35	68	7	9	85	17	8	15	14	-32	29	Poor
SL2	50	136	12	6	94	17	10	15	15	-37	32	Poor
SL3	44	97	7	9	86	17	8	7	15	-23	31	Poor
SL4	43	111	12	10	82	17	9	7	15	-43	17	Very Poor
SL5	39	80	7	7	92	17	9	8	15	-38	18	Very Poor
SL6	42	137	12	11	78	17	8	23	14	-50	24	Poor
SL7	33	59	7	9	87	17	9	13	15	-40	21	Poor
SL8	38	73	7	7	93	17	8	15	15	-40	22	Poor

UCS – Uniaxial compressive strength, SHV – Shmidt hammer Value, Ra – Rating, Jv- Volumetric count, RQD – Rock quality designation, Sp. – Spacing of discontinuity, Con. – Condition of discontinuity, GWC – ground water condition, Ori – Orientation of discontinuity, RMR – Rock mass rating

Shear Strength and Modulus of Deformation ‘Ed’ of Rock Mass

For the stability of rock mass shear strength parameters, namely cohesion and angle of friction, are very important as they provide the resistance to the sliding of rock mass under the influence of gravity. The shear strength parameters at each critical slope section have been determined from RMR. The Shear strength parameters of rock mass as determined from RMR are summarized in Table 5.2. The standard RMR table gives the range in which the cohesion and angle of friction of the rock mass will fall. Further, in order to get the cohesion and angle of friction for a specific value of RMR, Bieniawski, 1976 has proposed the following relations.

$$C^* = 0.05 \text{ RMR} \quad \dots\dots\dots 5.3$$

$$\Phi^* = 0.5\text{RMR} + 5 \quad \dots\dots\dots 5.4$$

C* and Φ* are the specific value of cohesion and angle of friction for a given RMR value.

For the present study an attempt has also been made to empirically find out the Modulus of deformation ‘Ed’ of the rock mass by using RMR. Deformability means the capacity of rock to strain under applied loads or in response to unloads. For this purpose the empirical relation proposed by Agarwal et al (1991) has been used, which is given by eq 5.5 and the results thus, obtained are presented in table 5.2

$$Ed = 10^{(RMR-30)/50} \quad \dots\dots\dots 5.5$$

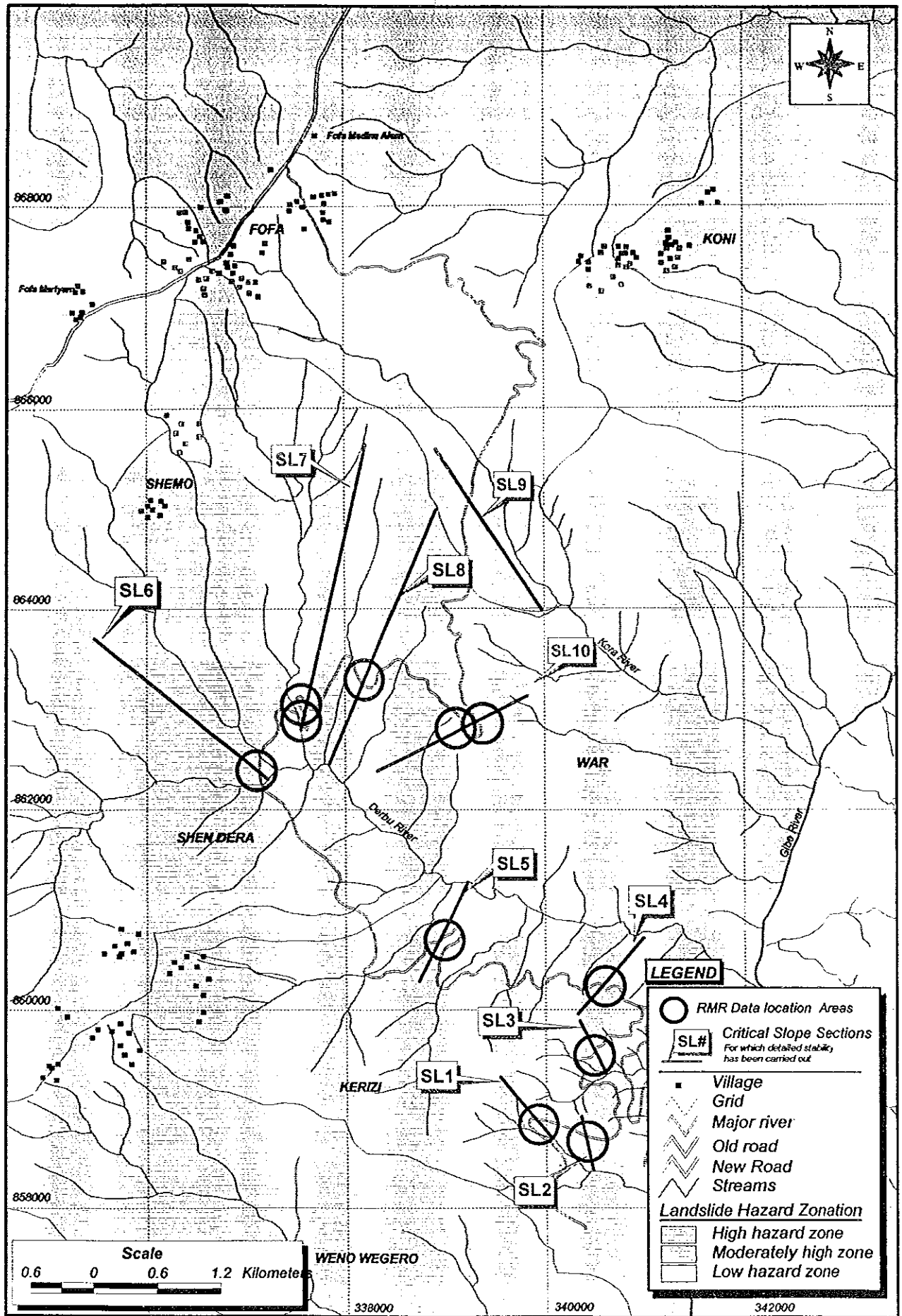


Fig. 5.1 Map showing the critical slope sections and RMR data collection areas

Table 5.2 Shear strength Parameters and Modulus of Deformation 'Ed' as determined from RMR

S.No	RMR Data Location (UTM) E,N	RMR	Shear strength Parameters				Modulus of Deformation 'Ed' in (Mpa) as determined by equation 5.5
			C (Range)	Φ (Range)	C*	Φ^*	
SL1	340029,858825	29	100-200	15-25	150	20	955
SL2	340632,858673	32	100-200	15-25	160	21	1096
SL3	340494,859222	31	100-200	15-25	155	21	1050
SL4	340976,859881	17	< 100	< 15	85	14	550
SL5	339014,860732	18	< 100	< 15	90	14	575
SL6	337117,862493	24	100-200	15-25	120	17	759
SL7	337521,863266	21	100-200	15-25	105	16	660
SL8	337661,863094	22	100-200	15-25	110	16	692

*C** is the specific value of Cohesion for a given RMR as determined using Eq. 5.3
 *Φ^** is the specific value of angle of friction for a given RMR as determined using Eq. 5.4

5.3.2 Soil Classification

The northern part of the study area is covered with soil. The 'Total estimated hazard' (TEHD) values indicates that most of the soil covered areas fall under moderately hazard zone. However, little soil covered areas fall under high hazard zone. From field manifestations of instabilities two critical soil slopes, SL9 and SL 10, have been identified which are potentially unstable (Fig. 5.1). Thus, these two slope sections are studied in detail for their instability.

For the purpose of detailed stability analysis, soil samples have been collected from these critical slopes (SL9 & SL 10) and were analyzed for the classification and the index properties. According to AASHTO classification, both the soil samples have been classified as clayey soil with dry unit weight of 16.7 kN/m³. The natural water content of soil sample taken from slopes SL9 and SL10 are 47.3% and 48.6%, respectively. The soils have also been classified as inorganic clay of low to medium plasticity with (LL) =46%, PL=25.9%, PI=20.1%) for SL9 soil and (LL) =48.5%, PL=23.3%, PI=25.2%) for SL10 soil sample. Table 5.3 presents the Index Properties, as determined from the soil samples collected from critical slope sections.

With the limitation of time and resources it was not possible to conduct the tests to determine the cohesion and angle of shearing resistance of the soil, as these tests are very sensitive and it needs proper sampling and testing methods. However, the values for cohesion and angle of

shearing resistance have been taken from USBR standard table (Small Dams, USBR, 1982). Table 5.4 presents the Shear strength properties and Unit weight of soil used in stability analysis for critical slope sections

Table 5.3 Index Properties, as determined from the soil samples collected from critical slope sections

Sample From	Depth (cm)	Origin	Color	Soil Type	Index Value				Classification
					LL*	PL*	PI*	Moisture content %	
SL9	90	Residual	Light yellow	Clay	46.0	25.9	20.1	47.3	CL
SL10	95	Residual	Reddish brown	Clay	48.5	23.3	25.2	48.6	CL

Table 5.4 Shear strength properties and Unit weight of soil at critical slope sections

Parameters	Samples from SL9	Samples from SL10
Cohesion (C) in T/m ² *	7.1	7.1
Friction angle (P) in degree*	25	25
Unit weight (S) in T/m ³ *	1.7	1.7
* values are taken from USBR, 1982		

5.4 Discontinuity Analysis

Discontinuities are structural weakness planes upon which movement can take place. The presence or absence of discontinuities has a very important influence upon the stability of rock slopes and the detection of these geological features is most critical part of the stability investigation. When the rock mass contains discontinuity surfaces dipping towards the slope face at angles between 30° and 70°, simple sliding can occur and the stability of the slope is significantly lower than those in which only horizontal and vertical discontinuities are present (Hoek et al, 1977).

The rock mass exposed on the critical slope sections in the study area is traversed by discontinuity planes mainly, joints, faults, and dykes. In order to work out the preferred orientations of these discontinuity planes, structural data, mainly joints has been collected from all critical rock slope sections. For each discontinuity plane the azimuth of the 'Dip-

Direction' clockwise in relation to magnetic North from 0° to 360°, has been measured, whereas, amount of dip was measured along it's true dip direction in the vertical plane.

Later, the structural discontinuity data has been analyzed using Spheristat 2.0 and Microdem computer programs. For data analysis the data were fed in Spheristat 2.0, as Dip direction /Dip amount. The poles were then plotted on a Schmidt projection, lower hemisphere. Using the density analysis facility of the program the poles were contoured on 'Schmidt' counting net. Thus, the preferred orientations of discontinuity planes were determined. Further, the major plane dip directions and dips were plotted in Microdem computer program, which has been later utilized for the Kinematic check to determine the possible mode of failure. Figure 5.2 and Table 5.5 presents the preferred orientations, as observed on various critical rock slope sections in the study area.

Table 5.5 Preferred orientations, as observed on various critical rock slope sections in the study area.

Slope section	Location (UTM)		Number of Joint sets	Preferred Orientation of Discontinuity Planes Dip Direction/ Dip Amount		
	Northing	Easting		J1	J2	J3
SL1	858825	340029	3	N028°/83°	N 182°/63°	N 145°/41°
SL2	858673	340632	3	N193°/72°	N021°/77°	N216°/59°
SL3	859222	340494	3	N312°/82°	N258°/49°	N213°/21°
SL4	859881	340976	3	N139°/75°	N253°/49°	N169°/39°
SL5	860732	339014	3	N297°/77°	N356°/54°	N316°/40°
SL6	862493	337117	2	N100°/42°	N080°/46°	--
SL7	863266	337521	3	N270°/85°	N269°/54°	N326°/60°
SL8	863094	337661	2	N318°/82°	N213°/61°	--

5.5 Geometry and Geology of the Critical slope Section

For the detailed stability analysis cross sections has been prepared along all critical slope sections. The Geometry of slope sections in terms of slope direction and inclination, upper slope direction, inclination and the height of the slope are presented in Fig.5.3(a), (b),(c) and Table 5.6. Geological cross sections have been prepared along all the critical slope sections. The geological details for these cross sections were visually observed along the road cut and the natural outcrops. Further, the geological cross section prepared by the Project Authorities for the tunnel alignment has also been utilized to project the geology along the critical slope sections.

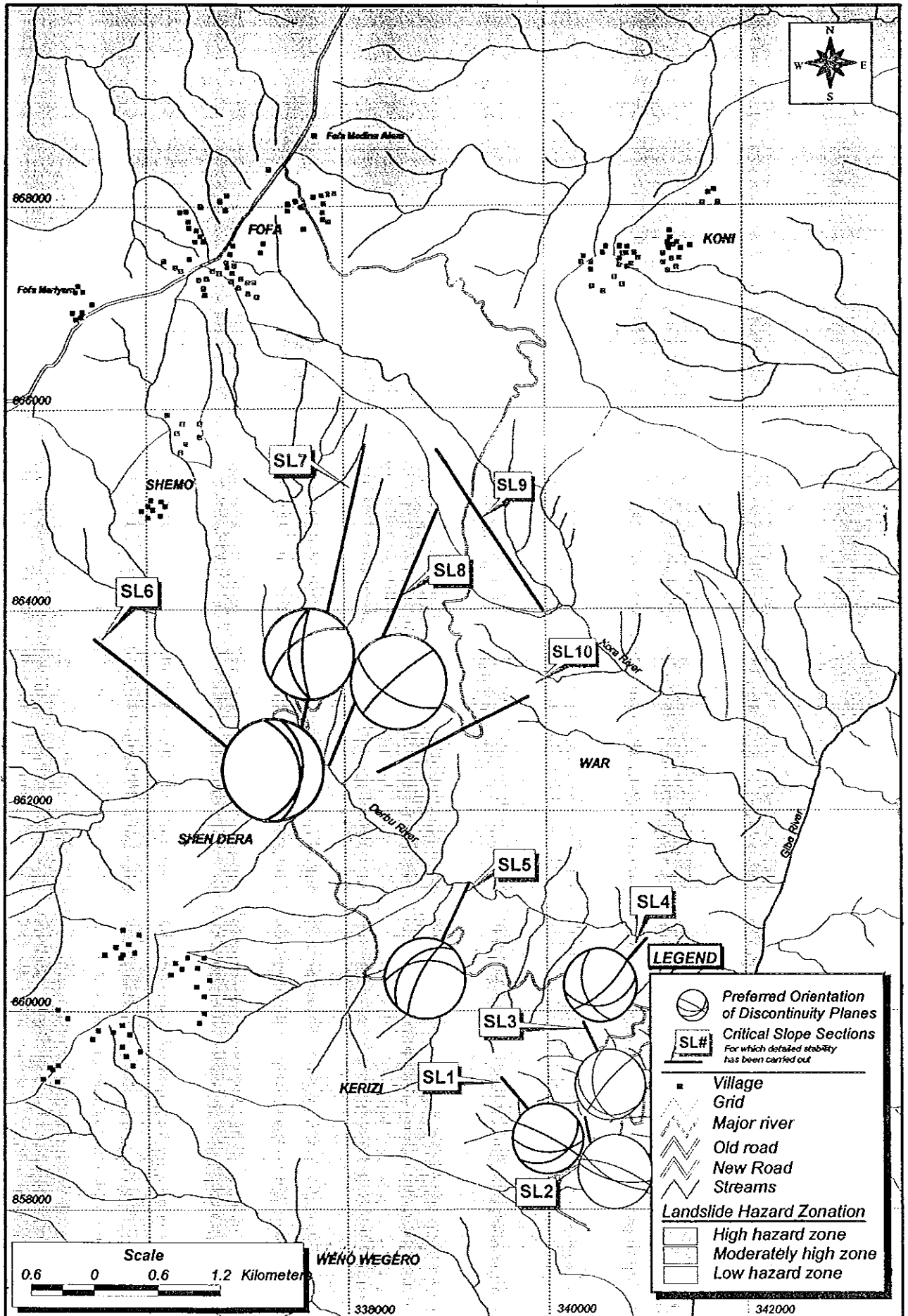


Fig. 5.1 Map Showing the Landslide Hazard zone and critical slope sections and Preferred Orientation of Discontinuity Planes

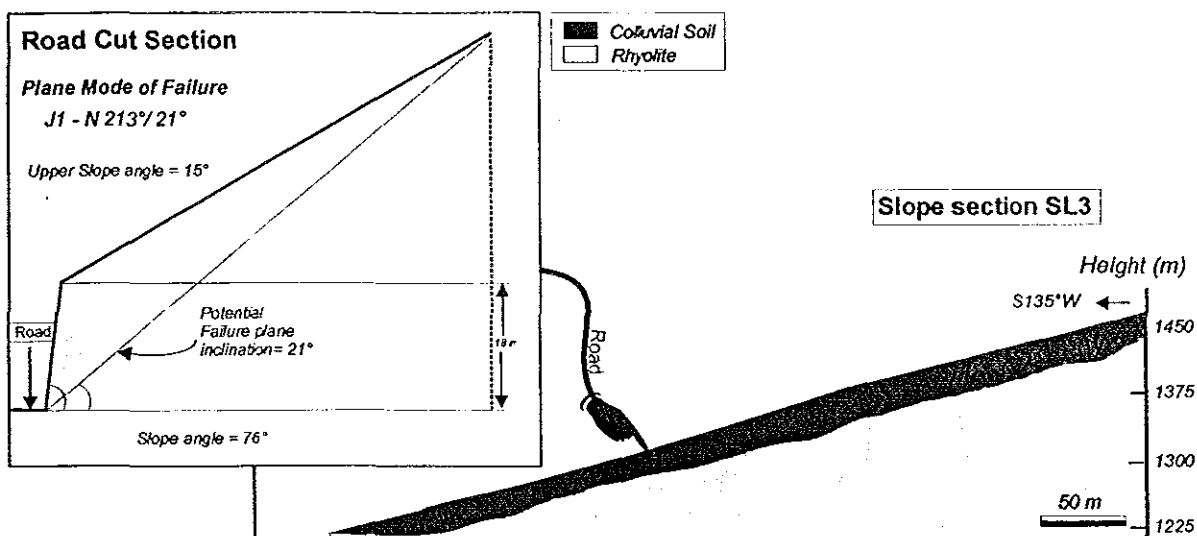
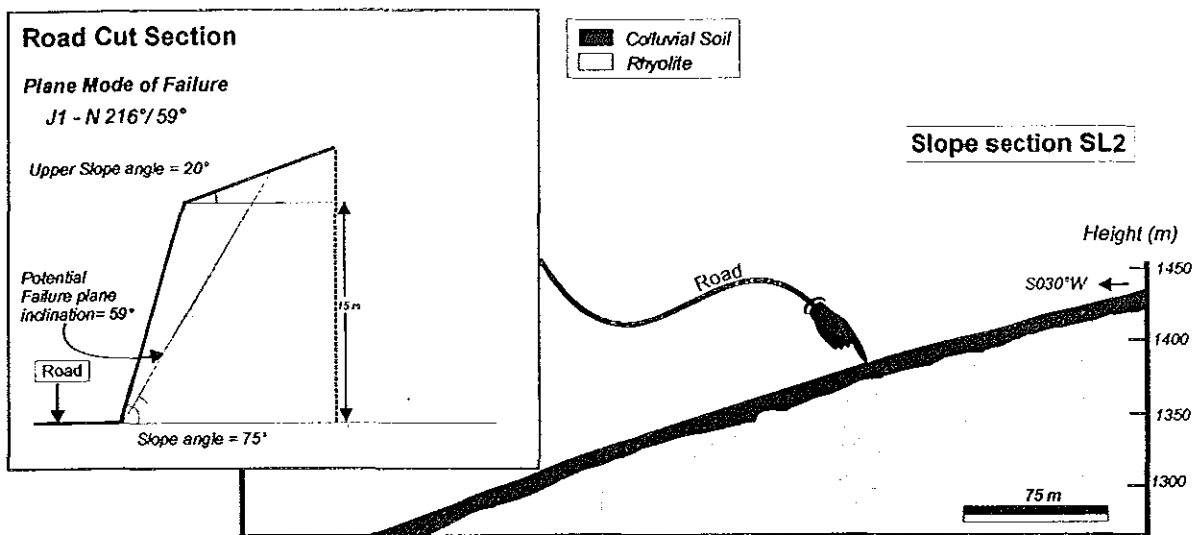
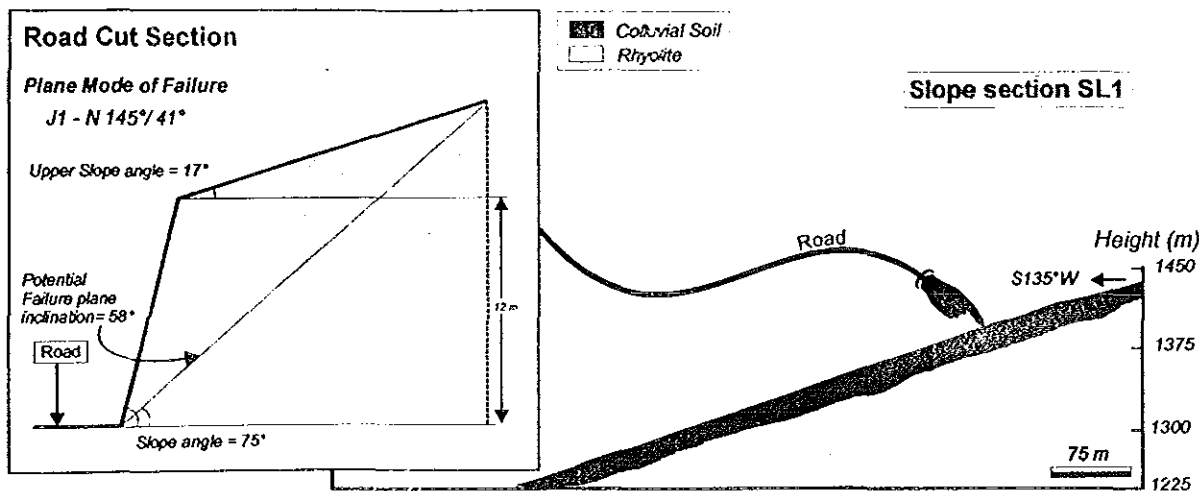


Figure 5.3(a) Geological cross sections and Geometry along the critical slope sections.

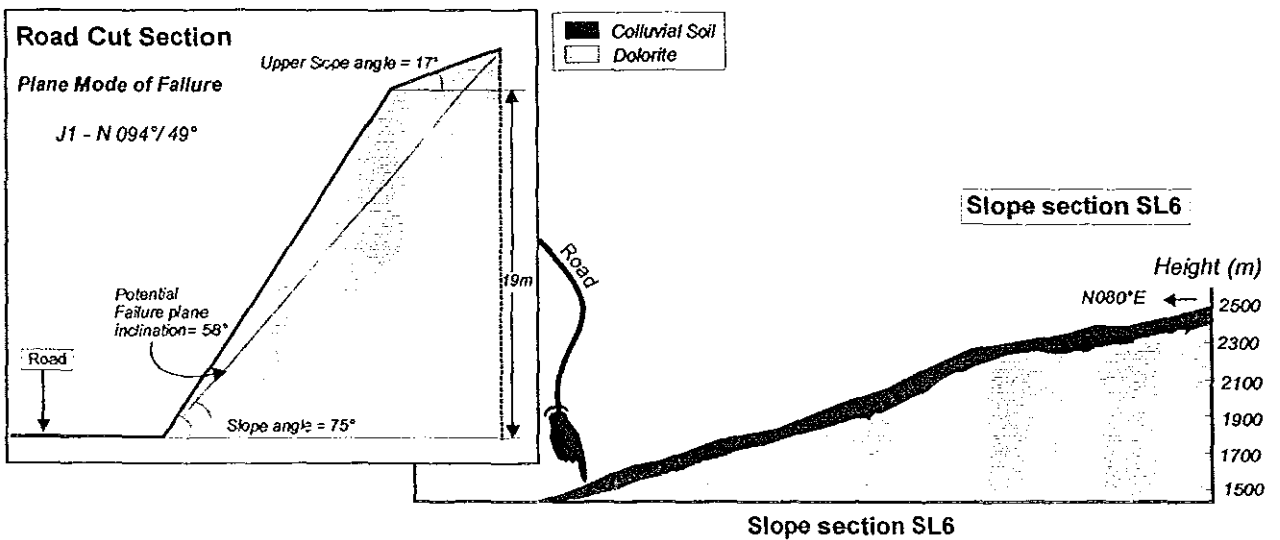
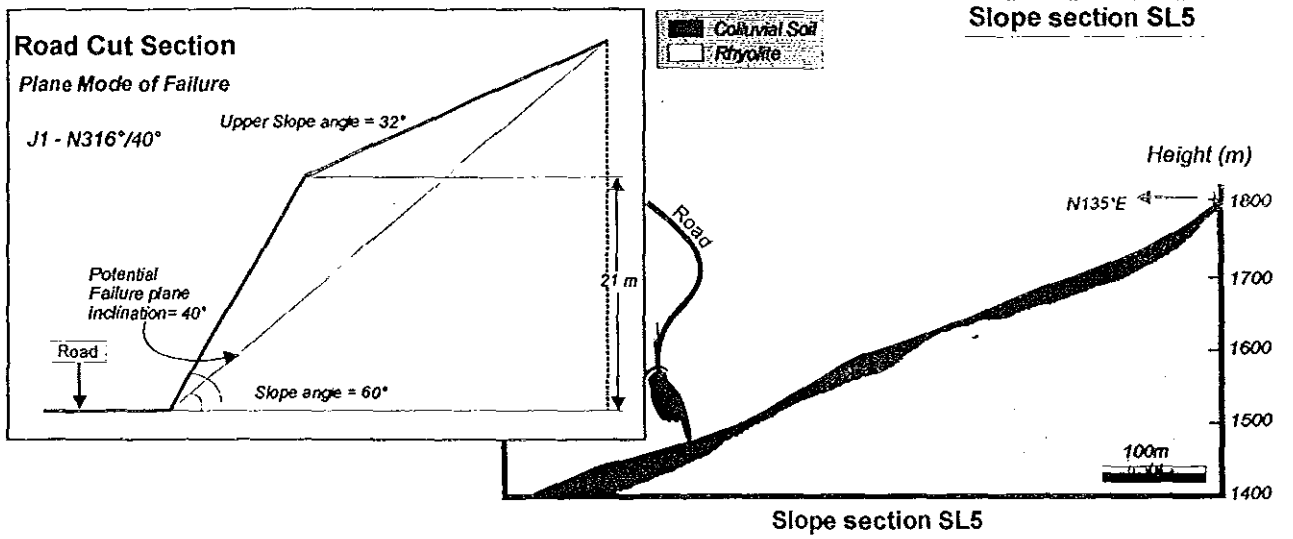
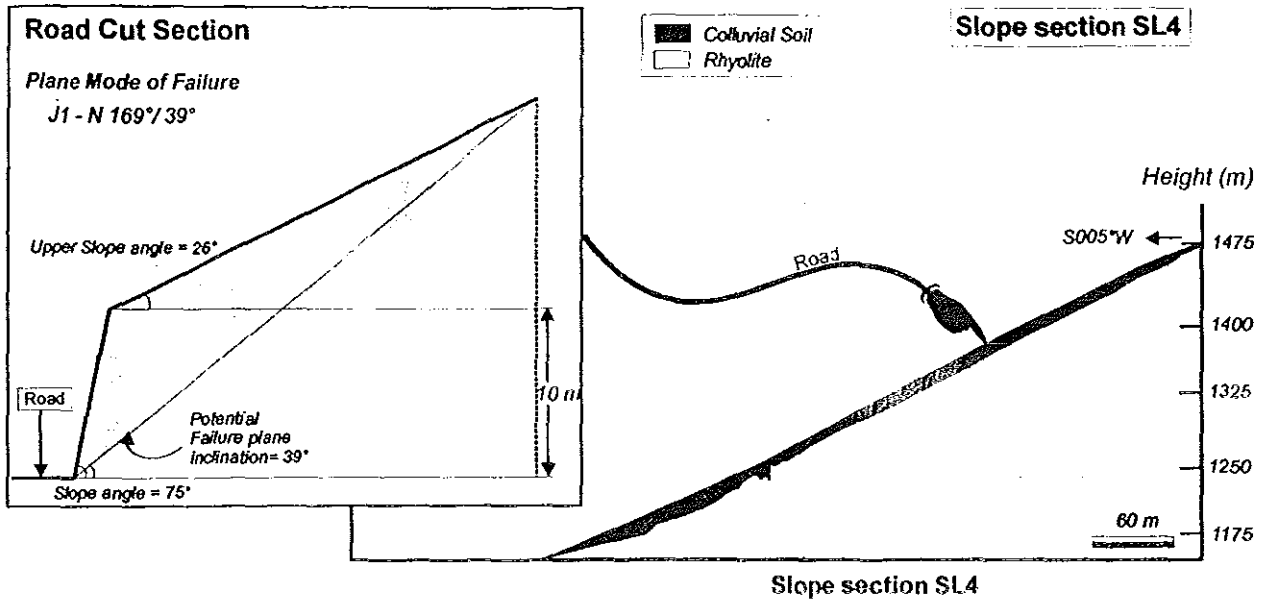


Fig. 5.3 (b) Geological Cross section and Geometry along critical slopes

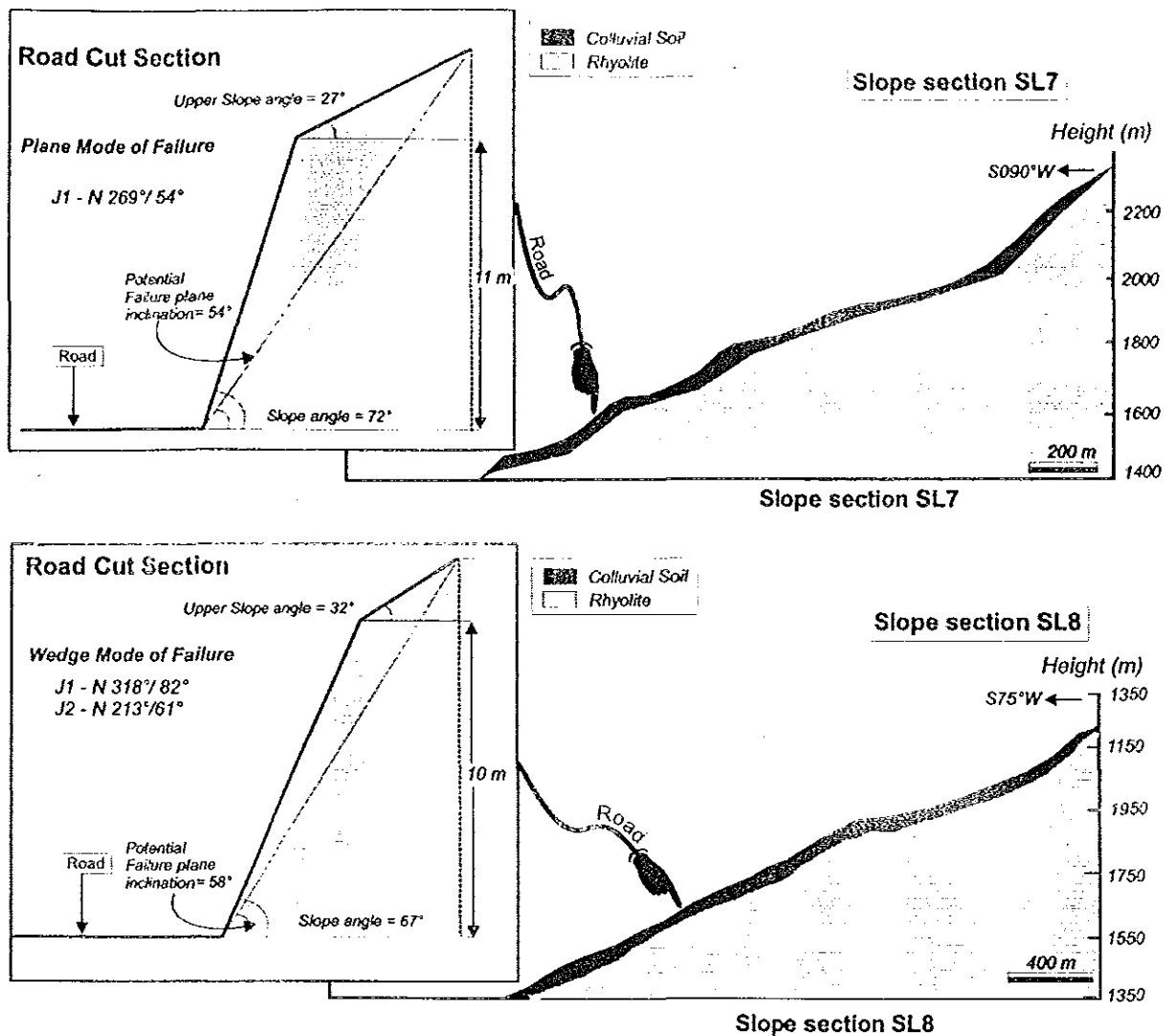


Fig. 5.3 (c) Geological Cross sections and the geometry along Critical slopes.

Table 5.6 The Geometry of Critical Slope Sections

Slope Section	Slope Face		Upper Slope Face		Height (m)
	Direction	Inclination	Direction	Inclination	
SL1	N 170 ⁰	75 ⁰	N 170 ⁰	17 ⁰	12
SL2	N 210 ⁰	74 ⁰	N210 ⁰	20 ⁰	15
SL3	N 335 ⁰	76 ⁰	N 335 ⁰	15 ⁰	18
SL4	N 185 ⁰	78 ⁰	N 185 ⁰	26 ⁰	15
SL5	N 315 ⁰	60 ⁰	N 315 ⁰	24 ⁰	18
SL6	N 080 ⁰	57 ⁰	N 080 ⁰	20 ⁰	19
SL7	N 270 ⁰	72 ⁰	N 270 ⁰	27 ⁰	11
SL8	N 270 ⁰	67 ⁰	N 270 ⁰	32 ⁰	10

5.6 Kinematic Check

Different types of slope failure are associated with different geological structures and it is important that the slope designer should be able to recognize the potential stability problems during the early stage of project. Markland developed a simple test which is designed to establish the possibility of a wedge failure in which sliding takes place along the line of intersection of two planar discontinuities. Plane failure is also covered by this test since it is a special case of wedge failure. If the contact is maintained on both planes, sliding can only occur along the line of intersection and hence this line of intersection must daylight in the slope face.

Thus, in a rock slope the failure will only occur if the following conditions are satisfied;

$$\text{Plane failure} \quad \alpha_f > \alpha_p > \phi \quad \dots 5.6$$

$$\text{Wedge failure} \quad \alpha_f > \alpha_i > \phi \quad \dots 5.7$$

Where:

α_f is the slope angle

α_p is the dip of the potential failure plane

α_i is plunge of the line of intersection

ϕ is the angle of internal friction of the two wedges forming plane

For the kinematics check, Markland test has been applied to all 8 critical rock slope sections. Structural data, along with slope inclination and a 'phi circle' corresponding to angle of friction of the rock mass has been plotted on equal area projection 'Schmidt Net'. The angle of friction has been estimated from the RMR data. Figure 5.4(a) & (b) presents the stereo plots to demonstrate Markland test for critical rock slope sections. It has been found that out of total 8 critical rock slope sections 7 slope sections satisfy the condition for Plane mode of failure (Plate 5.1), whereas, only one slope section satisfy the condition for wedge mode of failure. Two slope sections, namely SL9 and SL10 are soil slope sections and will have circular or rotational mode of failure. Thus, these slopes have been further analyzed for their Factor of safety under existing and anticipated worst conditions. Table 5.7 presents the possible mode of failures of critical slope sections in the study area.

5.7 Limit Equilibrium Analysis for Critical Slope Sections

Limit Equilibrium Method of analyzing stability of rock or soil slopes is a very effective and efficient method to quantitatively assess the stability condition of a slope. This method requires to determine Factor of Safety between the resisting forces to the driving forces.

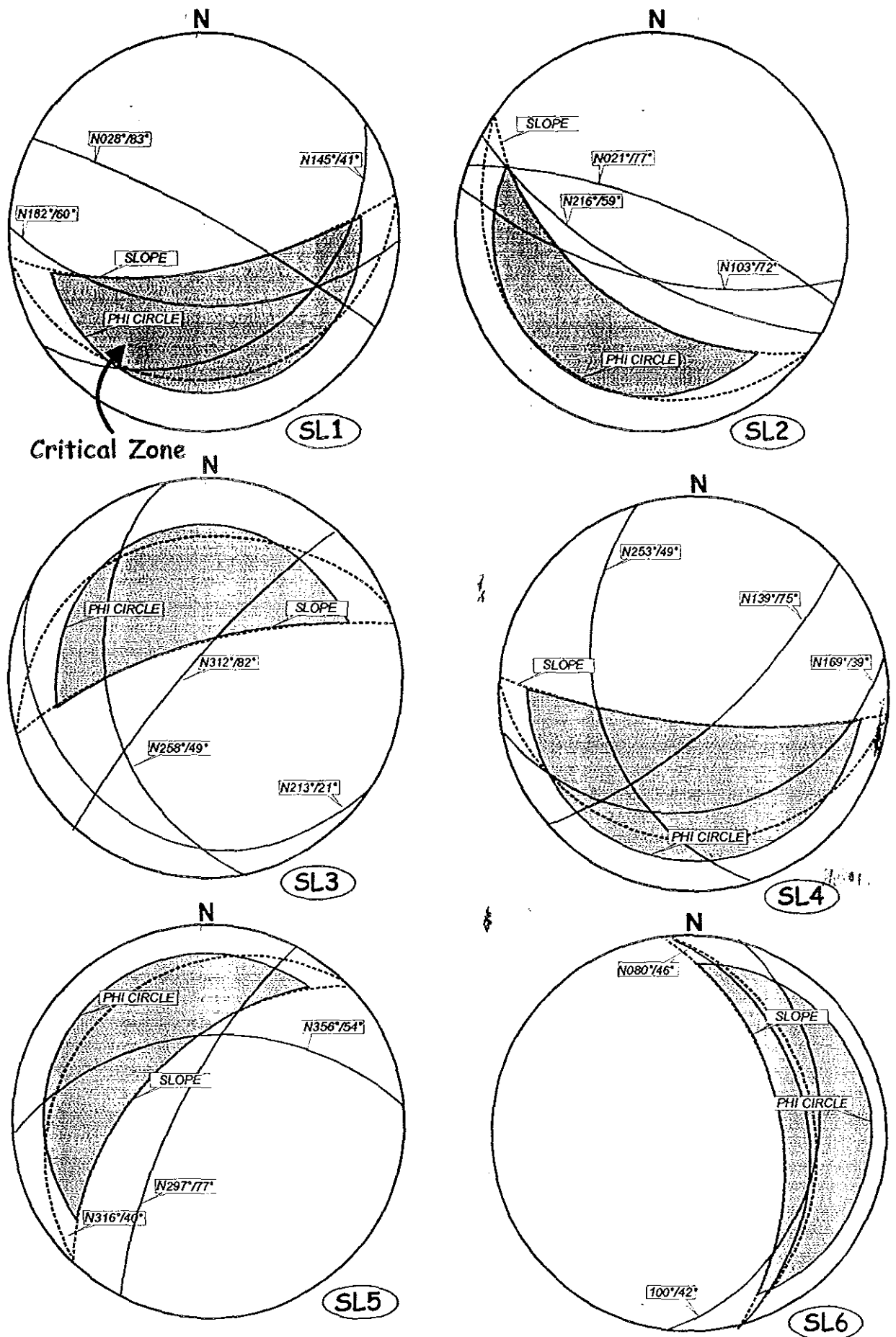


Fig.5.4 (a) Possible Mode of Failure in Critical rock slopes Sections

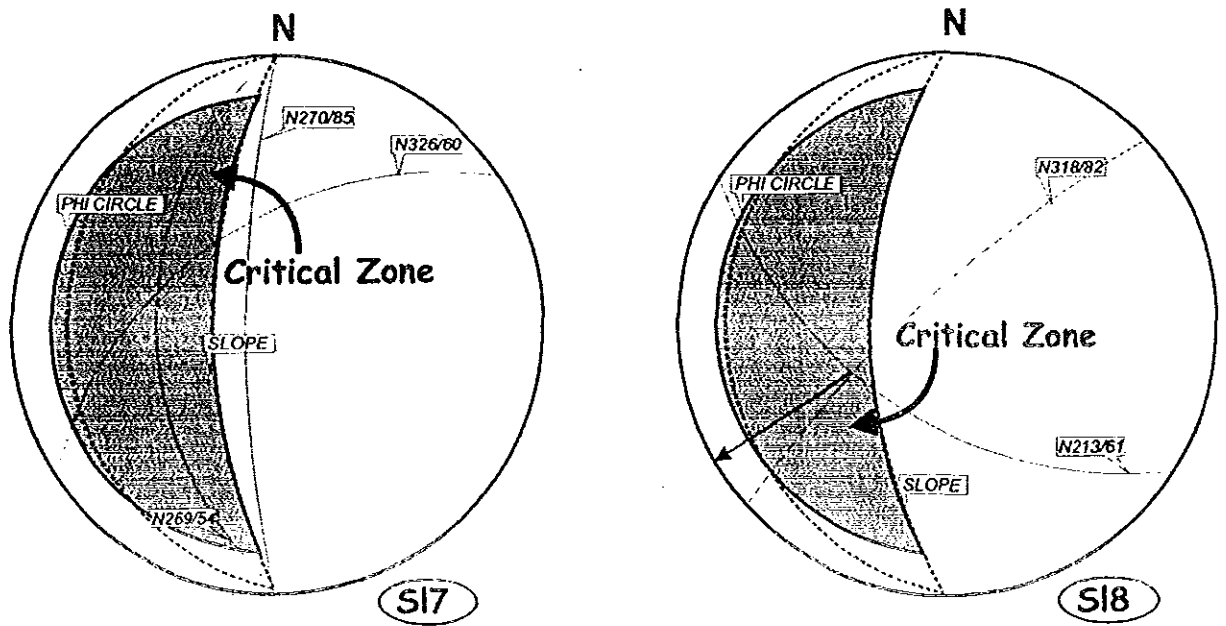


Fig. 5.4 (b) Possible Mode of Failure in Critical Rock slope Sections

The various forces involved in the stability condition of a rock slope are weight of the sliding rock mass over a failure plane or on two intersecting discontinuity planes, cohesive force on the discontinuity plane/s, uplift water forces acting along the discontinuity plane and the vertical water force acting on the back face of the tension crack.

Table 5.7 Possible mode of failures of critical slope sections in the study area.

Slope Section	Location (UTM)		Slope Section		Angle of Friction	Possible Mode of Failure		
	Northing	Easting	Direction	Slope Angle		Plane Failure	Wedge Failure	Circular Failure
SL1	858825	340029	N 170 ⁰	75 ⁰	20	J3 N 145 ⁰ /41 ⁰	No	No
SL2	858673	340632	N 210 ⁰	74 ⁰	21	J3 N 216 ⁰ /59 ⁰	No	No
SL3	859222	340494	N 335 ⁰	76 ⁰	21	J3 N 213 ⁰ /21 ⁰	No	No
SL4	859881	340976	N 185 ⁰	78 ⁰	14	J3 N 169 ⁰ /39 ⁰	No	No
SL5	860732	339014	N 315 ⁰	60 ⁰	14	J3 N 316 ⁰ /40 ⁰	No	No
SL6	862493	337117	N 080 ⁰	57 ⁰	17	J2 N 80 ⁰ /46 ⁰	No	No
SL7	863266	337521	N 270 ⁰	72 ⁰	16	J2 N 269 ⁰ /54 ⁰	No	No
SL8	863094	337661	N 270 ⁰	67 ⁰	16	No	W J1(N318/82), J2 (N213/61)	No
SL9	864996	339248	N 115 ⁰	68 ⁰	25 ⁰	No	No	Yes
SL10	863700	339160	N295 ⁰	61 ⁰	25 ⁰	No	No	Yes

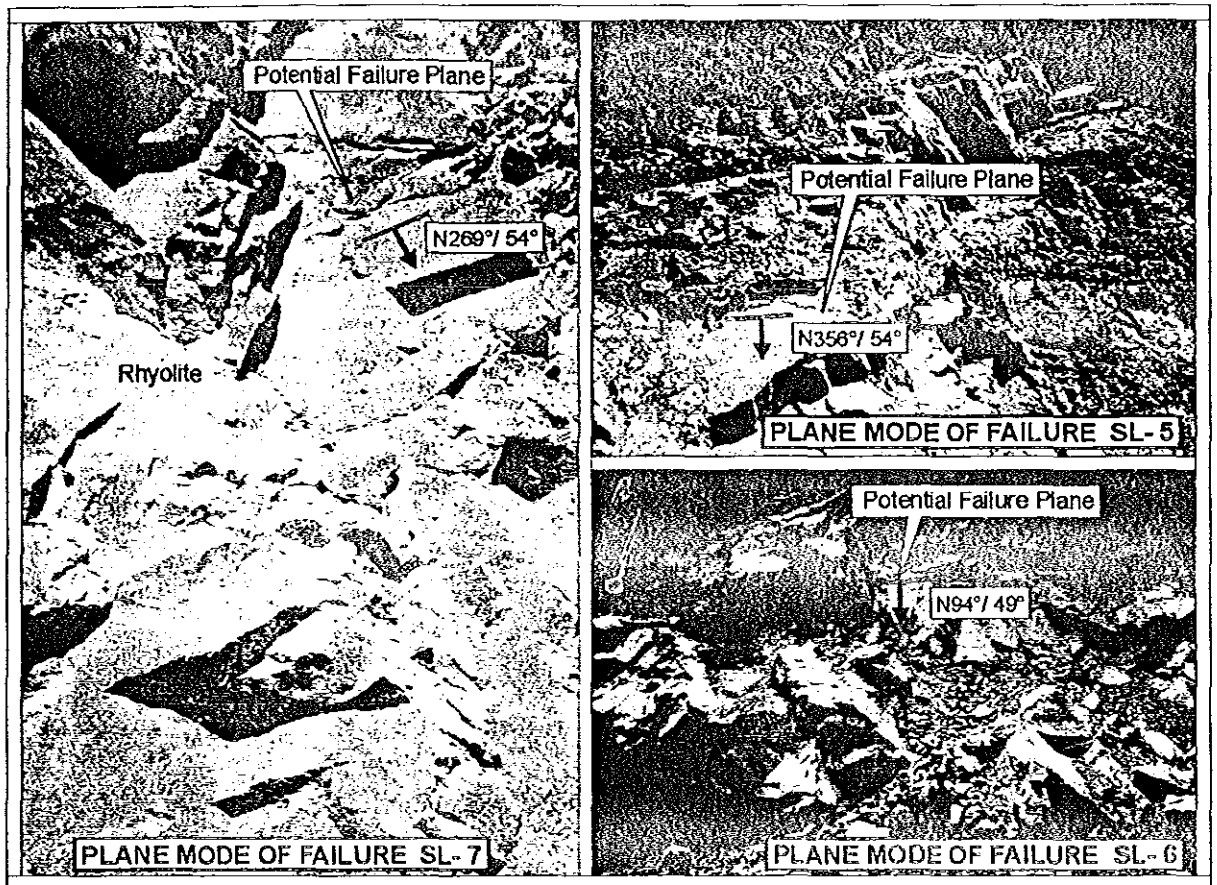


Plate 5.1 Possible plane mode of failure in rock mass

5.7.1 Factor of Safety analysis

Factor of safety (FOS) is the ratio of the total force available to resist sliding to the total force tending to induce sliding. For the present study, for all critical slope sections the factor of safety has been determined for static and dynamic conditions under varying water saturation situations. The factor of safety has been determined for existing and possible worst conditions, represented by following six conditions;

- i) Static dry condition – when slope is not subjected to any water saturation and static conditions prevail.
- ii) Static moderately saturated condition – when the slope is subjected to moderate saturation, this condition may occur during moderate rains and if static conditions prevail.
- iii) Static fully saturated condition – when the slope is subjected to full saturation, this condition may occur during very heavy rains and static conditions prevail.

- iv) *Dynamic dry condition* – when slope is not subjected to any water saturation and earthquake occurs.
- v) *Dynamic moderately saturated condition* – when the slope is subjected to moderate saturation, this condition may occur during moderate rains and during that period earthquake occurs.
- vi) *Dynamic fully saturated condition* – when the slope is subjected to full saturation, this condition may occur during very heavy rains and if during that period earthquake occurs.

Out of above 6 mentioned conditions, the existing condition of the critical slope sections is represented by static dry conditions. However, the possible anticipated worst conditions may be represented by Dynamic moderately saturated conditions. Since, the probability of Dynamic fully saturated conditions is very low as, it will be a very rare chance that earthquake activity occurs during very heavy rains. Thus, for all the critical slope sections the slopes has been designed for anticipated worst conditions.

5.7.1.1 Plane Mode of Failure Analysis

Plane failure occurs when the strike of the discontinuity plane is nearly parallel to the strike of the slope and daylight on the slope face. For the present study in total 7 critical slope sections satisfies the Markland condition for Plane failure. Therefore, these critical slope sections have been analyzed for their factor of Safety under static and dynamic conditions for varying water saturation situations.

The failure analyses have been carried out by using modified plane failure analysis technique of Sharma et al, 1995. This technique facilitates to account for inclined upper slope surface. The factor of safety, for slopes having plane mode of failure have been calculated for static and dynamic conditions under varied water saturated conditions. The saturation conditions have been represented as; dry slope; tension crack half filled; and tension crack completely filled with water. Fig 5.5 shows the geometry of slope and various force vectors involved in the analysis. In the modified technique of plane failure analysis (Sharma et al., 1995), the following assumptions have been made;

- i) For saturated condition the tension crack is fully filled with water. The water in the tension crack seeps along the failure surface and escapes out on the slope face through the sliding plane, where it day lights on the slope face.

- α_f - Slope face angle
- α_s - Upper slope surface angle
- α_p - Dip of potential failure plane
- α_t - Angle of tension crack
- h - Height of Slope
- Z - Height of tension crack
- W - Weight of sliding block
- U - Uplift water force acting on the block
- V - Water force in the crack acting on the rear face of the block

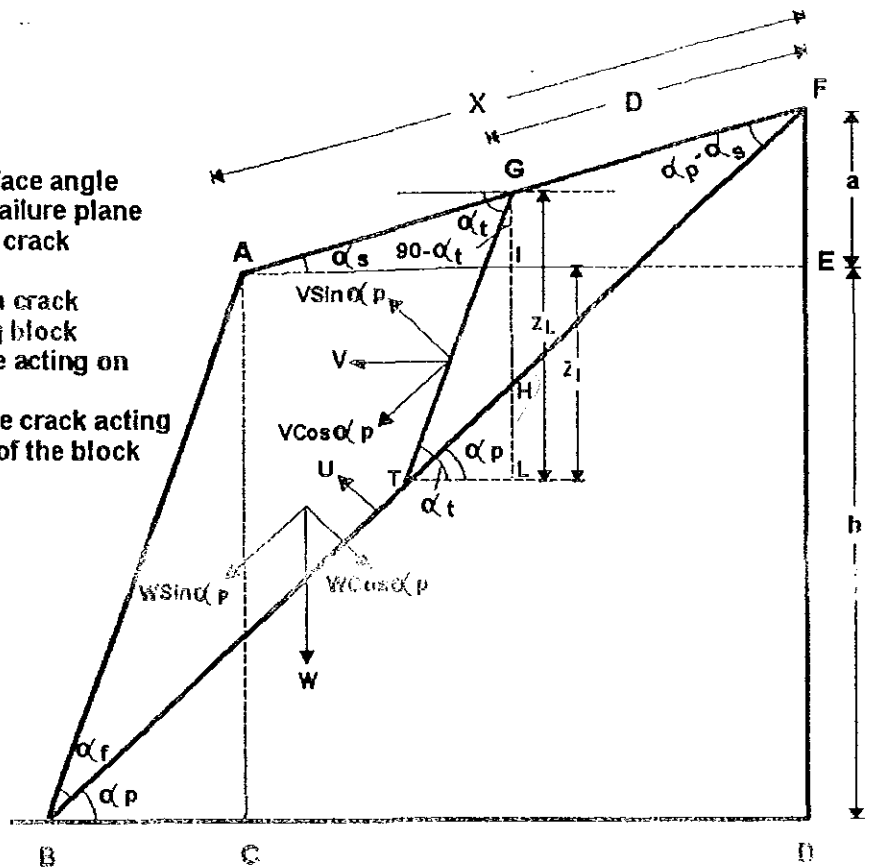


Fig. 5.5 Geometry of the slope for modified technique (Sharma et.al, 1995).

- ii) There is no resistance to sliding on the lateral boundaries of the sliding rock mass.
- iii) For moderately saturated condition the tension crack (Z_L) is half filled and the water level in the crack $Z_w = 0.5 Z_L$. The water in the tension crack seeps along the failure surface and escapes out on the slope face through the sliding plane, day lighting on the slope face.
- iv) For dry condition the rock mass is completely dry and $Z_w = 0$.
- v) The upper slope inclination must be less than the inclination of the failure plane, i.e. $\alpha_s < \alpha_p$.

As per the modified technique of plane failure analysis (Sharma et.al, 1995) the area, weight, horizontal water forces and uplift water forces are calculated by the following equations;

Area of sliding mass:

$$A = (h - Z_1) \operatorname{cosec} \alpha_p \quad \dots\dots\dots 5.8$$

Where:

$$Z_t = \frac{Z \sin \alpha_t}{(\sin \alpha_t - \tan \alpha_p \cos \alpha_t)} \quad \dots\dots 5.9$$

$$Z_l = Z_t - IG \quad \dots\dots 5.10$$

$$Z = h \left[\left(1 - \frac{\cot \alpha_f}{\cot \alpha_s} \right) + \sqrt{\frac{\cot \alpha_f}{\cot \alpha_p}} \times \left(\frac{\cot \alpha_p \cot \alpha_s}{\cot \alpha_s - 1} \right) \right] \quad \dots\dots 5.11$$

$$IG = \frac{h \left[\sqrt{\cot \alpha_f \cot \alpha_p} - \cot \alpha_f \right]}{\cot \alpha_s} \quad \dots\dots 5.12$$

Weight 'W' of the sliding mass:

$$W = \frac{1}{2} \gamma [(h+a)X - DZ_l] \quad \dots\dots 5.13$$

Where, γ is the unit weight of the rock, X and D are the slope distance A respectively and a is the height EF as shown in Fig. 5.5.

$$X = h \left(\frac{\cot \alpha_f}{\cos \alpha_s} \right) \times \left(\frac{\tan \alpha_p - \tan \alpha_f}{\tan \alpha_s - \tan \alpha_p} \right) \quad \dots\dots 5.14$$

$$D = \frac{Z}{\tan \alpha_p \cos \alpha_s - \sin \alpha_s} \quad \dots\dots 5.15$$

$$a = h \left(\frac{\tan \alpha_s}{\tan \alpha_f} \right) \times \left(\frac{\tan \alpha_p - \tan \alpha_f}{\tan \alpha_s - \tan \alpha_p} \right) \quad \dots\dots 5.16$$

Horizontal water force, V

$$V = \frac{1}{2} \gamma_w Z_w^2 \sin^2 \alpha_t \quad \dots\dots 5.17$$

Where, γ_w is the unit weight of water and Z_w is the water level in the tension crack.

Uplift water force, U

$$U = \frac{1}{2} \gamma_w Z_w \sin \alpha_t (h - Z_l) \operatorname{cosec} \alpha_p \quad \dots\dots 5.18$$

and moderate saturation conditions prevail, all 7 slope sections would be unstable, except for slope section SL 2 which has a FOS of 1.45.

Table 5.8 Input Parameters for the determination of Factor of Safety for Plane failure analysis of Critical Slope Sections

Slope Section	Slope angle α_f	Upper Slope angle α_s	Failure Plane angle α_p	Tension Crack angle α_t	Cohesion (ton/m ²) C	Angle of Friction ϕ	Unit weight (kN/m ³)		Horizontal Earthquake Acceleration α	Height (m) H
							Rock γ	Water γ_w		
SL 1	75°	17°	41°	63°	15	20°	2.41	1	0.08g	12
SL 2	79°	20°	59°	90°	16	21°	2.41	1	0.08g	15
SL 3	76°	15°	21°	90°	15.5	20.5°	2.41	1	0.08g	18
SL 4	78°	26°	39°	90°	8.5	13°	2.41	1	0.08g	15
SL 5	60°	24°	40°	77°	9	15°	2.41	1	0.08g	21
SL 6	57°	46°	49°	83°	12	20°	2.41	1	0.08g	19
SL7	72	27	54	85	10.5	15.5	2.41	1	0.08g	11

Therefore, there is a need to provide some form of remedial measures to the slope sections which have a FOS less than 1.0 for the anticipated adverse conditions. Though, slope section SL 2 and SL 7 demonstrates a FOS of 1.45 and 1.13, respectively for the existing slope geometry, but these may become unstable for other geometric configurations. The change of slope geometry is very likely to happen as the road is still in construction and the road widening is in progress. Therefore, keeping all considerations an attempt has been made to workout a safe design for all critical slope sections, including SL 2 and SL 7. The slope design and other remedial measures are discussed in detail in Chapter 6.

5.7.1.2 Wedge Mode of Failure Analysis

Wedge mode of failure occurs when two structural discontinuities planes strikes obliquely and there line of intersection daylight on the slope face (Plate 5.2). The sliding of rock mass will be on these two intersecting planes in the direction in which the line of intersection plunge. For the wedge failure to occur the kinematic condition defined as $\alpha_f > \alpha_i > \phi$ has to be satisfied. Where, ' α_f ' is the inclination of the slope face, ' α_i ' is the plunge of the line of intersection of the two wedge forming planes and ' ϕ ' is the angle of friction (Hoek and Bray, 1989).

In the study area only one slope section, SL8 satisfy the kinematic condition for wedge mode of failure. The two discontinuity planes involved in this slope section are J1 and J2 which have an orientation N318°/82° and N213°/61°, respectively. The plunge of line of intersection is oriented in N 232°/58°. The angle of friction as obtained from RMR and it is 16°. Thus,

detailed stability analysis for this slope has been carried out for static and dynamic conditions under varied water saturation conditions.

Table 5.9 Stability Condition of Critical Slopes having Plane Mode of Failure

Section Line	FACTOR OF SAFETY					
	Static Condition			Dynamic Condition		
	Dry	Moderately Saturated	Fully Saturated	Dry	Moderately Saturated	Fully Saturated
SL 1	0.42	0.35	0.16	0.36	0.28	0.13
SL 2	1.67	1.54	1.31	1.57	1.45	1.23
SL 3	1.06	1.04	1.00	0.85	0.84	0.81
SL 4	0.44	0.42	0.38	0.38	0.36	0.33
SL 5	0.62	0.58	0.52	0.56	0.51	0.46
SL 6	0.38	0.38	0.37	0.33	0.33	0.32
SL 7	1.19	1.22	1.07	1.21	1.13	0.91

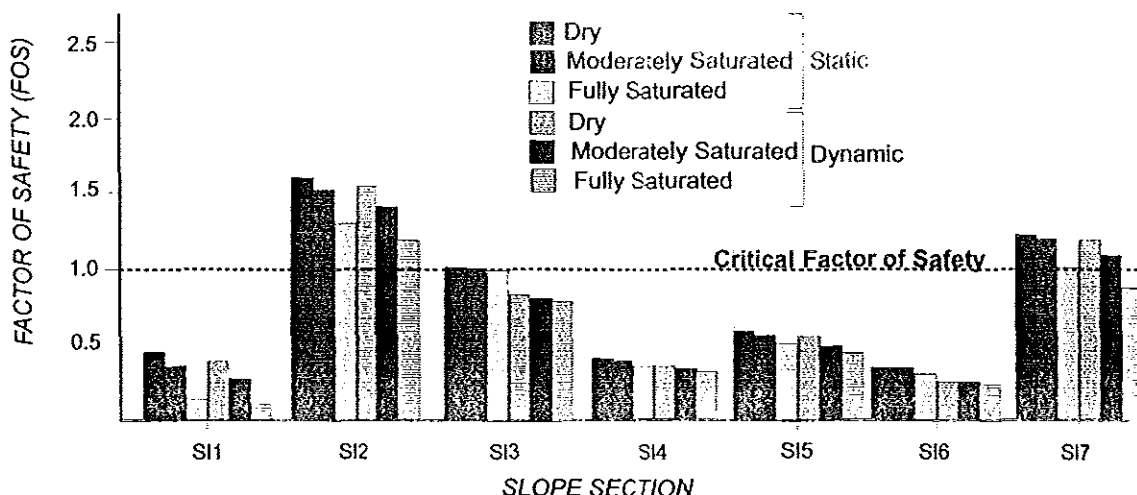


Fig 5.6 Stability condition of critical slopes having plane mode of failure for existing and anticipated worst conditions

In order to calculate the factor of Safety of SL8 having possible wedge mode of failure computer program SASW has been used. This computer program is based on the "Comprehensive Solution" of wedge failure proposed by Hoek and Bray (1989), a brief description about SASW is given at Annexure v.

The input parameters required for SASW Program are: number of slope; number of joint sets; number of cases; dip of the Ith joint plane (deg); C (I) cohesion of Ith joint plane (Ton/m²);

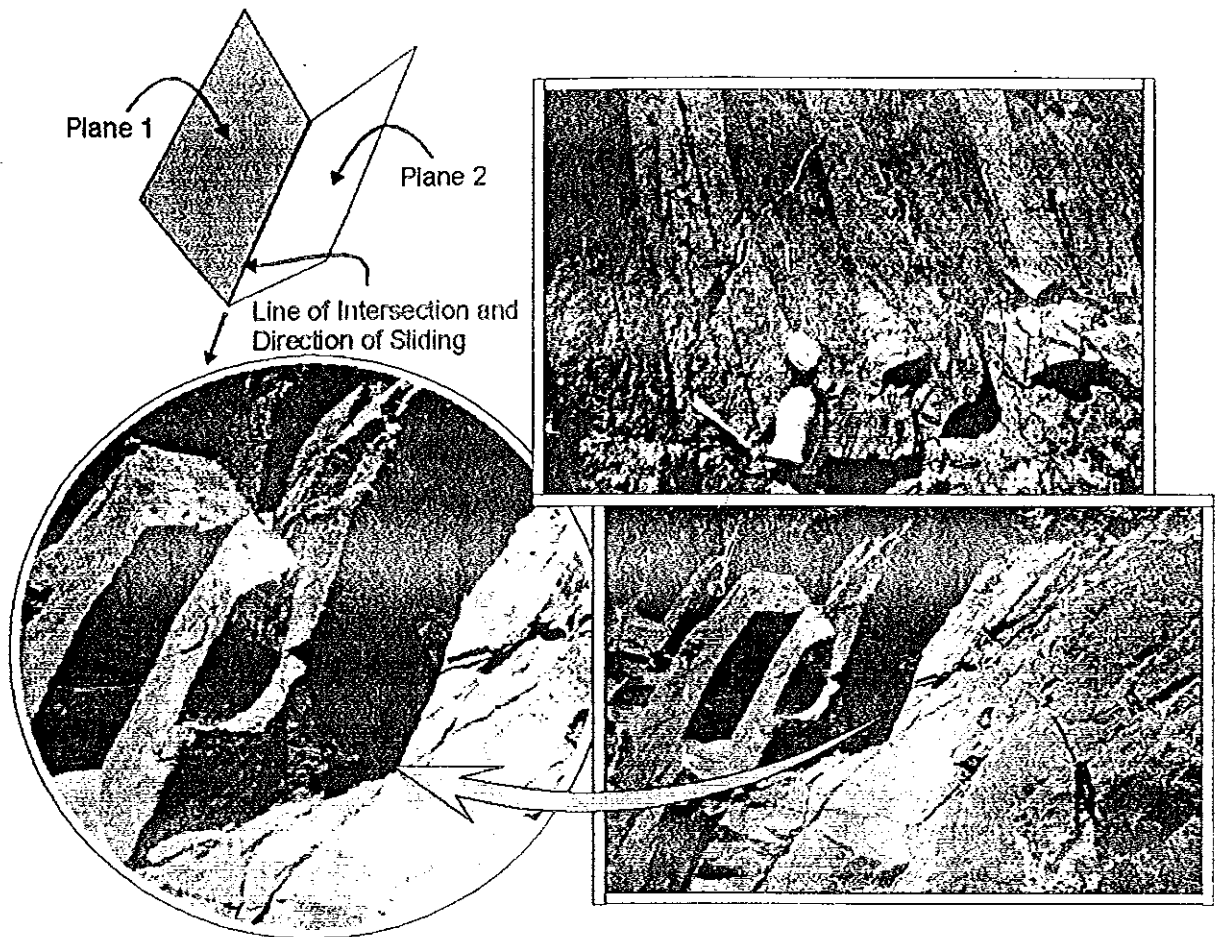


Plate 5.2 Wedge Mode of Failures along the road cut

friction angle (ϕ) of i th joint plane (deg); angle of slope of upper surface; dip direction of the upper surface; angle of rock slope; dip direction of the rock slope; height of the crest of the slope above toe of intersection; unit weight of the rock (γ_r); unit weight of water (γ_w); coefficient of horizontal acceleration near the crest of the slope (α); corresponding earth quake magnitude; water level above toe of intersection; and pore water pressure factor (0, for dry; 1, for wet slope).

Thus, the various input parameter used for the analysis of Slope SL8 are;

- i) Dip and dip direction of two wedge forming planes, this has been derived after analyzing the structural discontinuity data for their preferred orientation.
- ii) Slope geometry i.e. slope inclination, upper slope inclination and the height of the slope, obtained after preparing a slope cross section from topographical map on 1:50,000 and for road cut procuring cross section on 1:350 scale from the Project Authorities. The geometry of slope (SL8) is shown in Figure 5.3.

- iii) The shear strength parameters, cohesion 'C' and angle of friction ' ϕ ' have been derived from RMR data collected from the field (Table 5.1)
- iv) The horizontal earthquake acceleration ' α ' has been taken as 0.08g, the derivation of ' α ' has already been explained in the previous paragraph.

The input data sheet for critical slope section SL8 having wedge mode of failure is given at table 5.10.

The Factor of Safety has been calculated for SL8 critical slope sections having possible wedge mode of failure under static and dynamic conditions for varied water saturation conditions. The results thus, obtained are presented in Table 5.11.

Table 5.10 Input Data Sheet for Wedge failure Analysis for SL 8 Slope Section

<i>Input parameters</i>		<i>Road Cut Section</i>	<i>Entire Slope Section</i>
<i>Plane 1</i>	<i>Dip Direction</i>	N318°	N318°
	<i>Amount</i>	82°	82°
<i>Plane 2</i>	<i>Dip Direction</i>	N213°	N213°
	<i>Amount</i>	67°	67°
<i>Upper Slope Surface</i>	<i>Direction</i>	N270°	N270°
	<i>Inclination</i>	32°	32°
<i>Slope Face</i>	<i>Direction</i>	N270°	N270°
	<i>Inclination</i>	67°	32°
<i>Height of Slope</i>	<i>meters</i>	10	900
<i>Cohesion 'C'</i>	<i>Tons/m²</i>	11	
<i>Angle of friction 'ϕ'</i>	<i>degree</i>	20°	
<i>Unit weight of Rock</i>	<i>Tons/m³</i>	2.454	
<i>Unit weight of Water</i>	<i>Tons/m³</i>	1	
<i>Earthquake horizontal acceleration 'α'</i>	—	0.08	
<i>Corresponding earthquake magnitude (Richter Scale)</i>	—	7	
<i>Pore water pressure factor</i>	<i>No units</i>	0(dry), 0.5 (moderately saturated), 1.0 (fully saturated)	

Perusal of table 5.11 indicates that the road cut slope section is stable for the existing condition (static dry) and will remain stable even for dynamic conditions when it is dry but the entire slope section is not stable for existing and other anticipated conditions. However,

for anticipated worst condition represented as dynamic moderately saturated, both road cut slope section and the entire slope will be unstable, as for these conditions the FOS is zero. Therefore, there is a need to design suitable remedial measures for this slope section so that it will remain stable under the anticipated worst conditions.

Table 5.11 Stability Condition of Critical Slopes having Wedge Mode of Failure

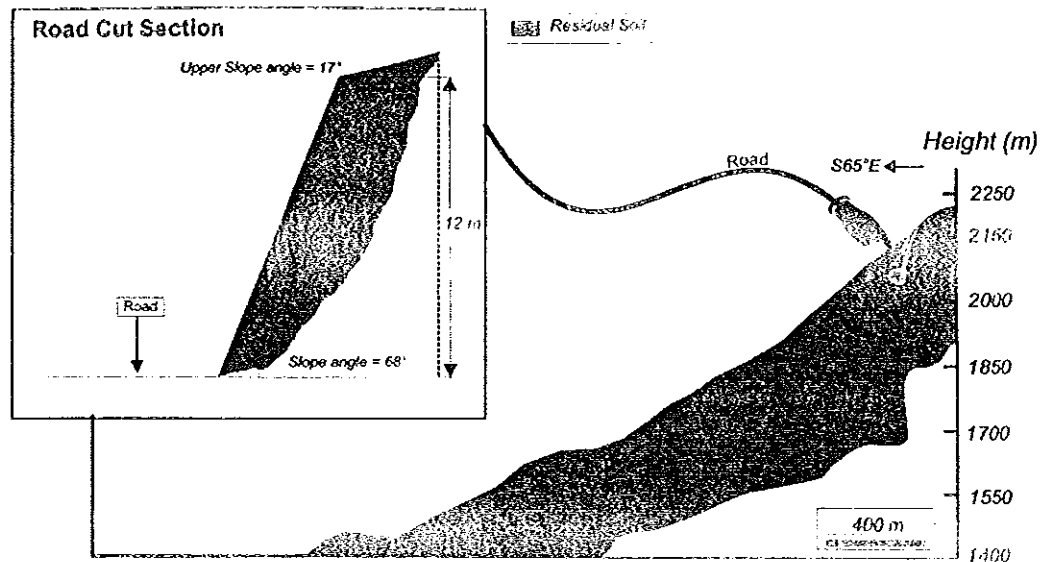
<i>Section Line</i>		<i>FACTOR OF SAFETY</i>					
		<i>Static Condition</i>			<i>Dynamic Condition</i>		
		<i>Dry</i>	<i>Moderately Saturated</i>	<i>Fully Saturated</i>	<i>Dry</i>	<i>Moderately Saturated</i>	<i>Fully Saturated</i>
SL 8	Road Cut Slope	22.8	0.0	0.0	20.9	0.0	0.0
	Entire Slope	0.57	0.0	0.0	0.56	0.0	0.0

5.7.1.3 Circular Mode of Failure Analysis

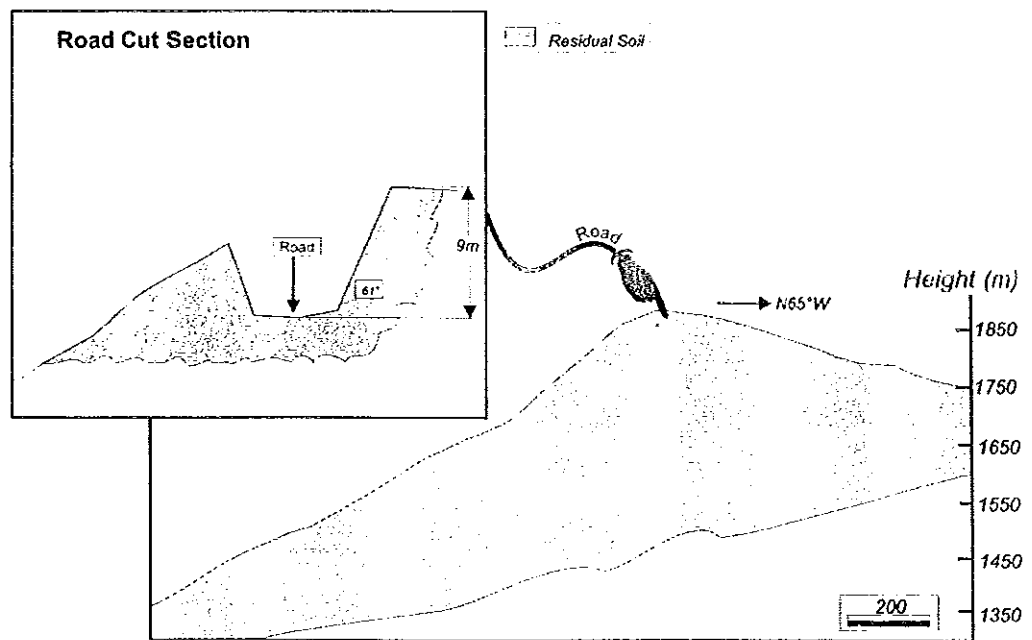
The conditions under which circular failure will occur arise when the individual particles in a soil or rock mass are very small as compared with the size of the slope and these particles are not interlocked as a result of their shape. In the case of soil, well defined structural pattern do not exists and the failure surface is free to find the line of least resistance through the slope. According to Hoek et al (1977), for circular failure analysis the following assumptions are made;

- i) The material forming the slope is assumed to be homogeneous, i.e its mechanical properties do not vary with direction of loading.
- ii) The shear strength of the material is characterized by a cohesion (c) and friction angle (ϕ) which are related by the equation, $\tau = c + \sigma \cdot \tan \phi$
- iii) Failure is assumed to occur on a circular surface, which passes through the toe of the slope.
- iv) A vertical tension crack is assumed to occur in the upper surface or in the face of the slope.
- v) The location of the tension crack and of the failure surface is such that the factor of safety is minimum for the slope geometry and the ground-water conditions considered.
- vi) A range of groundwater conditions, varying from a dry slope to heavy recharge, are considered in the analysis.

The northern part of the study area is covered with soil and according to the Total estimated hazard (TEHD) values, most of the soil covered areas fall under moderately hazard zone and low hazard zone. However, little soil covered areas fall under high hazard zone. In these zones based on the field manifestations of instability (as discussed in para. 5.2), two critical slope sections, namely SL9 and SL10, were identified (Fig. 5.1).



Slope Section SL 9



Slope section SL 10

Fig. 5.7 Critical Slope section for Rotational Mode of Failure

For the detailed stability analysis cross sections has been prepared (Fig 5.7) along both the critical slope sections, i.e. SL9 and SL10.

The Geometry of slope sections includes slope direction and inclination, upper slope direction and inclination and the height of the slope.

The stability analysis for circular mode of failure has been carried out by SARC computer program. This program is based on the Bishop's method of determining Factor of Safety for circular failure. The program calculates factor of safety for all possible slip circles and finally it workout slip surface for which factor of safety is minimum. It also provides the center and radius for the slip surface for which factor of safety is minimum. A brief description of SARC is given at Annexure V.

In order to perform the stability analysis, cross sections for each of the slope, has been prepared. The geological details for these cross sections were visually observed along the road cut and the natural outcrops. Further, the geological cross section prepared by the Project Authorities for the tunnel alignment has also been utilized to project the geology along the critical slope sections.



Plate 5.3 Critical soil slope section SL 10, having possible circular mode of failure

For the identification of soil present on both the critical slope sections, samples were collected and classification tests have been conducted. According to AASHTO classification, both soil slope sections has clayey soil with dry unit weight 16.7 kN/m^3 , and natural water content of 47.3% and 48.6% for SL9 and SL10 slope, respectively. The soils have also been classified as inorganic clay of low to medium plasticity with $LL=46\%$, $PL=25.9\%$, $PI=20.1\%$ for soils on SL9 slope section and $LL=48.5\%$, $PL=23.3\%$, $PI=25.2\%$ for soils present on SL10 slope section. The input data required for SARC has been presented in table 5.12.

The Factor of Safety has been calculated for both critical slope sections having possible Circular mode of failure under static and dynamic conditions for varied water saturation conditions. The results thus, obtained are presented in Table 5.13. Besides, the factor of safety has been calculated for the conditions when the cohesion will be zero, i.e. the worst condition which may occur in combination of other static and dynamic conditions under varied water saturation situations.

Table 5.12 Input data sheet for possible circular mode of failure.

Parameters	Critical Slope Sections	
	Slope section SL 9	Slope section SL 10
N	20	24
X(I), Z(I) I = 1 to N	(0,1364),(3,1364),(6,1365),(7,1366),(8,1367), (10,1368),(12,1369),(15,1372),(19,1375), (21, 1377),(24,1379),(25,1380),(27,1381),(29,1383) ,(32,1384),(34,1385),(36,1386),(39,1387),(43,1 387.5),(45,1387.8)	(0,1946),(1.35,1947),(2.8,1948),(6,1949), (8.6,1950),(11,1952),(13.6,1952.7),(17,195 4.4),(18,1955.5),(20.3,1956.6),(23.5,1958), (26,1959),(32,1961),(35,1963),(38,1964),(43,1964.4),(47,1964.3),(51,1964),(54,1964 ,(56,1964),(59,1963.8),(62,1963.7),(65,196 3),(68,1962.4)
C	0	0
PHI	25	25
GAMA	1.7	1.7
GAMAW	1	1
BBAR	0.0 (Dry), 0.1(MS), 0.2 (FS)	0.0 (Dry), 0.1(MS), 0.2 (FS)
AH	0.4 (Dynamic), 0 (Static)	0.4 (Dynamic),0 (Static)
AVR	0.08	0.08
EQM	7(Dynamic), 0 (Static)	7(Dynamic), 0 (Static)
NENP	0	0
ENTX (I)	0	0
ENTY (I)	1364	1946
NEP	0	0
NOPT	0	0
XEXITI	10	11
XEXITL	36	62
GAP	26	51
N	Number of profile coordinates (<50)	
(X,Z)	Coordinates of profile points	
C	Cohesion of soil	
PHI	Angle of shearing resistance	
GAMA	Unit weight of soil	
GAMAW	Unit weight of water	
BBAR	Pore water pressure/ (GAMA*Average Height of slice)	
AH	Horizontal component of earthquake acceleration near crest of slope	
AVR	Vertical component of earthquake acceleration /AH	
EQM	Corresponding earthquake magnitude on Richter Scale	
NENP	Number of entry points of slip surface	
ENTX	X-coordinate of entry point of circle	
ENTY	X-coordinate of entry point of circle	
NEP	Number of exit points (0, when no individual point is given)	
NOPT	0 when only minimum factor of safety is required, 1 when all FOS	
XEXITI	X-coordinate of first exit point of circle	
XEXITL	X-coordinate of last exit point of circle	
GAP	Horizontal distance between consecutive exit points	

Perusal of table 5.13 indicates that slope SL9 is stable for existing conditions (Static dry condition) as the factor of safety is 2.53. The slope will remain stable even for anticipated worst condition (dynamic moderately saturated condition) as the FOS for this condition is 1.23. However, if somehow, the cohesion for soil mass becomes zero the slope will be

unstable for all static and dynamic condition, though practically it would be very rare chance that cohesion becomes zero.

Table 5.13 Stability Condition of Slope having possible wedge mode of failure

<i>Slope Section</i>	<i>Condition</i>	<i>FOS</i>	<i>Weight of wedge</i>	<i>Coordinate of center of critical slip circle</i>	<i>Exit point of slip circle</i>	<i>Radius of slip circle</i>
SL 9	SD, C=7.1T/m ²	2.53	.50E+03	(10.17, 1387.81)	(36.00, 1386.00)	25.89
	SD, C=0	0.79	.56E+03	(-1.05, 1406.18)	(36.00, 1386.00)	42.19
	SMS, C=7.1T/m ²	2.40	.52E+03	(10.47, 1387.32)	(36.00, 1386.00)	25.57
	SMS, C=0	0.69	42.19	(-1.05, 1406.18)	(36.00, 1386.00)	42.19
	SFS, C=7.1T/m ²	2.26	.52E+03	(10.55, 1387.20)	(36.00, 1386.00)	25.48
	SFS, C=0	0.58	.56E+03	(-1.05, 1406.18)	(36.00, 1386.00)	42.19
	DD, C=7.1T/m ²	1.31	.55E+03	(11.18, 1386.17)	(36.00, 1386.00)	24.82
	DD, C=0	0.39	.56E+03	(-1.05, 1406.18)	(36.00, 1386.00)	42.19
	DMS, C=7.1T/m ²	1.23	.55E+03	(11.18, 1386.17)	(36.00, 1386.00)	24.82
	DMS, C= 0	0.33	.56E+03	(-1.05, 1406.18)	(36.00, 1386.00)	42.19
	DFS, C=7.1T/m ²	1.15	.55E+03	(11.18, 1386.17)	(36.00, 1386.00)	24.82
	DFS, C=0	0.39	.56E+03	(-1.05, 1406.18)	(36.00, 1386.00)	42.19
SL 10	SD, C=7.1T/m ²	3.70	.14E+04	(22.09, 1986.06)	(62.00, 1963.70)	45.74
	SD, C=0	1.10	.10E+02	(-6.12, 1970.30)	(11.00, 1952.00)	25.06
	SMS, C=7.1T/m ²	3.45	.14E+04	(22.09, 1986.06)	(62.00, 1963.70)	45.74
	SMS, C=0	0.94	.10E+02	(-6.12, 1970.30)	(11.00, 1952.00)	25.06
	SFS, C=7.1T/m ²	3.45	.11E+04	(22.06, 1994.82)	(62.00, 1963.70)	50.63
	SFS, C=0	0.89	.49E+01	(2.88, 1958.23)	(11.00, 1952.00)	10.23
	DD, C=7.1T/m ²	1.41	.18E+04	(25.64, 1973.62)	(62.00, 1963.70)	37.69
	DD, C=0	0.47	.10E+02	(-6.12, 1970.30)	(11.00, 1952.00)	25.06
	DMS, C=7.1T/m ²	1.25	.14E+04	(21.42, 1988.40)	(62.00, 1963.70)	47.51
	DMS, C=0	0.40	.10E+02	(-6.12, 1970.30)	(11.00, 1952.00)	25.06
	DFS, C=7.1T/m ²	1.18	.15E+04	(22.89, 1983.26)	(62.00, 1963.70)	43.73
	DFS, C=0	0.31	.10E+02	(-6.12, 1970.30)	(11.00, 1952.00)	25.06
SD	<i>Notations used in the table</i>					
SMS	Static Dry					
SFS	Static Moderately Saturated					
DD	Static Fully Saturated					
DMS	Dynamic Dry					
DFS	Dynamic Moderately saturated					
C	Dynamic Fully Saturated					
FOS	Cohesion					
	Factor of Safety					

From the results, the stability condition of slope SL10 is similar to that of SL9 as for existing condition (Static dry condition) the slope is stable as the factor of safety is 3.70. The slope will remain stable even for anticipated worst condition (dynamic moderately saturated condition) as the FOS for this condition is 1.25. However, for the condition when cohesion of the soil mass becomes zero the slope will be critically stable (FOS = 1.1) for the existing condition, but for anticipated worst conditions this slope will be unstable.

The slopes which are susceptible to failure by various modes like, plane, wedge or circular mode of failures can be stabilized by various methods. These methods could be as simple as altering the geometry of the slope or comparatively complicated and difficult like providing reinforcement and retaining structures. The important factors which influence the stability of the slope are; i) slope angle ii) dip of the failure plane or plunge of the line of intersection of two wedge forming planes iii) shear strength parameters, cohesion and angle of internal friction and finally the water saturation condition.

For the stability condition either of the above mentioned factors may have comparatively high or low influence. Some of the factors may be responsible in inducing the forces for sliding where as, the others may contribute in providing the resistance to the sliding. The net result of these factors will define whether the slope is going to slide, under the given conditions, or it will be stable. The relationship of the factors responsible for inducing sliding and the factors responsible to provide resistance to the sliding is defined by the limit equilibrium. Factor of safety can be defined as the ratio of the total forces available to resist sliding to the total forces available to induce sliding. If the factor of safety is less than unity, it implies that the resistive forces are less than that of the forces which induce sliding. Thus, for the condition when the FOS is less than 1.0 the slope may fail, provided it is subjected to a triggering factor, natural or man made. The factor of safety of a potential unstable slope may be improved by providing several methods such as, safe slope design by altering the geometry of the slope, reinforcement by providing rock bolts, retaining structures, shotcreting etc.

6.1 Overall Stability Condition

In the present study it has been identified that there are ten critical slope sections out of which 7 slope sections have potential plane mode of failure, 1 slope section accounts for wedge mode of failure and remaining 2 slope sections are potentially unstable for possible rotational mode of failure. Figure 6.1 shows the overall stability condition of critical slope sections.

The detailed stability analysis of the critical slope sections having possible plane mode of failure indicates that for the existing conditions i.e static dry, only 2 slope sections (SL2 and SL 7) are stable, the remaining 5 slope sections (SL1, SL3, SL4, SL5 and SL6) are unstable. For the anticipated adverse condition (AAC), represented by moderate saturation with

dynamic condition, slope SL2 is stable and slope SL7 is critically stable. However, the remaining slope sections (SL1, SL3, SL4, SL5 and SL6) would be unstable for AAC. Therefore, there is a need to provide some form of remedial measures to the slope sections which have a FOS less than 1.0 for the anticipated adverse conditions (AAC). Though, slope section SL 2 and SL 7 demonstrates a FOS of 1.45 and 1.13, respectively for the existing slope geometry, but these may become unstable for other geometric configurations. The change of slope geometry is very likely to happen as the road is still in construction and the road widening is in progress. Therefore, keeping all considerations an attempt has been made to work out a safe design for all critical slope sections, including SL 2 and SL 7.

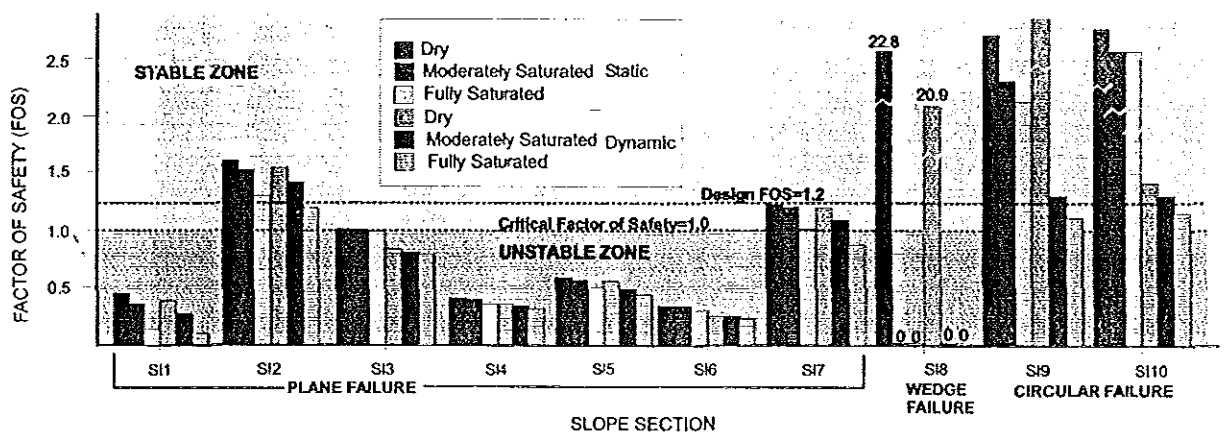


Fig. 6.1 Overall Stability of critical slopes under existing and possible worst conditions

The stability condition of road cut section having wedge mode of failure (SL8) will be stable for the existing conditions. However, for the entire slope section of SL8 demonstrates a FOS less than one, indicating slope is unstable for existing condition. For the AAC the road cut section and the entire slope section of SL8 is unstable. Therefore, some form of remedial measure has to be provided to this slope section.

The stability condition of slope sections having rotation mode of failure indicates that both the slope sections (SL9 and SL 10) are stable for existing and anticipated worst conditions. The slope sections are even stable for the dynamic full saturated conditions. However, for the worst condition when cohesion is taken zero both the slope sections become unstable. Though practically cohesion can never be zero, particularly for the soils present on these slope sections, which are clay soils (CL).

6.2 Remedial Measures for Slope Sections Having Plane Mode of Failure

6.2.1 Slope Design

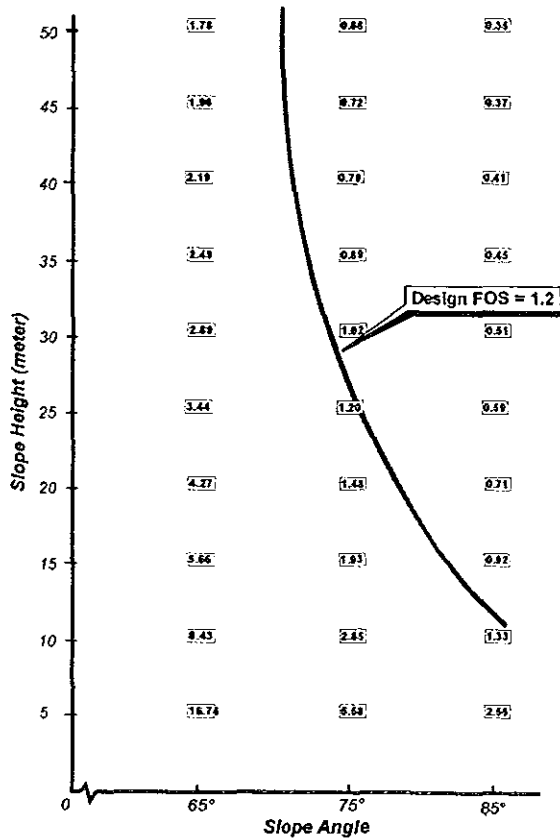
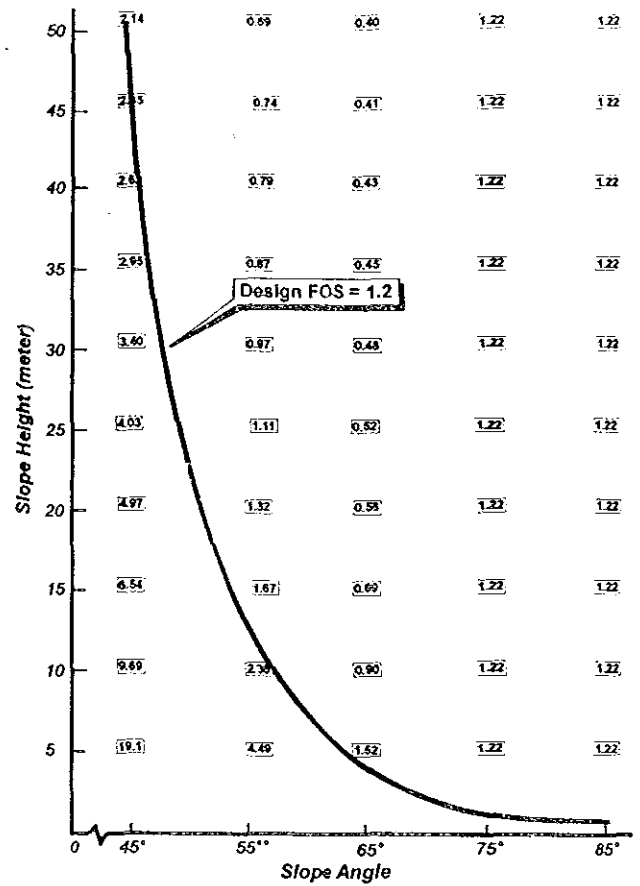
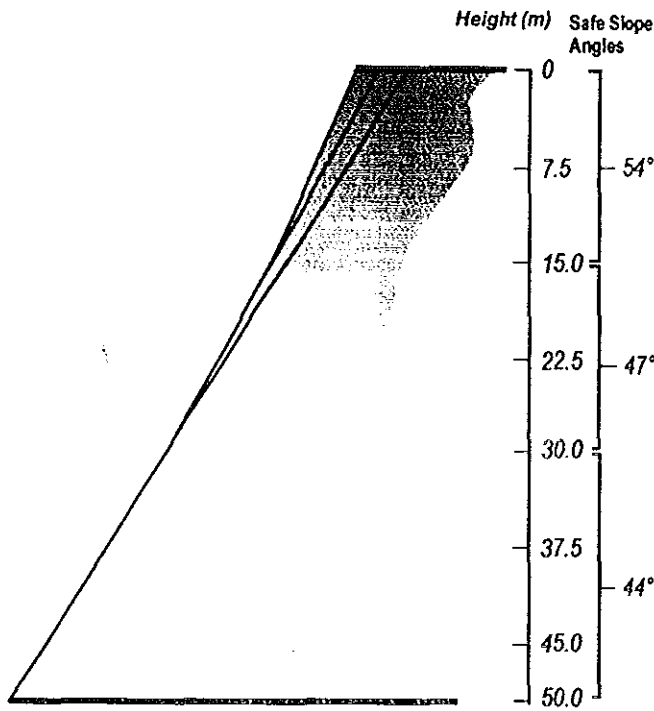
The safe slope angles for a given slope can be obtained by adopting technique proposed by Hoek and Bray, 1989. In this technique, the factor of safety is obtained by assuming different slope angles and slope heights. The factor of safety, as calculated for each combination of slope angle and slope height, is marked over a graph sheet by taking slope angles on X-axis and height on Y-axis. Later, a contour curve corresponding to a factor of safety equal to 1.2 is drawn. Thus, the safe slope angles for different slope heights are obtained from this graph. Based on these safe slope angles a slope cross section is prepared in which height of the slope is considered from top to bottom.

In the present study for the critical slope sections having plane mode of failure a safe slope design has been worked out by adopting the technique proposed by Hoek and Bray, 1989. For this purpose for each critical slope section the height is varied from a minimum to a maximum value for a given slope angle. Similarly the slope angle for each slope has been varied from a minimum (more than failure plane angle) to a maximum upto 85° . The factor of safety has been determined for the anticipated adverse conditions represented by moderately saturation with dynamic condition. Thus, the calculated factor of safety for each combination of slope angle and slope height is plotted over a graph in which the slope angle is taken on the X axis and the height is taken on Y axis. Further, a contour representing a FOS of 1.2 has been drawn over the graph to work out the safe slope angles. Hoek and Bray (1989) have recommended safe design FOS equal to 1.2 for the road cuts. The safe slope angles for different heights, as determined by the above techniques are presented in Table 6.1. Figure 6.2(a,b,c) shows the design for SL 1, SL2, SL3,SL4,SL5 and SL7 slope sections.

6.2.2 Rock Bolting

Rock bolts are used to reinforce jointed rock much as reinforcing bars supply tensile resistance in reinforced concrete. In rock slope, tunneling and underground mining, steel rod inserted in a hole drilled in the face of a rock formation to support the sides or roof of the excavation. These are equally effective in natural and cut slopes, as these rock bolts act as a binding tools between the two rock blocks on the either sides of the discontinuity plane. The bolt may be provided with an expanding device to grip the rock at the far end of the hole or

Slope Section SI1



Slope Section SL2

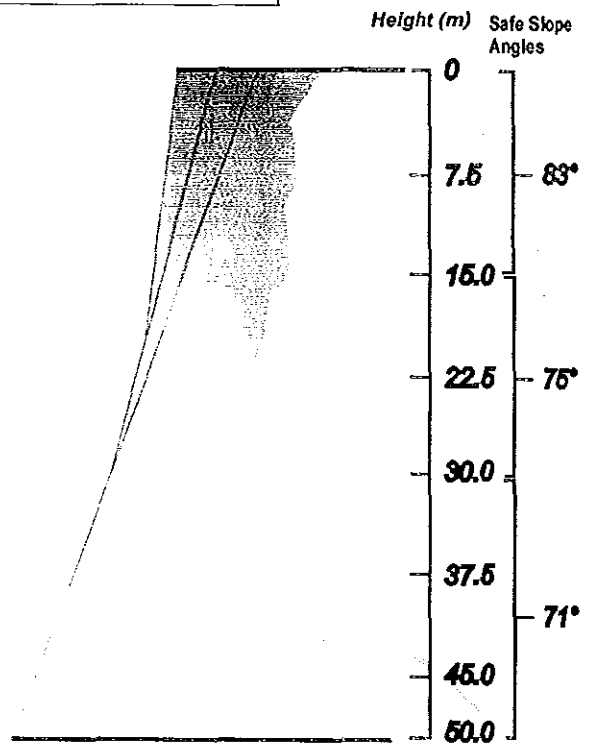


Fig. 6.2 (a) Slope Design and safe slope angles for anticipated worst conditions

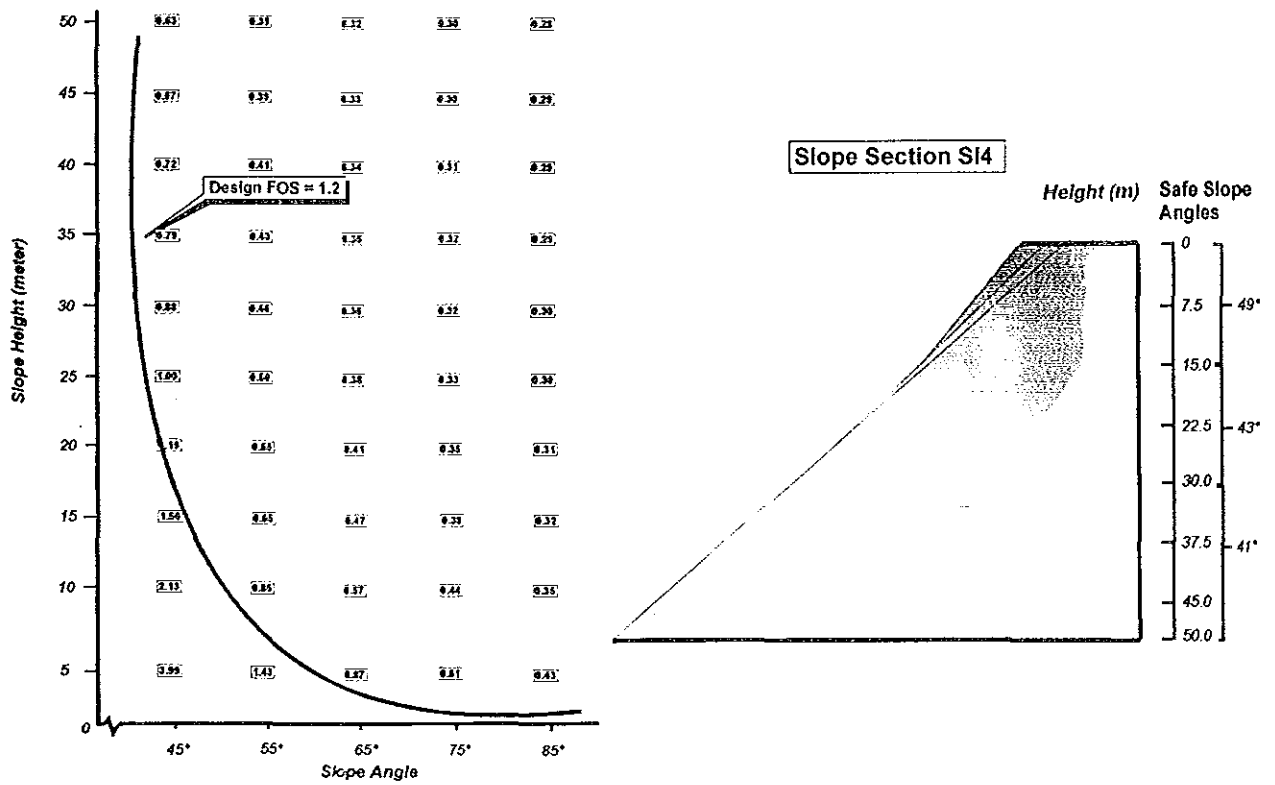
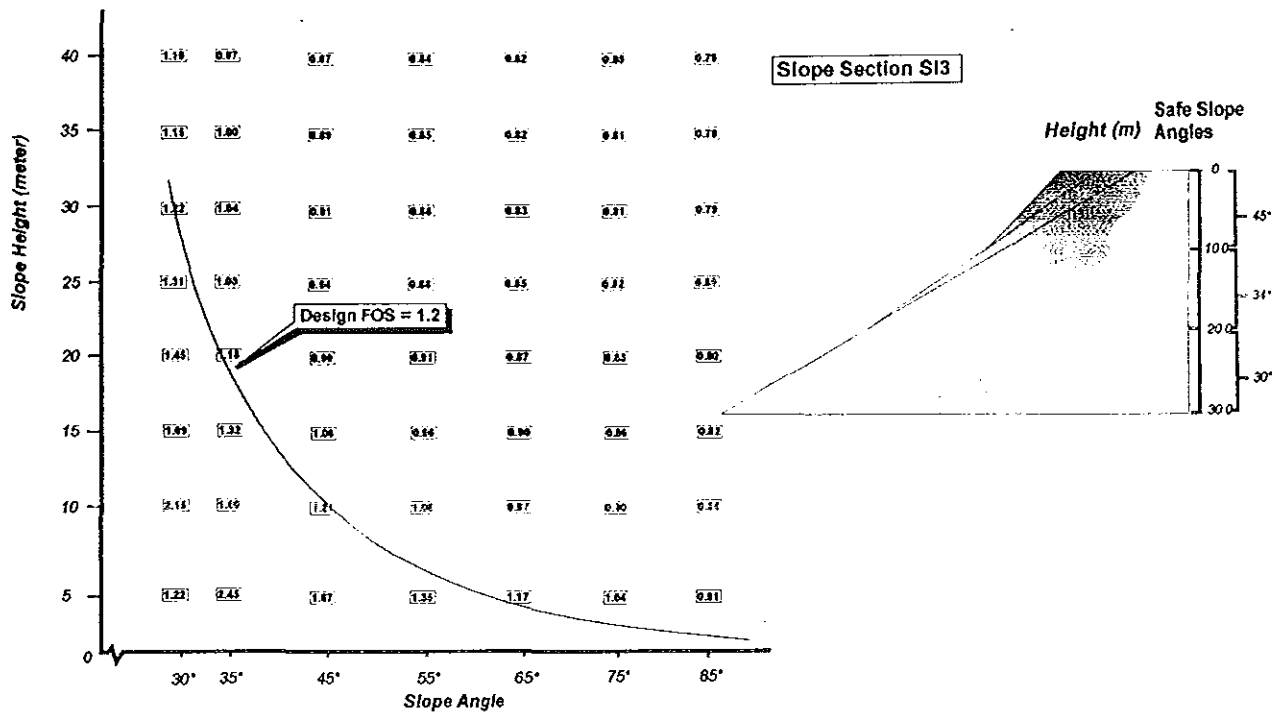
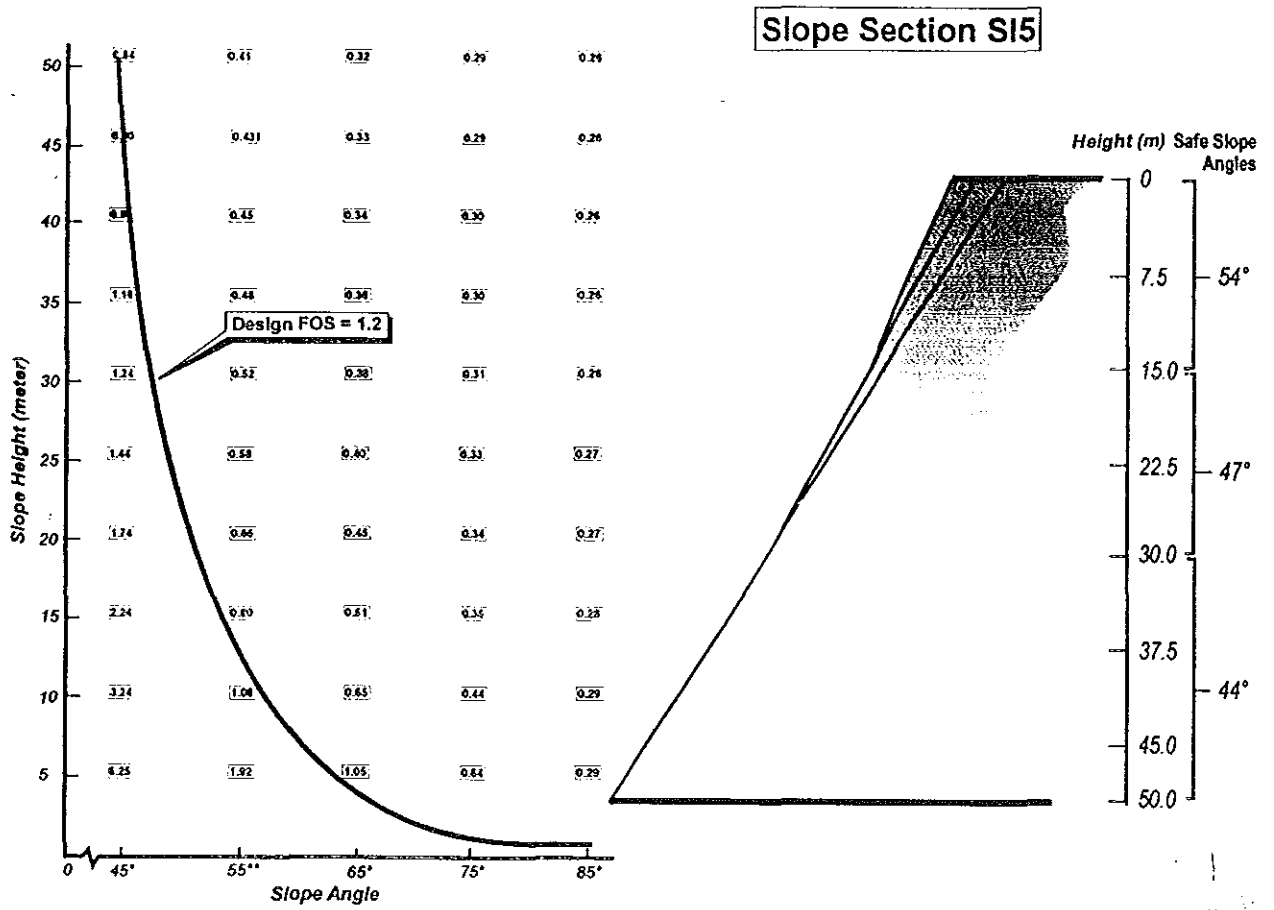


Fig. 6.2(b) Slope Design and safe slope angles for anticipated worst conditions



Slope Section SL7

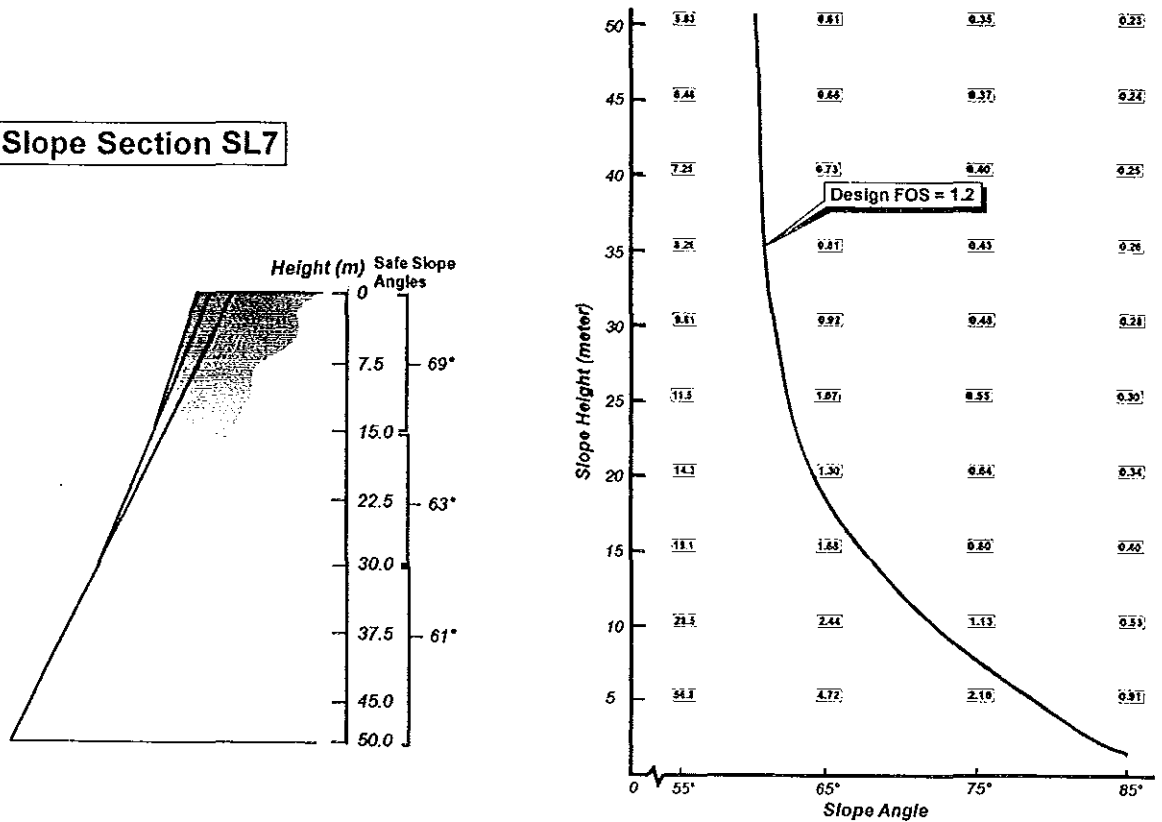


Fig.6.2 (c) Slope Design and safe slope angles for anticipated worst conditions

may be bonded to the rock by means of expanding cement. Rock bolts may be used singly or in rows. There are static and tensioned rock bolts. Tensioned rock bolts should be used only where a force is needed to counteract the forces making the structure unstable.

Table 6.1 Safe slope Design angles for different height

Slope Section	Height* (m)	Slope Angle	Slope Section	Height* (m)	Slope Angle
SL 1	0 - 15	54°	SL 2	0 - 15	83°
	15 - 30	47°		15 - 30	75°
	30 - 50	44°		30 - 50	71°
SL 3	0 - 10	45°	SL 4	0 - 15	49°
	10 - 20	34°		15 - 30	43°
	20 - 30	30°		30 - 50	41°
SL 5	0 - 15	54°	SL 7	0 - 15	69°
	15 - 30	47°		15 - 30	63°
	30 - 50	44°		30 - 50	61°

* Height is measured from top to bottom

In most cases static bolts should be used. The logic behind a static bolt is that if the structure is safe enough to drill into and install rock bolts, it already has an inherent factor of safety. If the stability of the structure is adversely affected in the future the static bolt will automatically go into tension with the exact amount of force and in the exact location that it should.

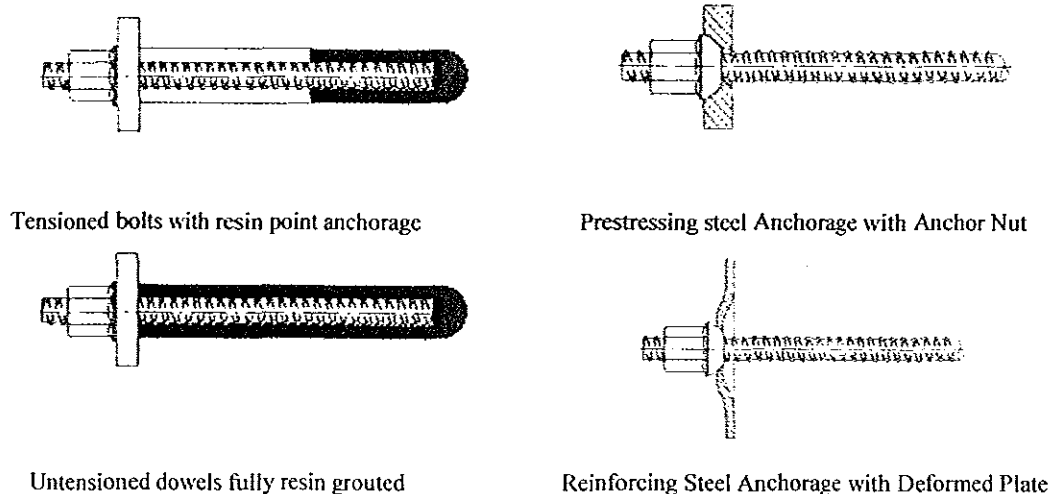


Fig 6.3 Different Type of Rock Bolts

Slope Section SL6 can not be stabilized by altering its geometry, as the factor of safety calculated for various combinations of slope angle and slope height is less than unity. Therefore, this slope section may be stabilized by providing rock bolts. An attempt has been

made to work out the reinforcement force and the number of rock bolts required to stabilize this slope section. For this purpose a factor of safety is considered as 1.2 and the required reinforcement force has been calculated by using eq. 6.1 or eq 6.2. The reinforcement force has been calculated for anticipated adverse conditions. However, the other factors like weight, area, uplift water pressure and the water pressure in tension crack has been calculated by using equations 5.8 to 5.18 (Chapter 5).

The reinforcement force for static condition is determined by using eq. 6.1. where the FOS is taken equal to 1.2

$$F = \frac{CA + (W \cos \alpha_p - U - V \sin \alpha_p) \tan \phi}{W \sin \alpha_p + V \cos \alpha_p - T \cos \beta} \quad \dots\dots\dots 6.1$$

The reinforcement force for static condition is determined by using eq. 6.2. where the FOS is taken equal to 1.2

$$F = \frac{CA + [W(\cos \alpha_p - \alpha \sin \alpha_p) - U - V \sin \alpha_p] \tan \phi}{W(\sin \alpha_p + \alpha \cos \alpha_p) + V \cos \alpha_p - T \cos \beta} \quad \dots\dots\dots 6.2$$

Where, C is the cohesion, α is the horizontal earthquake accelerations, ' β ' is an angle of the bolt installed from plane of sliding plane and 'T' is the bolt tension. The horizontal earthquake acceleration has been taken as 0.08g, since the study area falls in MM intensity scale 7 (Fig. 1.4) therefore, the horizontal acceleration for MM intensity 7 will fall in 0.07 to 0.1 ranges (Johnson et al., 1988). An average value 0.08g has been considered for the present analysis.

Table 6.2 Recommended bolt number and separation of bolts for SL 6 slope section

Installation Angle (β)	Total Reinforcement Force (Tons)	No of Bolts of 11 Tons/m ²	Separation of Bolts (m)
45°	38.74	4	3.56
51°	41.27	4	3.34
57°	44.68	4	3.09
65°	51.19	5	2.70
73°	61.30	6	2.25
79°	73.08	7	1.89
83°	84.42	8	1.63
89°	111.32	10	1.24

After calculating the amount of tension required to support the sliding rock mass for different installation angle for a design FOS, 1.2, for anticipated adverse conditions, the number and spacing between bolts is calculated for 11 ton bolt capacity. Table 6.2 shows the reinforcement force required to stabilize the slope section SL 6.

A perusal of table 6.2 indicates that if a Rock bolt is installed at an angle of 45° the required reinforcement force will be minimum i.e 38.74 Tons. This is the total force required to stabilize the total slope face of length 12.54 m. Therefore, if 11 tons capacity rock bolts are used, total 4 Rock bolts will be required at 3.5m in one section. Further, these Rock bolts may be provided laterally 3.5 center to center as per the plan shown through Figure 6.4

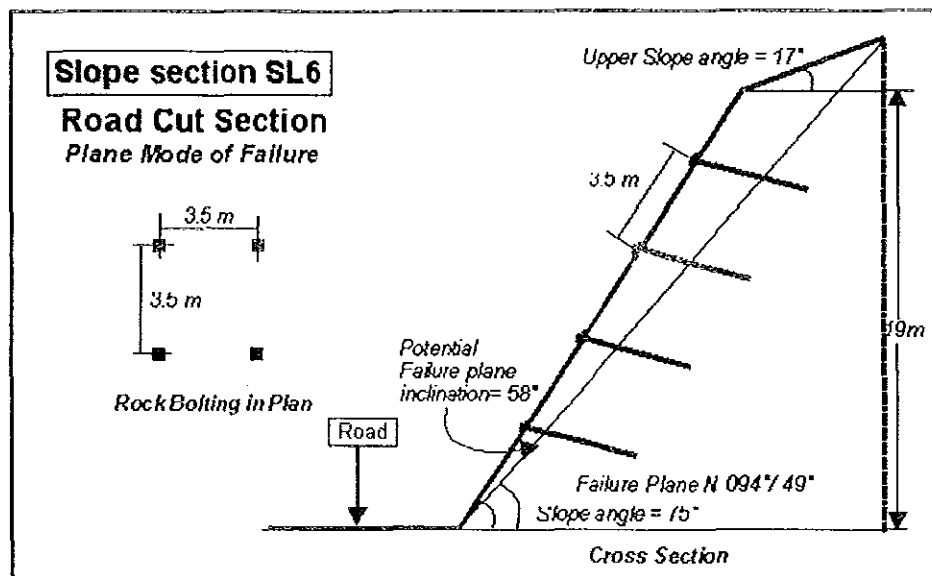


Fig. 6.4 Rock bolt plan for Slope Section SL6 Designed for Anticipated Adverse Condition

6.3 Remedial Measures for Slope Section Having Wedge Mode of Failure

The stability condition of road cut section having wedge mode of failure (SL8) will be stable for the existing conditions. However, for the entire slope section of SL8 demonstrates a FOS less than one, indicating slope is unstable for existing condition. For the AAC the road cut section and the entire slope section of SL8 is unstable. Therefore, some form of remedial measure has to be provided to this slope section.

As indicated from the stability results, slope section SL8 in it's road cut section is stable when there is no influence of water saturation i.e. when slope is dry. Even under dynamic condition

when slope would be dry the FOS is as high as 20.9. However, when there is an influence of water saturation the slope section becomes unstable for static and dynamic conditions. Therefore if somehow, the drainage is controlled the slope section may demonstrate stable condition.

In order to improve the drainage conditions horizontal collection drain in the crest region on upper slope may be provided which may collect the rain water and drain it away from the slope face. In addition to this on the upper slope surface and on the slope face shotcreting with wire mesh and random Rock bolts, may also be provided. In addition to this it is suggested to provide perforations in between the shotcreting surface, so that the water if any trapped, in between the shot creating layer and the slope face, be drained out.

6.4 Remedial Measures for Slope Section Having Rotational Mode of Failure

As already discussed in the previous paragraph there are two Critical soil slope sections SL 9 and SL 10, both the slope sections are stable for existing and anticipated worst conditions. However, if somehow, the cohesion for soil mass becomes zero the slope will be unstable for all static and dynamic condition, though practically it would be very rare chance that cohesion becomes zero. As such there is no need to provide any remedial measures as the slopes are stable for all conditions, however, there may be small soil failures of local nature in the road cut sections, and this may be due to the toe support removal, particularly during the rainy season. Therefore, it is suggested to provide retaining walls along the road cut. The retaining wall may be provided with perforated weep holes, this may help in draining any excess water trapped in between the wall and the soil face, which may generate pore water pressure. In addition to this along the road side, just at the junction of the wall, a lined drain should also be provided. This will help in draining the water which may damage the foundation of the retaining wall. However, presently the Project Authorities are using gabion wall to retain the soil cut sections along the road.

A landslide hazard zonation (LHZ) map is an important tool for designers, field engineers, and geologists. It is used to classify the land surface into zones of varying degree of hazard, based on the estimated significance of causative factors which influence the stability. The LHZ map is a rapid technique of hazard assessment of the land surface.

The LHEF rating scheme is a numerical system which is based on major inherent causative factors of slope instability such as geology, slope morphometry, relative relief, landuse and land cover and ground water conditions. Factors like rainfall and seismicity are not included for the purpose of landslide hazard zonation mapping. Thus, for the present study the facet map was prepared and according to the LHEF rating scheme various other thematic maps were prepared utilizing the facet map as base map.

The project area is dominated by three geological units, rhyolite, dolerite intrusions with in rhyolite and rhyolitic tuff. There are also trachytes interbedded with rhyolite. The area is also cut by northeast-southwest trending major lineaments with subordinate north-west oriented ones identified on air photographs.

Based on the TEHD values, 54% of the slopes in the study area falls in High Hazard, 34% in the Moderately Hazard and only 12% of the area falls in Low Hazard. From these results it can easily be concluded that the study area, in general, is prone to landslide activity. However, a slope may only fail when the driving forces exceeds the resisting forces and the orientation of discontinuities is such that they favor sliding, either on single discontinuity or on a wedge formed by two intersecting discontinuities. Slopes may also fail when the slope material is homogeneous like soils or slope material comprises of highly weathered and fractured rock mass. Moreover, even if slope is potentially unstable, it does not mean that slope is actually going to fail, until or unless there is some driving force which triggers sliding, such as heavy water saturation or earthquake loading.

For the present study, about 54% of the area falls in the High hazard zone, indicating that this area is most susceptible to land slides. With an intension to study the slopes falling in High Hazard zones, 8 critical slope sections in rock slopes were identified as potential unstable, based on certain field manifestations of instability. In addition to this two slope sections were identified to posse instability in soil sections. A detailed stability analysis has been carried out

by limit equilibrium method. In the present study it has been identified that there are ten critical slope sections out of which 7 slope sections have potential plane mode of failure, 1 slope section accounts for wedge mode of failure and remaining 2 slope sections are potentially unstable for possible rotational mode of failure.

The detailed stability analysis of the critical slope sections having possible plane mode of failure indicates that for the existing conditions i.e. static dry, only 2 slope sections (SL2 and SL 7) are stable, the remaining 5 slope sections (SL1, SL3, SL4, SL5 and SL6) are unstable. For the anticipated adverse condition (AAC), represented by moderate saturation with dynamic condition, slope SL2 is stable and slope SL7 is critically stable. However, the remaining slope sections (SL1, SL3, SL4, SL5 and SL6) would be unstable for AAC. Therefore, there is a need to provide some form of remedial measures to the slope sections which have a FOS less than 1.0 for the anticipated adverse conditions (AAC). Though, slope section SL 2 and SL 7 demonstrates a FOS of 1.45 and 1.13, respectively for the existing slope geometry, but these may become unstable for other geometric configurations. The change of slope geometry is very likely to happen as the road is still in construction and the road widening is in progress. Therefore, keeping all considerations an attempt has been made to workout a safe design for all critical slope sections, including SL 2 and SL 7.

The northern part of the study area is covered with soil and according to the Total estimated hazard (TEHD) values, most of the soil covered areas fall under moderately hazard zone and low hazard zone. However, little soil covered areas fall under high hazard zone. In these zones based on the field manifestations of instability two critical slope sections were identified. The stability analysis for circular mode of failure has been carried out by SARC computer program. From the results, the stability conditions for both soil slope sections are stable for existing condition (Static dry condition). The slope will remain stable even for anticipated worst condition (dynamic moderately saturated condition) as the FOS for this condition is 1.25.

In the present study for the critical slope sections having plane mode of failure a safe slope design has been worked out by adopting the technique proposed by Hoek and Bray, 1989. For this purpose for each critical slope section the height is varied from a minimum to a maximum value for a given slope angle. Similarly the slope angle for each slope has been varied from a minimum (more than failure plane angle) to a maximum up to 85°. Slope Section SL6 can not be stabilized by altering its geometry, as the factor of safety calculated

for various combinations of slope angle and slope height is less than unity, therefore, this slope section may be stabilized by providing rock bolts.

In order to improve the stability condition of wedge failures the horizontal collection drain in the crest region on upper slope may be provided which may collect the rain water and drain it away from the slope face. In addition to this on the upper slope surface and on the slope face shotcreting with wire mesh and random Rock bolts, may also be provided.

In the case of soil slopes, it is suggested to provide retaining walls along the road cut. The retaining wall may be provided with perforated weep holes, this may help in draining any excess water trapped in between the wall and the soil face, which may generate pore water pressure.

References

- Agarwal, C.K., Mehrotra, V.K. and Mitra, Subhash, 1991, "Need of Long Term Evaluation of Rock Parameters in the Himalayas Proc.", 7th International Congress Rock Mech., Aachen, Germany.
- Anbalagan R, Raghuvanshi T.K, Sharma R (1996) "Stability studies in the Reservoir slopes of Kishau Dam, Garhwal Himalaya, India Workshop on Design Practices in Earthquake Geotechnical Engineering, Department of Civil Engineering, Indian Institute of Technology Roorkee, India
- Anbalagan, R., (1992), "Landslide Hazard Evaluation and Zonation mapping in mountaneous Terrain". Elsever Science Publ., Eng.Geol.32. Amesterdam, pp269- 277
- Anbalagan, R., Sharma,S., Raghuvanshi. T.K. "Rockmass Stability Evaluation using Modified SMR Approach" Nati. Sympo. On Rock Mechanics, 1992, PP258 – 268
- Arora, K.R., (1997): Soil mechanics and foundation engineering. Bhargave printers, New Bell, F.G., (1983): Engineering geology and geotechniques, Boston, pp 497
- Bieniawski, Z.T., 1989, "Engineering Rock Mass Classifications", John Willey and Sons, New York.
- Coordinated National programme on "Landslide Hazard Mitigation", Department of Science and Technology, New Delhi, India, 2003.
- Ethiopian Electric power corporation (EEMCO), 2003 GiigeiGibe II Hydro electric power project Geotechnical report, Addis Ababa, Ethiopia
- Ethiopian Electric power corporation (EEMCO), 2004, GiigeiGibe II Hydro electric power project Geotechnical report for tunnel alignment, Addis Ababa, Ethiopia
- Goodman, R. E., (1989): Introduction to Rock Mechanics, second edition, John Wiley and Sons, NY.
- Haboudane, D., Bonn, F., Royer,A. (2002)"Land Degradation and Erosion Risk mapping by Fusion of Spectrally Based information and Digital Geomorphometric attributes", Int.J. Remote sensing. Vol. 23. No.18, Taylor &Francis Pub. Pp3795-3820.
- Hoek E. and Brown E.T. 1980. Underground Excavations in Rock . London: Institution of Mining and Metallurgy 527 pages
- Hoek, E., 1976, "Rock Slopes, Rock Engineering for Foundation and Slopes", V. 1, pp. 157-171.
- Hoek,E. & John Bray (1977). Rock Slope Engineering. The institution of Mining and Metallurgy, London. The Institution of Mining and Metallurgy, London

- JanodInc., Janod Ltd., 2002, "Rock Bolting and Grouting" Site built and maintained by PanTechnica Corporation, internet source.
- Johnson, R. B. (1988): Principles of Engineering Geology. John Wiley and Sons, Inc., USA.
- Kazmin v., (1972): Geology of Ethiopia, Explanatory note to the geological map of Ethiopia 1:2000.000, Geogolitical Survey of Ethiopia, Addis Ababa
- Leake Mariam Asfaw, (1996) : Catalogue of Ethiopian Earth Quakes, Earth quake parameters , strain release and seismic risk, Geophysical Observatory, Faculty of Science, Addis Ababa university
- Ayalew L., (1999) "The Effect of Seasonal Rainfall on Landslides in the Highlands of Ethiopia".
- Ayalew L., (2001) "Weathered Rockmass Characterization Considering Uncertainty, with an Example from GilgelGibe Hydropower Project in Ethiopia". PHD Thesis, Shaker Verlag, Germany.
- Mengesha, T. Tadiwos, C. and Workineh, H. (1996) "Exploration of the Geological map of Ethiopia, 2nd edition EIGS Bull.No2, Addis Ababa, Ethiopia
- Pachauri, A.K, and Pant, M., 1992, "Landslide Hazard Mapping based on geological attributes", Engi.geol. 32, Elsever Science Publ., Amesterdam, pp81-100.
- Robert, F. Legget, 1962 "Geology and Engineering Geology", Mc Graw-Hill, NewYork, PP410-417.
- Romana, M., 1985 "New Adjustment Ratings for application of Bieniawski Classification to Slopes". Inte. Sympto. On the role of rock mechanics ISRM, zacatecas, pp 49 – 53.
- Saha, A.K , Gupta, R.P., Arora,M.K. 2002. "GIS based Landslide Hazard zonation in the Bhagirathi Vally , Himalayas", inte. Jor. Remote Sensing, Vol. 23, No. 2, pp 357 –369.
- Sharma S., Raghuvanshi T.K and Anbalagan R.,1995. "plane failure analysis based on modified techniques"
- Singh, B, and Goel, R.K., 1998, "Software for Engineering Control of Landslide and Tunnelling Hazard", A.A. Balkema Publishers, Netherlands.
- USBR,1987. "Design Of Small Dams". United States Dep. Of The Interior Bureau Of Reclamation, Washington, DC 904 pages
- U.S. Army Corps of Engineers, Different engineering manuals from internet, Washington, DC
- Woldegebriel, G., Aronson, J.L., Walter, R.C., 1990. "Geology, Geochronology, and Rift Basin Development in the central sector of the main Ethiopian Rift" , Geol. Soc.Am. Bull 102, PP439 -458.

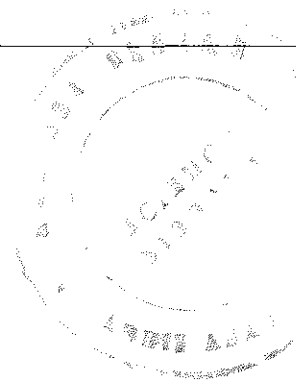
Yonas B.,(2004) "Legademi Gold Open Pit Mine Slope Stability & Underground Mine Geotechnical Study". Msc thesis, Addis Ababa University

Annexures

Annexure-I List of earth quakes between lat 4° 00 N and 10° 00 N and lon 35° 00 E and 40° 00 E since 1900 to 1993

No	LAT.	LON.	ML	No	LAT.	LON.	ML
1	8.02	38.41	3.3	45	8.9	39.86	4.1
2	8.02	38.41	3.3	46	9.1	40	4.3
3	9.72	38.58	3.5	47	9	39.94	4.2
4	9.6	39.65	4	48	9.1	40	4.1
5	5.5	37.43	4.9	49	9.1	40	4.4
6	8.85	38.7	4	50	9.1	40	4
7	5.62	36.57	4.1	51	9	39.94	4.2
8	8.7	39.75	4.1	52	8.7	39.75	4.3
9	9	39.94	4	53	9.1	40	4.2
10	8.7	39.75	4.5	54	9.1	40	4
11	9	39.94	4	55	9	39.94	4
12	8.9	39.86	4	56	9	39.94	4
13	8.9	39.86	4	57	9.1	40	4.3
14	4.3	36.7	6.2	58	8.9	39.86	4.52
15	6.9	36.9	6	59	9	39.94	4
16	5.1	36.9	6.3	60	9.1	40	4
17	5.8	37.2	5.9	61	9.1	40	4
18	5.8	36.8	5.3	62	7.95	38.7	4.2
19	5.6	37.2	5.1	63	7.56	38.98	4.5
20	4.3	35.7	5	64	9.75	39.5	3.7
21	5.6	36.9	5.7	65	7.03	38.59	
22	5.5	36.1	5.4	66	5.2	36.75	4.5
23	6.2	37.8	5.3	67	8.95	39.95	4.9
24	5.4	36.8	6.2	68	5.2	36.76	4.3
25	5.1	37.2	5.8	69	5.66	37.47	3.8
26	5.7	36.7	5.6	70	7.67	38.96	4.5
27	8.5	39.6	4.3	71	7.65	38.93	4.6
28	8.9	39.86	4.2	72	7.61	38.95	4.6
29	9	39.94	4	73	4.3	35.7	5
30	8.7	39.75	4	74	6.0	36.3	4.8
31	8.7	39.75	4.5	75	5.26	36.84	5.2
32	9	39.94	4.3	76	4.25	37	4.5
33	9	39.94	4.1	77	5.15	36.7	6.25
34	8.7	39.75	4.1	78	5.6	37.24	6.2
35	8.9	39.86	4.3	79	5.5	37.35	4.75
36	9	39.94	4.4	80	8	38.5	6.75
37	9	39.94	4.2	81	8.67	37.65	4.1
38	8.7	39.75	4	82	8.71	37.66	5.1
39	8.9	39.86	4.4	83	8.67	37.41	4.9
40	8.9	39.86	4	84	5.75	36.8	5.5
41	8.9	39.86	4				
42	8.9	39.86	4				
43	8.9	39.86	4				
44	8.7	39.75	4				

Dip of discontinuity Planar (B _j) Wedge (B _i)	I	<15°	0.2	Numbers of contour lines over 1cm length	Slope angle		
	II	16°- 25°	0.25				
	III	26°- 35°	0.3				
	IV	36°- 45°	0.4				
	V	> 45°	0.5				
Depth of soil cover	< 5 m		0.65			>12	>40°
	6-10 m		0.85			9-12	36°-40°
	11-15 m		1.30			8-6	25°-35°
	16-20 m		2.0			3-5	16°-25°
	> 20 m		1.20			<3	<15°
Slope Morphometry Escarpment Steep slope Moderately steep slope Gentle slope Very gentle slope	> 40°		2.0				
	36-40°		1.7				
	26°-35°		1.2				
	16°-25°		0.8				
	<15°		0.5				
Relative Relief Low Medium High	<100		0.3				
	101-300		0.6				
	>300		1.0				
Land use and land cover Agricultural land/ populated flat land Thickly vegetated forest land Moderately vegetated area Sparsely vegetated area with lesser ground cover Barren land			0.65				
			0.80				
			1.2				
			1.5				
			2.0				



Annexure- III - Rock mass Rating System (After Bieniawski 1989)

A. CLASSIFICATION PARAMETERS AND THEIR RATINGS									
Parameter		Range of values							
1	Strength of intact rock material	PointHead strength index	>10 MPa	4 - 10 MPa	2 - 4 MPa	1 - 2 MPa	For this low range - uniaxial compressive test is preferred		
		Uniaxial comp. strength	>250 MPa	100 - 250 MPa	50 - 100 MPa	25 - 50 MPa	5 - 25 MPa	1 - 5 MPa	< 1 MPa
	Rating	15	12	7	4	2	1	0	
2	Drill core Quality ROD		90% - 100%	75% - 90%	50% - 75%	25% - 50%	< 25%		
	Rating		20	17	13	8	3		
3	Spacing of discontinuities		> 2 m	0.6 - 2 m	200 - 600 mm	60 - 200 mm	< 60 mm		
	Rating		20	15	10	8	5		
4	Condition of discontinuities (See E)		Very rough surfaces Not continuous No separation Unweathered wall rock	Slightly rough surfaces Separation < 1 mm Slightly weathered walls	Slightly rough surfaces Separation < 1 mm Highly weathered walls	Slitkenned surfaces or Gouge < 5 mm thick or Separation 1-5 mm Continuous	Soft gouge > 5 mm thick or Separation > 5 mm Continuous		
			Rating		30	25	20	10	0
5	Ground water	Inflow per 10 m tunnel length (l/m)	None	< 10	10 - 25	25 - 125	> 125		
		(Joint water pressure) (Major principal σ)	0	< 0.1	0.1 - 0.2	0.2 - 0.5	> 0.5		
	General conditions	Completely dry	Damp	Wet	Dripping	Flowing			
	Rating		15	10	7	4	0		
B. RATING ADJUSTMENT FOR DISCONTINUITY ORIENTATIONS (See F)									
Strike and dip orientations		Very favourable	Favourable	Fair	Unfavourable	Very Unfavourable			
Ratings	Tunnels & mines	0	-2	-5	-10	-12			
	Foundations	0	-2	-7	-15	-25			
	Slopes	0	-5	-25	-50				
C. ROCK MASS CLASSES DETERMINED FROM TOTAL RATINGS									
Rating	100 - 81	80 - 61	50 - 41	40 - 21	< 21				
Class number	I	II	III	IV	V				
Description	Very good rock	Good rock	Fair rock	Poor rock	Very poor rock				
D. MEANING OF ROCK CLASSES									
Class number	I	II	III	IV	V				
Average stand-up time	20 yrs for 15 m span	1 year for 10 m span	1 week for 5 m span	10 hrs for 2.5 m span	30 min for 1 m span				
Cohesion of rock mass (kPa)	> 400	300 - 400	200 - 300	100 - 200	< 100				
Friction angle of rock mass (deg)	> 45	35 - 45	25 - 35	15 - 25	< 15				
E. GUIDELINES FOR CLASSIFICATION OF DISCONTINUITY conditions									
Discontinuity length (persistence)	< 1 m	1 - 3 m	3 - 10 m	10 - 20 m	> 20 m				
Rating	6	4	2	1	0				
Separation (aperture)	None	< 0.1 mm	0.1 - 1.0 mm	1 - 5 mm	> 5 mm				
Rating	6	5	4	1	0				
Roughness	Very rough	Rough	Slightly rough	Smooth	Slitkenned				
Rating	6	5	3	1	0				
Infilling (gouge)	None	Hard filling < 5 mm	Hard filling > 5 mm	Soft filling < 5 mm	Soft filling > 5 mm				
Rating	6	4	2	2	0				
Weathering	Unweathered	Slightly weathered	Moderately weathered	Highly weathered	Decomposed				
Rating	6	5	3	1	0				
F. EFFECT OF DISCONTINUITY STRIKE AND DIP ORIENTATION IN TUNNELLING**									
Strike perpendicular to tunnel axis					Strike parallel to tunnel axis				
Drive with dip - Dip 45 - 90°		Drive with dip - Dip 20 - 45°			Dip 45 - 90°		Dip 20 - 45°		
Very favourable		Favourable			Very unfavourable		Fair		
Drive against dip - Dip 45-90°		Drive against dip - Dip 20-45°			Dip 0-20° - Irrespective of strike°				
Fair		Unfavourable			Fair				

* Some conditions are mutually exclusive. For example, if infilling is present, the roughness of the surface will be overshadowed by the influence of the gouge. In such cases use A.4 directly.

** Modified after Wickham et al (1972).

SL4	RMR1	16	10	21	10	10	15	-40	4	17
		16	12	21	10	10	15	-40	4	17
		19	40	21	10	10	15	-40	7	17
		24	58	21	10	10	15	-40	12	17
	Average	18.8								
	RMR2	4	25	18	8	0	15	-40	4	17
		12	54	18	8	0	15	-40	12	17
		12	60	18	8	0	15	-40	12	17
	Average	9.3								
	RMR3	24	58	20	10	10	15	-40	12	17
		24	60	20	10	10	15	-40	12	17
		16	46	20	10	10	15	-40	4	17
		24	50	20	10	10	15	-40	12	17
	Average	22								
SL5	RMR1	20	12	19	8	10	15	-40	7	20
		20	42	19	8	10	15	-40	7	20
		25	48	19	8	10	15	-40	12	20
		17	26	19	8	10	15	-40	4	20
		20	34	19	8	10	15	-40	7	20
	Average	20.4								
	RMR2	20	58	18	8	5	15	-40	12	20
		12	44	18	8	5	15	-40	4	20
		15	46	18	8	5	15	-40	7	20
		15	40	18	8	5	15	-40	7	20
	Average	15.5								
SL6	RMR1	22	34	16	8	25	15	-50	7	17
		27	54	16	8	25	15	-50	12	17
		27	48	16	8	25	15	-50	12	17
	Average	25.3								
	RMR2	25	52	18	8	25	15	-50	12	15
		20	30	18	8	25	15	-50	7	15
		25	48	18	8	25	15	-50	12	15
		25	56	18	8	25	15	-50	12	15
		20	34	18	8	25	15	-50	7	15
		17	18	18	8	25	15	-50	4	15
	Average	22								
SL7	RMR1	16	22	21	10	10	15	-40	4	17
		16	32	21	10	10	15	-40	4	17
		16	26	21	10	10	15	-40	4	17
		19	36	21	10	10	15	-40	7	17
		16	24	21	10	10	15	-40	4	17
	Average	16.6								
	RMR2	19	28	33	10	10	15	-40	4	20
		19	32	33	10	10	15	-40	4	20
		19	20	33	10	10	15	-40	4	20
		22	46	33	10	10	15	-40	7	20
		19	30	33	10	10	15	-40	4	20
	Average	19.6								
	RMR3	32	58	9	8	20	15	-40	12	17
		27	38	9	8	20	15	-40	7	17
		27	46	9	8	20	15	-40	7	17

		32	48	9	8	20	15	-40	12	17
		24	20	9	8	20	15	-40	4	17
		22	16	9	8	20	15	-40	2	17
		24	32	9	8	20	15	-40	4	17
	Average	26.9								
SL8	RMR1	10	38	10	8	0	15	-40	7	20
		10	46	10	8	0	15	-40	7	20
		15	48	10	8	0	15	-40	12	20
	Average	11.7								
	RMR2	34	44	20	10	25	15	-40	7	17
		34	34	20	10	25	15	-40	7	17
		29	16	20	10	25	15	-40	2	17
		34	42	20	10	25	15	-40	7	17

Annexure- V: A Brief outline of SARC computer program

The computer program SARC is prepared by Prof. Bhawani Singh, Department of Engineering, Indian Institute of Technology. The program (x) is written in Fortran 77 and EXE files work in DOS environment. The users' manual is also indexed as IX.NEW for preparation of input data files. Further, typical input data files are also given as IX.DAT beginning with I. The corresponding out put files OX.DAT are added, beginning with O.

The typical computer commands are:

NE IX.DAT- To open input file

NE OX.DAT- To open out put file

X- Name of computer program

IX.DAT- Input file name

OX.DAT- Output file name

2- For execution

1- For help menu

NE OX.DAT- To see the output file OX.DAT

SARC

This program facilitates to compute the factor of safety with circular failure surface emerging at the toe. It analyses any general profile of the slope surface and for various forces that is pore water pressure, depth of tension crack at the top of the slope, depth of water in tension crack and earthquake force. In the first step it draws the various slip surfaces along which failure can take place. Then it calculates the radius and center of each slip surface.

In the next step, the factor of safety is computed using Bishop,s equation for various slip surfaces until a minimum factor of safety is obtained. The analysis evaluates critical acceleration for slopes with factor of safety less than unity and compute dynamic displacement utilizing coorelation developed by Lavania et al. (1987).

Annexure-I List of earth quakes between lat 4° 00 N and 10° 00 N and lon 35° 00 E and 40° 00 E since 1900 to 1993

No	LAT.	LON.	ML	No	LAT.	LON.	ML
1	8.02	38.41	3.3	45	8.9	39.86	4.1
2	8.02	38.41	3.3	46	9.1	40	4.3
3	9.72	38.58	3.5	47	9	39.94	4.2
4	9.6	39.65	4	48	9.1	40	4.1
5	5.5	37.43	4.9	49	9.1	40	4.4
6	8.85	38.7	4	50	9.1	40	4
7	5.62	36.57	4.1	51	9	39.94	4.2
8	8.7	39.75	4.1	52	8.7	39.75	4.3
9	9	39.94	4	53	9.1	40	4.2
10	8.7	39.75	4.5	54	9.1	40	4
11	9	39.94	4	55	9	39.94	4
12	8.9	39.86	4	56	9	39.94	4
13	8.9	39.86	4	57	9.1	40	4.3
14	4.3	36.7	6.2	58	8.9	39.86	4.52
15	6.9	36.9	6	59	9	39.94	4
16	5.1	36.9	6.3	60	9.1	40	4
17	5.8	37.2	5.9	61	9.1	40	4
18	5.8	36.8	5.3	62	7.95	38.7	4.2
19	5.6	37.2	5.1	63	7.56	38.98	4.5
20	4.3	35.7	5	64	9.75	39.5	3.7
21	5.6	36.9	5.7	65	7.03	38.59	
22	5.5	36.1	5.4	66	5.2	36.75	4.5
23	6.2	37.8	5.3	67	8.95	39.95	4.9
24	5.4	36.8	6.2	68	5.2	36.76	4.3
25	5.1	37.2	5.8	69	5.66	37.47	3.8
26	5.7	36.7	5.6	70	7.67	38.96	4.5
27	8.5	39.6	4.3	71	7.65	38.93	4.6
28	8.9	39.86	4.2	72	7.61	38.95	4.6
29	9	39.94	4	73	4.3	35.7	5
30	8.7	39.75	4	74	6.0	36.3	4.8
31	8.7	39.75	4.5	75	5.26	36.84	5.2
32	9	39.94	4.3	76	4.25	37	4.5
33	9	39.94	4.1	77	5.15	36.7	6.25
34	8.7	39.75	4.1	78	5.6	37.24	6.2
35	8.9	39.86	4.3	79	5.5	37.35	4.75
36	9	39.94	4.4	80	8	38.5	6.75
37	9	39.94	4.2	81	8.67	37.65	4.1
38	8.7	39.75	4	82	8.71	37.66	5.1
39	8.9	39.86	4.4	83	8.67	37.41	4.9
40	8.9	39.86	4	84	5.75	36.8	5.5
41	8.9	39.86	4				
42	8.9	39.86	4				
43	8.9	39.86	4				
44	8.7	39.75	4				

SASW computer program

This Program Calculates The Factor of Safety of Tetrahedral Wedge With Horizontal Slope Crest and With No Tension Crack

Name of Program SASW (Units Used Tonne - Meter - Degree)

Give Input Data In The Following Sequence

NO (Please repeat all following lines no times for no slopes)

Title of problem in one line (<80 characters)

NJT,NCASE

SAI(I),ALPHA(I),C(I),PHAI(I) (Please repeat above line NJT times)

SAI3,ALPHA3,SAI4,ALPHA4

H,GAMA,GAMAW,ETA,ACCN,RWL,PORE,EQM (Please repeat above line NCASE times)

The discontinuities are denoted by 1 and 2 , the upper ground surface by 3 and the slope face by 4

NO	=	Number of slopes
NJT	=	Number of joint sets
NCASE	=	Number of cases
SAI(I)	=	Dip of I th joint plane (deg.)
ALPHA(I)	=	Dip direction of I th joint plane (deg.)
C(I)	=	Cohesion of I th joint plane (T/sq.m)
PHAI(I)	=	Friction angle of I th joint plane (deg.)
	=	ARC TAN(J_r/J_a) for clay coated joints
SAI3	=	Angle of slope of upper ground surface
ALPHA3	=	Dip direction of the upper ground surface
SAI4	=	Angle of rock slope
ALPHA4	=	Dip direction of the rock slope
H	=	Height of the crest of the slope above toe of intersection
GAMA	=	Unit weight of rock (T/CU.M)
GAMAW	=	Unit weight of water(T/CU.M)
ETA	=	-1 means slope face overhangs toe of the slope
	=	+1 means slope face does not overhang
ACCN	=	Coefficient of horizontal acc. of earthquake near crest of slope
EQM	=	Corresponding earthquake magnitude
RWL	=	Water level above toe of intersection
PORE	=	Pore water pressure factor - 0 (for dry slope) or 1 (for wet slope)